2020

Adsorption Behavior of Chemically / Charged Modified Antibodies on Gold Nanoparticles

Samuel Okyem
Illinois State University, okyemsamuel@gmail.com

ADSORPTION BEHAVIOR OF CHEMICALLY/CHARGED MODIFIED ANTIBODIES ON GOLD NANOPARTICLES

SAMUEL OKYEM

82 Pages

Gold nanoparticles (AuNPs) have been exploited in the various domains of science such as drug delivery, bio-sensing, immunoassays and environmental sensors, due to their optical properties and intriguing surface chemistry. Different scientific procedures have been used to effectively immobilize antibodies onto AuNPs. Although acceptable outcomes have been achieved in the immobilization of antibodies onto AuNPs, the sensitivity of these immobilized antibodies to target antigen or binding sites is limited due to improper orientation of the antibodies. Also, the possibility of nanoparticle aggregation when exposed to proteins limits its biomedical applicability.

There is some evidence that the surface charge of antibodies is responsible for controlling the orientation upon adsorption to AuNPs. Antibodies have ubiquitous lysine residues which are protonated at physiological pH contributing to the total surface charge of the antibody. Chemical modification of antibodies by reacting with acrylic acid N-hydroxysuccinimide ester and thiosuccinimidylpropionate, acroleinate and thiopropionate lysine residues respectively, consequently controlling the surface charge of the antibodies and potentially impacting the orientation upon adsorption to AuNPs.

In this proceeding, novel analytical techniques are utilized to directionally adsorb charge modified antibodies onto citrate capped AuNPs to increase the amount of exposed active site.

Dynamic light scattering, fluorescence, nanoparticle tracking analysis and other analytical strategies have been used to study the adsorption dynamics, kinetics, and orientation of these charged modified antibodies on AuNPs. These fundamental investigations to elucidate the mechanism of protein-AuNP adsorption will lead to optimized bioconjugates that are necessary to realize the full potential of AuNP-enabled bio-nanotechnologies.

KEYWORDS. Charged Modified Antibody, Gold Nanoparticles, Immunoassay

ADSORPTION BEHAVIOR OF CHEMICALLY/CHARGED MODIFIED ANTIBODIES ON GOLD NANOPARTICLES

SAMUEL OKYEM

A Thesis Submitted in Partial
Fulfillment for the Requirement
for the Degree of

MASTER OF SCIENCE

Department of Chemistry

ILLINOIS STATE UNIVERSITY

2020

ADSORPTION BEHAVIOR OF CHEMICALLY/CHARGED MODIFIED ANTIBODIES ON GOLD NANOPARTICLES

SAMUEL OKYEM

COMMITTEE MEMBERS:

Jeremy D. Driskell, Chair

Jun-Hyun Kim

Chris Weitzel

ACKNOWLEDGMENTS

I would like to express my sincere gratitude and appreciation to Dr. Jeremy D. Driskell, for his guidance and support throughout the duration of my research. His mentorship has not only given me relentless efforts and dedication to continue strong with my journey as a chemistry student, it has also created a friendship connection between us. I would like to expand my appreciation to Dr. Chris Wietzel and Dr. Jun-Hyun Kim for taking their precious time to read my thesis and accepting to be part of my thesis committee. Their kind support has pushed me forward to be the best that I can be in everything.

My appreciation goes to the Illinois State Department of Chemistry for giving me the opportunity to do research and expand my knowledge in completing my thesis.
I would like to thank my friends and family who have been of great support, especially my mother, Florence Awuah, for her emotional and financial support, and believing in me.

My final gratitude is to the National science foundation (award # CHE-1807126) for funding this project.

S.O.

CONTENTS

	Page
ACKNOWLEDGMENTS	i
CONTENTS	ii
TABLES	v
FIGURES	vi
CHAPTER I: INTRODUCTION	1
Immunoassay and Gold nanoparticle (AuNP)	1
Time Evolution AuNP-Protein Corona	2
Strategies for Synthesizing Antibody-AuNP Conjugates	2
Covalent Immobilization of Antibodies onto AuNP	2
Direct Antibody Immobilization on AuNP	3
Orientation Directed Antibody-AuNP Synthesis	3
Protein/Antibody Gold Nanoparticle (AuNP) Interactions	4
Protein Triggered Aggregation of Nanoparticles	5
Thesis Objectives	6
Research Overview	6
CHAPTER II: PROBING ANTIBODY- AuNP AGGREGATION MECHANISM	8
Introduction	8
Materials and Methods	10
Reagents	10
Antibody Characterization at Different pHs	10
Antibody-AuNP Synthesis at Different pHs	11

Titration of Antibody-AuNP Conjugates 12

Antibody-AuNP Conjugate Unfolding Test 12

Antibody-AuNP Characterization and Stability Analysis 13

Results and Discussion 14

Effect of pH on Antibody Triggered Aggregation of AuNPs 14

Overview of Nanoparticle Stability and Aggregation Mechanism 17

pH Effect on Antibody Surface Charge 18

Effect of Antibody Unfolding on Nanoparticle Aggregation 20

Buffer Exchange of Stable Antibody-AuNPs to Lower pH 21

Effects of Titration with NaOH on Reversibility of Aggregates 26

Reducing Antibody Positive Charge through Chemical Modification Allows Synthesis of Conjugates at Lower pH 27

Conclusion 29

CHAPTER III: HIGH AFFINITY POINT OF INTERACTION ON ANTIBODY ALLOWS SYNTHESIS OF STABLE AND HIGHLY FUNCTIONAL ANTIBODY-AuNP CONJUGATES 31

Introduction 31

Materials and Methods 33

Reagents 33

Computational Simulation of Antibody Surface Charge 33

Antibody Chemical Modification and Characterization 34

Antibody-AuNP Synthesis 35

Kinetic of Antibody Adsorption onto AuNPs 35

Quantifying the Number of Antibodies bound Per AuNP 35
Quantitation of Conjugates Antigen Binding Site 37
Dissecting Antibody Orientation on AuNP 37
Instrumentation 38
Results and Discussion 38
Antibody Chemical Modification 38
Kinetics of Hard and Soft Antibody Corona Formation on AuNPs 45
Effect of pH on the Synthesis of AuNP-Antibody Conjugates 52
Quantifying Antibody bound Per AuNP 55
Quantitation of Antigen-binding Activity of Conjugates 61
Dissecting the Effect of Antibody on AuNP 65
Conclusion 67
CHAPTER IV: CONCLUSIONS AND OUTLOOKS 69
Research Summary 69
Outlooks and Future Direction 71
REFERENCES 72

TABLES

Table Page

1. DLS Size and Zeta Potential of Anti-HRP Antibody (MAHRP) at Different pHs. 20

FIGURES

Figure Page

1. Schematic illustration of conjugate synthesis at a pH 8.0 to form a stable monolayer 11
2. Schematic illustration of titration of conjugates to lower pH. 13
3. Evaluating the stability of antibody-AuNP conjugates at pH 6.0-8.5 16
4. Computational simulation of mouse IgG 2a antibody surface charge at four different pHs. Blue and red regions represent positive and negative potential, respectively, in a range of −5 kbT/e to + 5 kbT/e. The calculations were performed online using Adaptive Poison Boltzmann Solver (APBS). http://nbcr-222.ucsd. edu/pdb2pqr/ 19
5. Quantitation of antigen binding activity of conjugates after resuspension into buffer of pH 6, 6.5 and 8. MAHRP-AuNP conjugate synthesized at pH 8 is resuspended in buffer of pH 6, 6.5 and 8.5 for 24 hours 21
6. Size and particle distribution of MAHRP-AuNP conjugates synthesize at pH 6.0-8.5 in situ and stable conjuagtes titrated to pH 6.0-8.0. (A) Size of conjugates in nm for in situ synthesis and titrations. (B) Polydispersity Index (PDI) of in situ and titration conjugates. (C) DLS size 23
7. Surface plasmon resonance and Zeta potential of conjugates after titration into buffer of pH 6.0 and 6.5. (A) UV-visible spectra of MAHRP-AuNP conjuagtes synthesized at pH 8.0 and resuspended

in buffer of pH 5.0-6.5 for 4 hours. (B) UV-visible spectra of MAHRP-AuNP conjuagtes synthesized at pH 8.0 and resuspended in buffer of pH 5.0-6.5 for 24 hours. (C) Zeta potential of conjugates after resupesnion in buffer pH 6.0 , 6.5 and 8.0 for 4 and 24 hours 25

8. Reversibility of aggregation by addition of NaOH. (A) DLS Size distribution of conjugates synthesized at pH 6.0 (in situ) for 4 and 24 hours and titrated to higher pH by addition of 0.1 M NaOH. (B) DLS size distribution of conjugates incubated at pH 6.5 (in situ) for 4 and 24 hours. Dash lines represent size distribution of antibody-AuNP conjugates after addition of 0.1M NaOH 28

9. Surface plasmon resonance of acrylic acid NHS chemically modified MAHRP-AuNP conjugate synthesized in situ at pH 6.0, 6.5 and 7.5 29

10. Calculation of antibody (PDB-ID 1IGT) surface charge. Adaptive Poison Boltzmann equation solver on a CHARM-GUI was used for protein surface charge simulation. Blue and red regions represent positive and negative potential, respectively, in a range of −5 kbT/e to + 5 kbT/e 39

11. Chemical modification of the lysine residue with acrylic acid NHS (top) and reduced DSP (bottom). 41

12. Characterization of chemically modified and unmodified antibodies. Zeta potential of unmodified chemically modified antibodies at different pHs 42

13. Structure of antibody showing all cysteine residue (pink) are engaged in disulfide bond 42
14. Characterization of chemically modified and unmodified antibodies. The number of free thiols on unmodified and DSP-modified antibodies determined using Ellman's reagent 43
15. Characterization of chemically modified and unmodified antibodies. Result of equilibrium dialysis to determine the antigen-binding activity of the unmodified (UM) and modified antibodies (NHS and DSP). Negative control samples include an IgG isotype (ISCTR) control and buffer (EQ CONC) 44
16. Extinction spectra of Antibody-AuNP conjugates incubated for an hour. 46
17. Time evolution of antibody corona on AuNP. Demonstration of effect of centrifuging on antibody soft and hard corona 47
18. Kinetic of hard and soft antibody corona formation. (A) DLS size meaured of unmodified antibody-AuNP conjugates before removal of excess antibodies through centrifugation (in situ) and after removal of excess antibodies (purified). (B) Size of acrylic acid NHS-modified antibody-AuNP conjugates in situ and after purification. (C) DSP- modified antibody-AuNP conjugates size before (in-situ) and after (purified) purification 49
19. Zeta potential of unmodified and modified antibody-AuNP conjugates incubated for different time 50

20. Kinetics of catalytic activity of acrylic acid NHS-modified and unmodified antibody-AuNP conjugates. Reduction of para-nitrophenol to aminophenol by AuNP was evaluated to determine the time required for full saturation of AuNP surface by acrylic acid NHS-modified antibodies 51
21. Evaluating antibody-AuNP conjugate stability at different pH. Extinction spectra of (A) unmodified antibody-AuNP, (B) acrylic acid NHS-modified antibody-AuNP, and (C) DSP-modified antibody-AuNP conjugates at different pH 54
22. Hydrodynamic diameter of unmodified and modified antibody-AuNP conjugates at pH 6.5 measured with DLS 55
23. Schematic illustration of workflow for quantitation of the number of antibodies per AuNP using florescence and ICP-OES. 56
24. Quantitation of number of antibody/AuNP. (A) Florescence adsorption isotherm of unmodified antibody on AuNP obtained using native protein florescence and a highly sensitive CBQCA florescence assay 57
25. Quantitation of number of antibody/AuNP at selected pHs for chemically modified and unmodified antibodies 59
26. NTA size distribution of DSP-modified antibody-AuNP conjugate at (A) pH 6.5 and (B) pH 6.0 60
27. Determination of antigen binding activity of chemically modified and unmodified antibody-AuNP conjugates. (A) Moles of HRP

captured by each conjugate at selected pH. ICP-OES Au intensity at 242 nm was used to normalize HRP data.(B) Percentage of adsorbed antibody available for antigen binding 62

28. Workflow of HRP enzymatic assay for evaluating the antigen binding affinity of antibody-AuNP conjugates 63

29. Evaluating the effect of antibody overcrowding on antigen capture efficiency 66

CHAPTER I: INTRODUCTION

Immunoassay and Gold nanoparticle (AuNP)

Disease diagnosis is a critical area in medicine since it remains the first fundamental process of medical care. Diagnostic tools with high sensitivity and selectivity are in stark demand as they allow for early and effective diagnosis which decreases disease threats and mitigates the excessive use of drugs.

Immunoassays remain one of the most effective techniques for diagnosing infectious diseases, cancer, autoimmune disease, etc. Recent advancement in enzyme, fluorescence, chemiluminescence, and radio immunoassay have contributed to early diagnoses of disease and lower detection limits.[4] However, these techniques are labor intensive and may employ the use of hazardous chemicals, or require specialized facilities and highly skilled personnel. It is, therefore, necessary to explore alternative cost effective, highly sensitive and time efficient analytical techniques that require no specific training for use, e.g. pregnancy test strips, for various disease diagnosis. Gold Nanoparticles (AuNPs) having outstanding optical, chemical, electrical and catalytic properties have been exploited in drug delivery, therapeutics, bioimaging, biosensors and in immunoassays.[5,6] Recently, several advancements have been made in AuNP enabled immunoassays; nonetheless the applicability of these techniques are still limited due to their low sensitivity. This lower sensitivity is attributed to random orientation of antibody or antigen on the AuNP surface which decreases the number of accessible binding sites. In this research we seek to develop a technique leading to the formation of highly stabilized, functional, and selective antibody-AuNP conjugates with high sensitivity to promote implementation of AuNP-enabled immunoassays in disease diagnosis.

Time Evolution AuNP-Protein Corona

AuNPs for biomedical applications are mostly functionalized with aptamers, peptides, proteins, glycans, peptidoglycans, etc.[7,8] This biomolecule functionalized AuNP dictate the function of the AuNP. Various techniques have been used in studying the time evolution of protein corona on AuNP. Puntes and coworkers[9] studied protein corona formation on AuNP in cell culture medium supplemented with serum protein by measuring the Zeta potential and conjugates size at different incubation times. From their findings, the Zeta potential of AuNP which is a measure of the surface charge decreased exponentially with time, indicating the formation of strongly stabilized conjugates with time. Also, they observed that at early incubation time, several proteins with low affinity are loosely bound to the AuNP (soft corona), which desorbs upon centrifugation. However, as time evolves, a highly stabilized hard corona of protein is formed on AuNP. In this work, we intend to employ the use of zeta potential and size measurement to probe the required time needed to irreversibly adsorb chemically modified and unmodified antibodies onto AuNPs at different pHs.

Strategies for Synthesizing Antibody-AuNP Conjugates

Covalent Immobilization of Antibodies onto AuNP

Several methods exist for synthesizing AuNP-antibody conjugates. Among them is the use of heterobifunctional linkers, which uses one of its arms mostly containing a thiol group to bind selectively to the AuNP, and the other half reacts covalently with the antibody through 1-ethyl-3-(3-dimethylaminopropyl)carbodiimide/dicyclohexyl carbodiimide (EDC/DCC) coupling chemistry. In addition, covalent immobilization of antibodies on AuNP can be achieved by adsorbing small molecules containing carboxylate functional on to AuNP followed by coupling of antibodies through NHS (N-hydroxy succinimide), EDC, and DCC chemistry to form amide

bonds. Several other methods have been developed for covalent immobilization, however these immobilization techniques require more antibodies, and also results in fewer antibodies being immobilized onto AuNP.[10]

Direct Antibody Immobilization on AuNP

Antibody-AuNP conjugates can also be synthesized by directly incubating antibodies with AuNP.[11,12] Recent advancement in protein-AuNP chemistry reports electrostatic interaction between negatively charged citrate capped nanoparticles[13] and proteins as the primary driving force facilitating the adsorption of proteins onto AuNP. Subsequently, the interaction between free sulfhydryl and amino groups and the AuNP have been reported as secondary interactions leading to the formation of a hard corona of protein on AuNP.[9] Highly stable antibody-AuNP conjugates have been synthesized using this procedure. However, this immobilization technique is pH-dependent, thus stable conjugates can only be synthesized within a small pH range for each specific antibody isotype or host type dictated by the isoelectric points exhibited by these antibodies. In addition, direct immobilization of antibodies onto AuNPs results in random orientation of antibody on AuNP surface which may cause paratope masking thereby reducing the effectiveness of these conjugates in immunoassays.

Orientation Directed Antibody-AuNP Synthesis

Recently Richard M. Crooks and coworkers[14] employed the use of a heterobifunctional linker to control the orientation of antibodies on silver nanoparticles. The heterobifunctional linker consisted of either a disulfide or free sulfhydryl at one end and a hydrazine at the other half separated by a small alkyl group. In this work, the heterobifunctional linker is first immobilized onto the AuNP, followed by antibody immobilization. Hydrazine on the heterobifunctional linker preferentially reacts with the carbonyl of the polysaccharide at the Fc

end of the antibody, whereas the sulfur containing functionality at the other arm of the linker binds to the gold. This technique allowed the immobilization of antibodies onto AuNP and AgNP through the Fc (fragment crystallizable) end rendering the Fab (fragment antigen binding) end exposed for antigen binding. Protein A, which binds selectively to the Fc of antibodies, have also been utilized for directionally oriented antibody-AuNP conjugates synthesis.[15,16] Although a high fraction of antibodies is oriented correctly for effective antigen binding only a small number of antibodies are immobilized due to the bigger footprint of protein A on AuNP.

Protein/Antibody Gold Nanoparticle (AuNP) Interactions

Recent advancements in gold nanotechnology have rendered it very useful in biomedicine.[17] In order to maximize its usefulness in a biological environment it is pertinent to understand the fundamental interaction of biomolecules with AuNP. Various analytical techniques such as UV-visible spectrophotometry (UV-vis), dynamic light scattering (DLS), nanoparticle tracking analysis (NTA), and florescence correlation spectroscopy (FSC) have been employed to study the formation of protein corona on AuNP. However, a full, detailed, chemical mechanism for the formation of protein corona on AuNP is yet to be unraveled. Electrostatic interaction between negatively charged citrate capped AuNP and proteins have been reported as the main fundamental force that drives the adsorption of proteins onto AuNP.[13,18] Recent reviews on protein AuNP interactions also suggests the occurrence of secondary interaction between protein and AuNP,[19,9,20] which leads to the formation of irreversibly bound protein (hard corona) on AuNPs. These secondary interactions are reported to be driven primarily from free sulfhydryl groups of proteins. Trout et al.[21] deduced the interaction between DNA and AuNP to proceed through the conjugated amines on the purine and pyrimidine bases after conducting a computational adsorption study of methylamines on AuNP. Protein affinity for AuNP is also

known to increase with increasing molecular weight as a result of increasing points of interaction.[22] These findings suggest that antibodies of molecular weight 150 kDa will have a high binding affinity for AuNP. In this research, we seek to employ the use of UV-Vis, DLS and NTA to understand the mechanism of adsorption of both unmodified and chemically modified antibodies on AuNP, which will facilitate the development of a systematic procedure for synthesizing highly stable and active conjugates for biomedical applications.

Protein Triggered Aggregation of Nanoparticles

It is well-established that proteins can adsorb onto AuNPs to result in a stable Ab-AuNP conjugate, which resists aggregation under physiological conditions, e.g., high ionic strength. It is less commonly reported, however, that protein can actually trigger the aggregation of AuNPs.[23,24] In the case of some proteins, the aggregation has been attributed to adsorption and subsequent unfolding of the protein, which leads to destabilization and aggregation.[25] Other protein-triggered aggregation events have been attributed to a bridging mechanism.[26] In this case, proteins with positive charges on opposing sides of the macromolecule act as a bridge to electrostatically crosslink two negatively charged AuNPs, e.g., citrate-capped AuNPs. Accordingly, at lower pHs, antibodies will carry more positive charge and trigger AuNP aggregation. This will limit the pH range over which the proposed antibody-AuNP binding affinity experiments can be performed. Moreover, with respect to the long-term goal of the project, certain antibodies will not form stable conjugates at lower pH values for use in bioassays. To overcome this challenge, we propose to investigate the mechanism leading to nanoparticle aggregation at lower pHs. We hypothesize that if the mechanism of protein induced nanoparticle aggregation is through electrostatic bridging of antibodies then appropriate modification will convert the protonated lysine, e.g., positive charge, to a neutral or negatively

charged functional group to prevent protein-triggered aggregation via electrostatic bridging. This work will provide a pathway to form stable antibody-AuNP conjugate at any pH which proves to be optimal for antigen binding.

Thesis Objectives

Protein-AuNP conjugates have numerous promising biomedical applications, yet its utilization is limited due to the possibility of AuNPs aggregating upon exposure to proteins. Several interactions have been reported as the means through which protein induces aggregation of nanoparticles. In this research, a systemically developed workflow for synthesizing protein-AuNP conjugates at different pH is being used to evaluate the impact of protein charge on nanoparticle aggregation as well as the mechanism through which these aggregates are produced.

Preliminary studies in our lab indicate chemical modification of antibodies allows the synthesis of antibody-AuNP conjugates at several pHs, however synthesis of some of these conjugates require a long incubation time; understanding the underlying chemical interactions resulting in long incubation as a result of chemical modification of antibody is therefore essential. Here, we seek to employ various analytical techniques to investigate the effect of chemical modification on conjugate stability, adsorption kinetics, adsorption dynamics, and antigen-binding affinity.

Research Overview

The functionalization of AuNP surfaces with protein and other molecules defines its functions and surface properties.[18,27] Various analytical techniques have been employed to immobilize proteins onto AuNPs for several applications,[8,28] yet these immobilization techniques are pH dependent and are mostly unique to a specific protein. Existing methods for synthesizing antibody-AuNP conjugates mostly results in random orientation of antibodies on nanoparticle

surface, which may cause masking of protein active sites, leading to reduced effectiveness of these conjugates for biomedical applications. Although several attempts have been made to understand the chemical interaction between protein and nanoparticle, no definite conclusions have been reached.[29–31] It is, therefore, important to search for alternative universal techniques for synthesizing these conjugates to understand their chemistry that will improve the applicability of antibody-AuNP conjugates in biomedicine.

To this end, this research is aimed at developing a strategy to synthesize highly active, oriented, and stable antibody-AuNP conjugates for immunoassays. The primary objective of this research is to investigate the adsorption dynamics and kinetics of unmodified and chemically modified antibody onto AuNPs.

Antibodies ubiquitously contain lysine residues, which upon reacting with activated esters leads to their acetylation. Chemical modification therefore modifies the charge on lysine residues which results in a change in the total surface charge of the protein. We hypothesize that antibody surface charge will direct its orientation on AuNP and contribute to the synthesis of highly active, stable, and aggregation resistant antibody-AuNP conjugates. Previous findings imply antibodies adsorbs irreversibly onto AuNPs,[19] which removes the requirement of specialized coupling techniques for antibody-AuNP conjugate formation; also, antibody surface charge is known to dictate its orientation on AuNP which can be controlled with pH.[32] Lastly, chemical modification of antibodies alters the surface charge, defining its orientation on AuNP. Our main aim is to develop a universal technique for the synthesis of highly active and stable antibody-AuNP conjugates for AuNP-enabled immunoassays and biomedical applications.

CHAPTER II: PROBING ANTIBODY- AuNP AGGREGATION MECHANISM

Introduction

Gold nanoparticles (AuNPs) have remarkable physicochemical properties and high biocompatibility, and as a result they have been exploited in many emerging biomedical applications,[5,17] including drug delivery, photo-thermal therapy and disease diagnosis.[17,28,33,34] The surface chemistry of AuNPs allows it to adsorb several biomolecules such as protein, nucleic acids and lipids. However, the high surface energy of nanoparticles compared to the bulk metal makes it kinetically and thermodynamically unstable. Although most biomolecules form stable conjugates with AuNPs, an increase in surface energy due to biomolecule adsorption can trigger nanoparticle aggregation. Bovine serum albumin, immunoglobulin G and some other proteins have been shown to form stable conjugates with AuNPs at physiological pH,[35] while lysosomes and other proteins induce AuNP aggregation at physiological pH.[23,36] To this point, it becomes relevant to understand the mechanism by which these aggregations occurs, in other to help improve the utility of AuNP-protein conjugates in a biological setting and avoid *in vivo* detrimental effects. For some proteins, aggregation of AuNP is ascribed to the unfolding of protein upon adsorption followed by destabilization .[37] Also, other scientific evidence suggests that proteins may trigger nanoparticle aggregation by an electrostatic bridging mechanism.[38] For this mechanism, exposed positive charges on proteins act as an electrostatic bridge to crosslink negatively charged AuNPs, e.g., citrate capped AuNPs. Besides, the charge screening effect caused by the displacement of negatively charged citrate by proteins on AuNPs reduces the overall surface charge of the nanoparticles, decreasing the diffusion bilayer; the distance between two AuNPs and electrostatic repulsion between nanoparticles.[36] Diffusion bilayer depletion brings two adjacent AuNPs into proximity where Van der Waals attractive forces predominate

and may trigger the nanoparticle's collapse. Protein surface charge is, therefore, an important parameter to cause nanoparticle aggregation.

Research conducted by Katsuhiko and coworkers[39] established the importance of charged molecules on nanoparticle aggregation. In their work, they adsorbed various small molecules that contain thiols, amines and carboxylates, e.g., urea, cysteine, and glutathione, onto citrate capped AuNPs. Based on their findings, molecules with both amine and thiol functionality seem to facilitate aggregation of the AuNPs. In contrast, thiols and carboxylate containing molecules did not trigger the aggregation of nanoparticles. These results suggest either a possible charge screening of the negatively charged citrate capped AuNPs or bridging of the two AuNPs by amines upon displacement of citrate by the thiol-amine molecules.

The Driskell's lab demonstrated the effectiveness of pH in controlling the orientation of antibodies on AuNPs.[40] The percentage of available antigen-binding sites of antibodies adsorbed onto citrate capped AuNPs increased as a function of decreasing pH.[40] However, we observed aggregation of nanoparticles at pH below 7.5. This observation was attributed to an increase in protein positive charge with decreasing pH, which tends to induce nanoparticle aggregation through any of the mechanisms previously discussed. Protein surface charge is, therefore, an important parameter to consider when synthesizing protein nanoparticle conjugates.

Herein, we have employed several analytical techniques to elucidate which of these mechanisms drives the aggregation of antibody-AuNP conjugates. Knowledge of the aggregation mechanism can help mitigate the effect of a lower pH on nanoparticle aggregation. This will allow the synthesis of highly stable and oriented antibody-AuNP conjugates.

Materials and Methods

Reagents

A 60 nm citrate capped AuNPs at a concentration of 2.6×10^{10} particles/mL was used in all analyses. All antibody studies were performed using a mouse monoclonal anti-horseradish peroxidase IgG (clone 2H11) obtained from My BioSource. Horseradish peroxidase (HRP), 2,2′-azino-bis-(3-ethylbenzothiazoline-6-sulfonic acid) (1-Step ABTS) and potassium cyanide were obtained from Thermo Scientific (Rockford, IL). Phosphate buffers were prepared using anhydrous potassium phosphate dibasic and potassium phosphate monohydrate purchased from Mallinckrodt Chemicals, Inc. (Paris, KY) and Fischer Scientific (Fair Lawn, NJ), respectively. All experiments were performed using Nano pure deionized water from a Barnstead water purification system (Thermo Scientific, Rockford, IL).

Antibody Characterization at Different pHs

A 2 mg/mL mouse anti-HRP antibody solution was prepared from a 4.4 mg/mL commercial purchased stock solution by diluting in a 2 mM phosphate buffer (pH 7.5). This solution was further diluted in 2 mM buffers of different pHs. Resuspension of antibodies were carried out by diluting 50 μL of 2 mg/mL antibody at pH 7.5 to 500 μL with buffers of pH 5, 6, 7, 7.5, 8, and 9. The resulting anti-HRP solutions was concentrated using an Amicon filter (MWC 100 KDa) by centrifugation at 14,000 g for 10 min to an approximate volume of 20 μL. The concentrates were collected following results of the manufacturer's recommendation. The concentration of antibodies resuspended in buffers of different pH was determined by a NanoDrop 2000 (Thermo Scientific). A 90 % recovery was achieved consistently. Recovered antibodies were further diluted to 1 mg/mL and analyzed by DLS hydrodynamic diameter and

zeta potential measurements using a Malvern Zetasizer Nano ZSP. Prior to the DLS measurement, antibodies solutions were filtered using an Anotop 0.02-micron filter.

Antibody-AuNP Synthesis at Different pHs

AuNP-antibody conjugates were synthesized by first centrifuging 100 μL of AuNPs at 5000g for 5 min. Nanoparticle pellets were resuspended in 100 μL of 2 mM phosphate buffer of pH 6, 6.5, 7, 8 and 9. Three micrograms of antibody (200 nM final concentration) was incubated with 100 μL AuNPs at pH 6, 6.5, 7, 7.5, 8 and 9 in a low binding microcentrifuge tube for 3 h with gentle agitation. After incubation, the AuNP-antibody suspension was centrifuged at 5000g for 5 min to remove excess antibodies not adsorbed onto the AuNPs followed by resuspension in buffer of the same pH. The conjugates were further purified by performing the centrifuging/resuspension cycle three times.

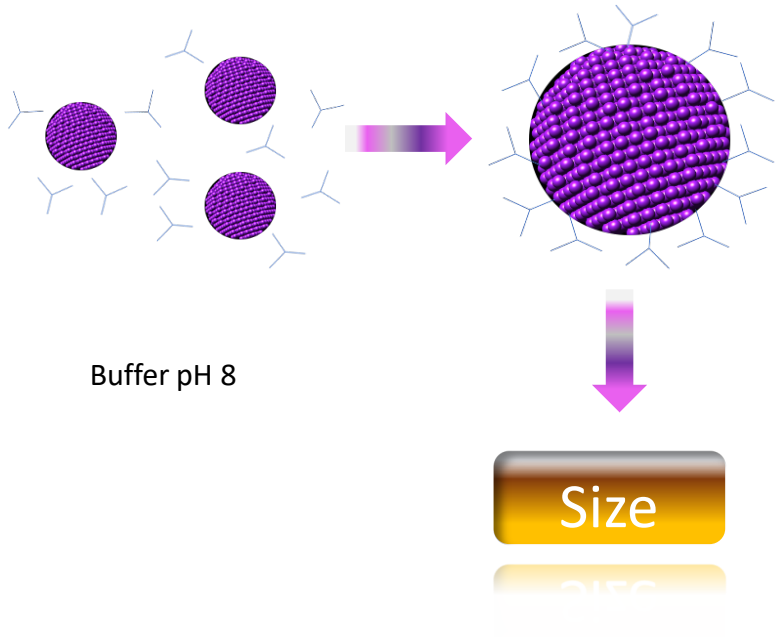

Figure 1. Schematic illustration of conjugate synthesis at a pH 8.0 to form a stable monolayer.

Titration of Antibody-AuNP Conjugates

Stable purified AuNP-antibody conjugate synthesized at pH 8.0 (Figure **1**) was centrifuged

at 5000g for 5 min. The supernatant was discarded whereas the pelleted conjugates were resuspended in a buffer of pH 6 or 6.5 and allowed to stand for 4 and or 24 hours (Figure **2**). The pH of AuNP-antibody suspension resuspended in the various buffer solutions was determined using litmus paper.

Antibody-AuNP Conjugate Unfolding Test

To determine the impact of AuNPs on antibody unfolding which can trigger nanoparticle aggregation, we employed the use of an established immunoassay technique to assess the antigen capture activity of antibodies adsorbed onto AuNPs. 100 μl of purified AuNP-antibody conjugates were incubated with 3 μg of HRP for 1 h. After incubation, excess uncaptured HRP was removed by centrifuging at 5000g for 5 min. The HRP captured conjugates were further washed three times to ensure the removal of all free HRP. Enzymatic activity of HRP captured by the conjugates was determined by the measuring the kinetics of oxidation of ABTS for 20 minutes, in a suspension made up of 10 μl HRP captured conjugates and 150 μl of ABTS using a Bio-Rad microplate reader. A standard HRP calibration was used to extrapolate the concentration of HRP captured by conjugates.

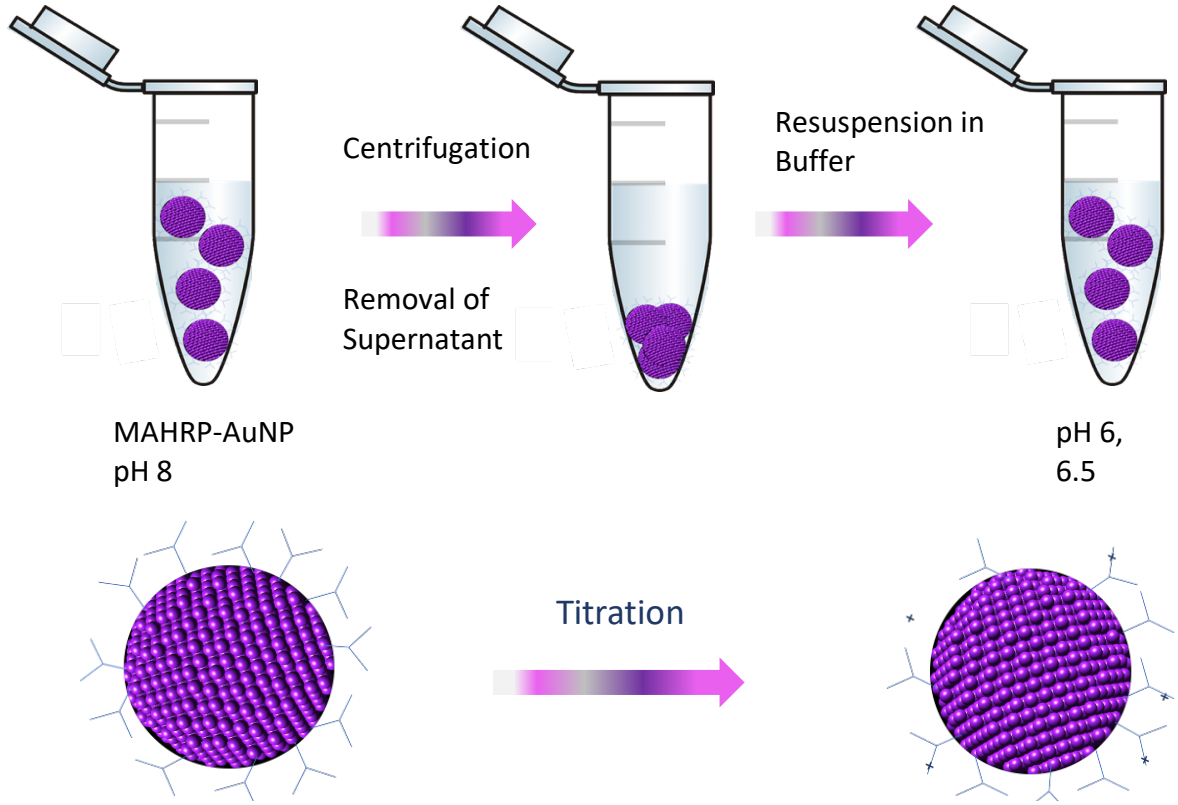

Figure 2. Schematic illustration of titration of conjugates to lower pH.

Antibody-AuNP Characterization and Stability Analysis

UV-VIS characterization. Surface plasmon resonance of AuNP-antibody conjugate was measured to evaluate the stability of the conjugates using a Cary 1 Bio UV−visible dual-beam spectrophotometer with spectral bandwidth of 0.2 nm. For this experiment 80 μL of conjugate was introduced into a microcuvette after which a UV-vis scan was obtained from 350 nm to 900 nm at 0.5 nm increments. An iMark microplate reader (Bio-Rad) was used in collecting absorbance at 415 nm for the HRP enzymatic assay.

DLS sized and zeta potential measurements. A Malvern Zetasizer Nano ZSP operating with non-invasive back scatter optics was used to carry out conjugate size and zeta potential measurements. A folded capillary cuvette was filled with desired buffer followed by careful introduction of 20 μL of conjugate to the bottom of the cuvette by the aid of a capillary pipette

tip. Before size and zeta potential measurements, the conjugates were equilibrated at 25 ^{O}C for 30 s. Conjugates size and zeta potential measurements were performed in triplicate and each measurement consisted of the analysis sequence of size-zeta potential-size. This sequence was adopted to confirm no aggregates were generated during the zeta potential measurement. For each size and zeta potential measurement, fifteen separate runs were averaged.

Results and Discussion

Effect of pH on Antibody Triggered Aggregation of AuNPs

Mukherjee and co-workers[31] reported the time evolution of protein corona on AuNPs using cell lysate and a 20 nm AuNP. They observed a large particle size of about 200 nm during the first 30 min of the incubation whereas a smaller conjugate with a size of 52-73 nm was observed during later times. This observed phenomenon was attributed to the formation of nanoparticle clusters resulting from bridging of protein between exposed sticky ends of AuNPs at the initial stages of the incubation. Although this aggregation is reversible, proteins having enough localized positive charge can strongly crosslink with negatively charged AuNPs to facilitate irreversible aggregation. Cedervall et al[38] analyzed the effect of IgG and fibrinogen concentration on the aggregation of polystyrene nanoparticles. From their results, large aggregates were observed when a low concentration of IgG was added to polystyrene nanoparticles while no or small aggregates were observed at high concentration of IgG. The generation of aggregates at low antibody concentration was ascribed to the bridging of IgG between exposed ends of polystyrene nanoparticles since the nanoparticle surface is not fully coated at low protein concentration. However, upon increasing the concentration of IgG, the nanoparticle surface becomes fully saturated; hence, no exposed nanoparticle surface exists for bridging to occur. Findenegg and co-workers[41] also investigated the effect of pH and electrolyte

concentration on the bridging aggregation of silica nanoparticles with lysozyme. They observed aggregation of silica nanoparticles when pH was less than the isoelectronic point (pI) of lysozymes. This observation was attributed to lysozymes acting as an electrostatic bridge between silica nanoparticles due to an increase in positive surface exposed on lysozyme at a pH below lysozyme's pI. Here we seek to investigate the mechanism and effect of antibody surface charge on AuNP aggregation.

To evaluate the impact of antibody surface charge on AuNP aggregation, we synthesized AuNP-antibody conjugates at pHs ranging from 5.0-8.5. Excess antibodies were incubated with citrate capped AuNPs for 4 h when synthesizing these conjugates (**Figure 1**). The resulting antibody-AuNP conjugates were centrifuged to remove non adsorbed antibodies and its stability was monitored using UV-vis spectrophotometry and dynamic light scattering to measure the surface plasma resonance and the size of antibody-nanoparticle conjugates, respectively.

A

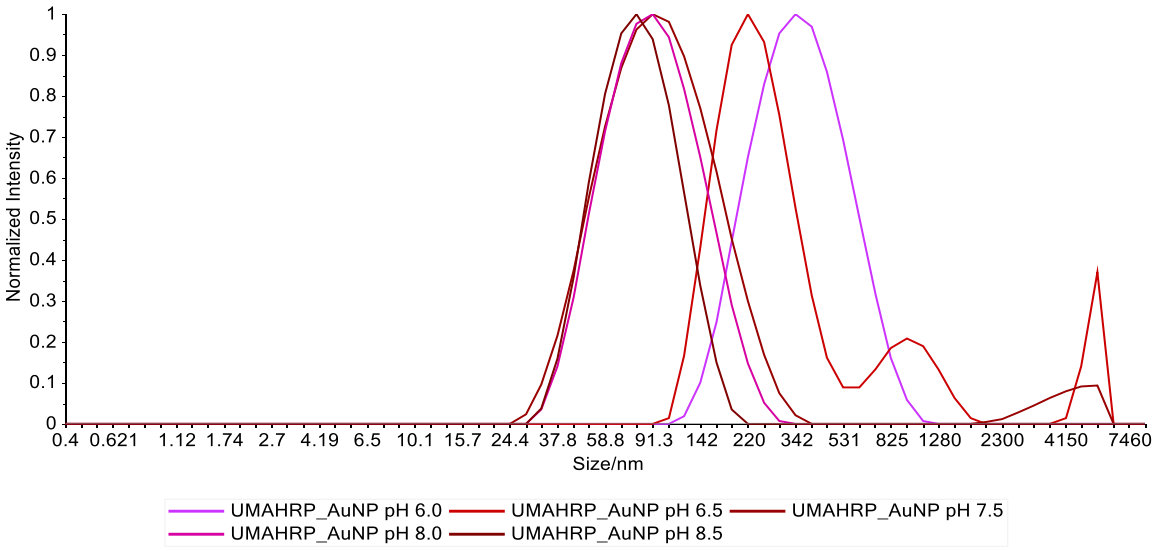

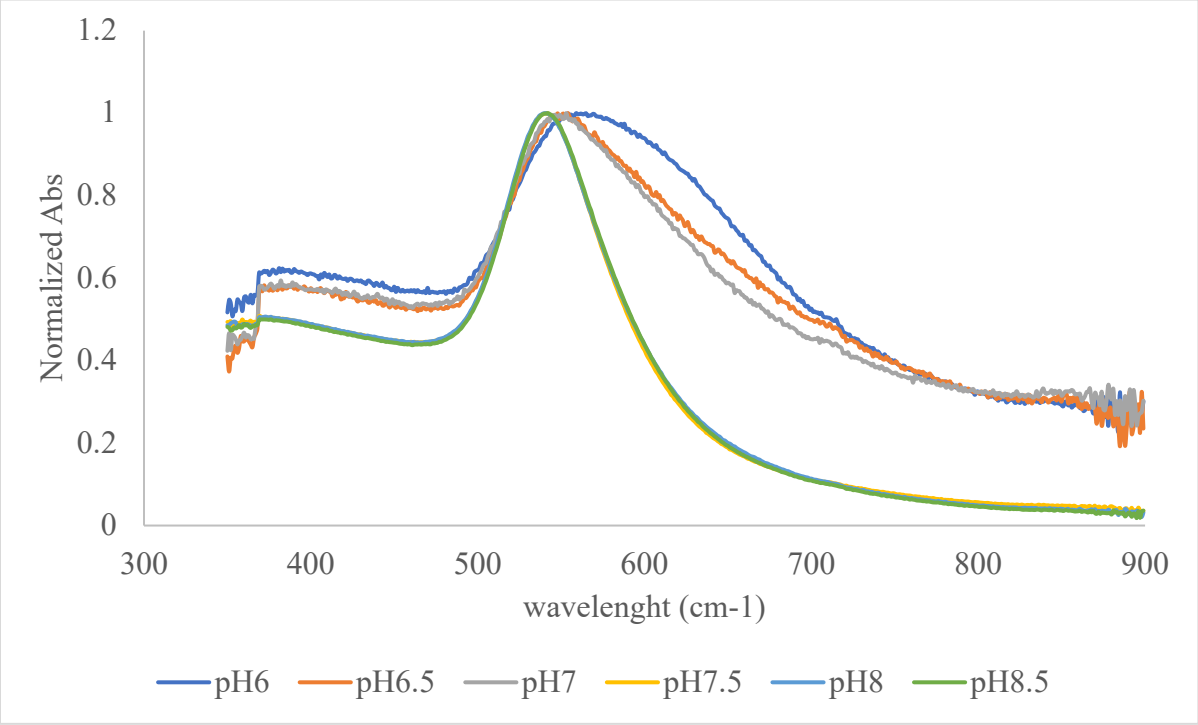

Figure 3. Evaluating the stability of antibody-AuNP conjugates at pH 6.0-8.5.

(A) Size distribution of MAHRP-AuNP conjugates synthesized at pH 6-8.5. (B) UV-visible spectrum of MAHRP-AuNP conjugates synthesized at different pH by adding excess antibodies to AuNP and incubating for 1 h.

A mean hydrodynamic diameter of 87 ± 4 nm was recorded for AuNP-antibody conjugates at pH 7.5 and above, whereas conjugate sizes greater than 200 nm were observed for conjugates synthesized below pH 7.5 (**Figure** 3A). Similarly, a broad and a red shifted SPR band ~ 9 nm was observed for conjugates synthesized below pH 7.5 (**Figure 3B**). In addition, the zeta potential of nanoparticles became less negative upon protein adsorption. These results indicate protein triggered aggregation of AuNPs at pH less than 7.5. We propose that protein surface charge is therefore responsible for causing nanoparticles aggregation, thus, increased positive patches on the surface of antibodies at lower pH may cause nanoparticles to aggregate.

Overview of Nanoparticle Stability and Aggregation Mechanism

Nanoparticles in close proximity may interact with each other through short-range van der Waals forces leading to the formation of clusters or aggregates.[42,43] The aggregation of these particles is both kinetically and thermodynamically controlled. While these theories can be efficiently used to explain the stability of many colloidal particles, it also provides significant insight on nanoparticle stability with extended modification.[44] For the kinetic model, nanoparticles must collide inelastically to promote aggregation. The collision rate depends on the root mean velocity, the number density of nanoparticles, temperature, and the energetics (repulsive and attractive forces) of the particles. Thermodynamically controlled aggregation of AuNPs is mostly explained using Derjaguin–Landau–Verwey–Overbeek (DLVO) theory, which calculates the total interaction potential between two particles as a function of their radius of curvature and the distance between them.[42] Electrostatic repulsive forces and van der Waals attractive forces are assumed to be the most predominant interactions that exist between these particles in the DVLO theory. One of these two interactions is more significant, depending on the distance between the particles. Thus, electrostatic repulsive forces that depend on the Debye length predominate at a longer distance, whereas van der Waals attractive forces predominate at a certain shorter distance. Nanoparticle Zeta potential directly correlates with the Debye length and it is mostly employed in calculating the surface potential in DVLO theory, hence can be used to predict the nanoparticle stability threshold.

Additionally, steric interactions, osmotic potential resulting from competition between solvent molecules to solvate proteins on AuNPs within a distance lower than two times the monolayer thickness of protein,[45,46] and elastic interaction between proteins at a distance less than the monolayer thickness of proteins, also play a critical role in the stability of the protein

functionalized nanoparticle. From these theories, you can predict the experimental requirement needed to maintain nanoparticle stability in solution. Consequently, in this chapter we seek to use the above theories to explain our experimental results in order to establish the mechanism by which protein induces nanoparticle aggregation.

Several mechanisms have been proposed for protein-induced nanoparticle aggregation using kinetic and thermodynamic models.[26,37–39,43,47] Among these mechanisms, electrostatic bridging, van der Waals attraction of nanoparticles resulting from surface charge depletion upon protein adsorption,[26,42] and protein unfolding [3623,37,48]are the most discussed. The aggregation of AuNPs by antibodies may proceed either through the bridging of localized positively charged surface of antibodies with negatively charged citrate capped AuNPs, by the reduction of AuNPs surface charge when citrates are displaced by antibodies or by the hydrophobic interaction between unfolded proteins on nanoparticles.

pH Effect on Antibody Surface Charge

Immunoglobulin G (IgG), the most abundant antibody in serum of vertebrates, is a globular glycoprotein with a molecular weight of about 150 kDa produced by plasma B cells. It is made up several amino acids, including basic amino acids such as arginine, lysine, and histidine.[52] Most of these basic amino acids are relatively solvent accessible; hence their side chains can be easily protonated or deprotonated depending on the pH of a solution. The surface charge of IgG can, therefore, be substantially altered by pH, as protonation of these amino acids creates positive charges, which results in positive patches on the surface of the protein.

Initially, to affirm our hypothesis of the impact of pH on antibody surface charge, we conducted a computational simulation of IgG (PDB-ID 1IGT) surface charge with an online molecular dynamics platform using adaptive poison Boltzmann solver (APBS) (http://nbcr-

222.ucsd.edu/pdb2pqr/).[49,51] As shown in **Figure 4,** with red and blue indicating regions of negative and positive charges, respectively, pH has a significant impact on IgG surface charge.

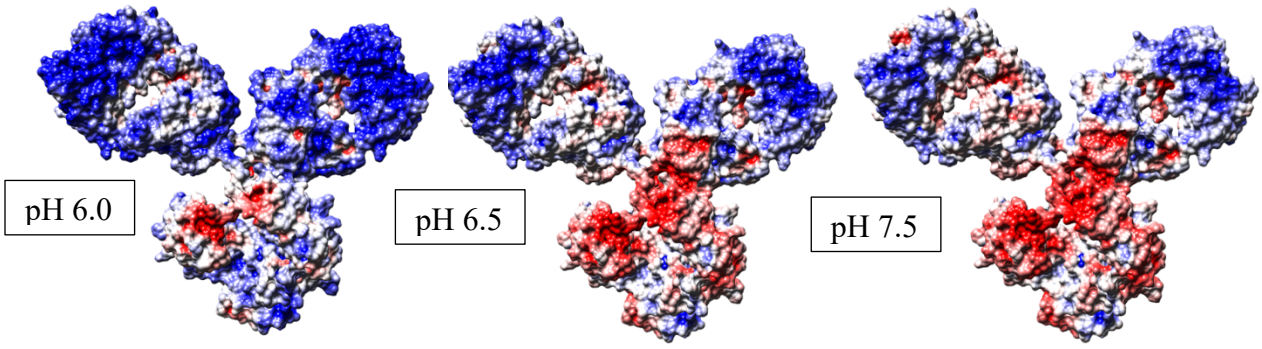

Figure 4. Computational simulation of mouse IgG 2a antibody surface charge at four different pHs. Blue and red regions represent positive and negative potential, respectively, in a range of −5 kbT/e to + 5 kbT/e. The calculations were performed online using Adaptive Poison Boltzmann Solver (APBS). http://nbcr-222.ucsd. edu/pdb2pqr/.[49–51]

The effect of pH on IgG surface charge was evaluated experimentally to examine our hypothesis. In this experiment, a mouse monoclonal anti-HRP (MAHRP) IgG was suspended in buffers of pH 5, 7, 8 and 9. The zeta potential, as well as the size of IgG, were measured using a Zetasizer Nano ZSP (Malvern instruments). We recorded a decrease in the negative zeta potential of MAHRP as the pH decreases. Thus, zeta potentials of -13.68, -9.39, -6.67 and, -0.21 mV were recorded at pH 9, 8, 7 and 5, respectively. Additionally, there was no significant change in protein size at different pHs (**Table 1**). These results indicate a significant alteration of IgG surface charge by solution pH whilst maintaining antibody integrity. Moreover, there was no

significant change of protein size before and after zeta potential measurement as shown in **Table 1**, confirming no aggregation of proteins during the zeta potential measurement.

Table 1. DLS size and zeta potential of anti-HRP antibody (MAHRP) at different pHs.

pH (2 mM /0.3% NaCl)	**Average Size Before Zeta (nm)**	**Average Zeta Potential (mV)**	**Average Size After Zeta (nm)**
5	14.65	-0.21	13.31
7	13.80	-6.67	12.95
8	16.32	-9.39	17.00
9	14.73	-13.63	14.11

Effect of Antibody Unfolding on Nanoparticle Aggregation

The unfolding of proteins upon adsorption onto nanoparticles has also been proposed as one of the mechanisms that can drive nanoparticle aggregation. Link et al. recently reported that, BSA induced the aggregation of nanoparticles by a BSA-BSA interaction; thus, unfolding of BSA upon adsorption to nanoparticles exposed hydrophobic surface that can interact with other exposed BSA hydrophobic sites leading to nanoparticle aggregation. To this end, we probed the effect of antibody unfolding on nanoparticle aggregation by measuring its antigen binding activity, hypothesizing that the antigen binding capabilities of antibodies will be lost if the antibody unfolds. Here, stable purified AuNP-mouse anti-HRP conjugates resuspended in buffer of pH 6, 6.5, and 8 for 24 h were incubated with HRP for an hour and the enzymatic activity of HRP captured by AuNP-mouse anti-HRP conjugates was analyzed by an ABTS HRP assay.

From the enzymatic rates measured, (**Figure 5**) MAHRP-antibody adsorbed onto AuNPs was still active for antigen capture. This result suggests no drastic unfolding of antibodies adsorbed onto AuNPs that can trigger nanoparticle aggregation.

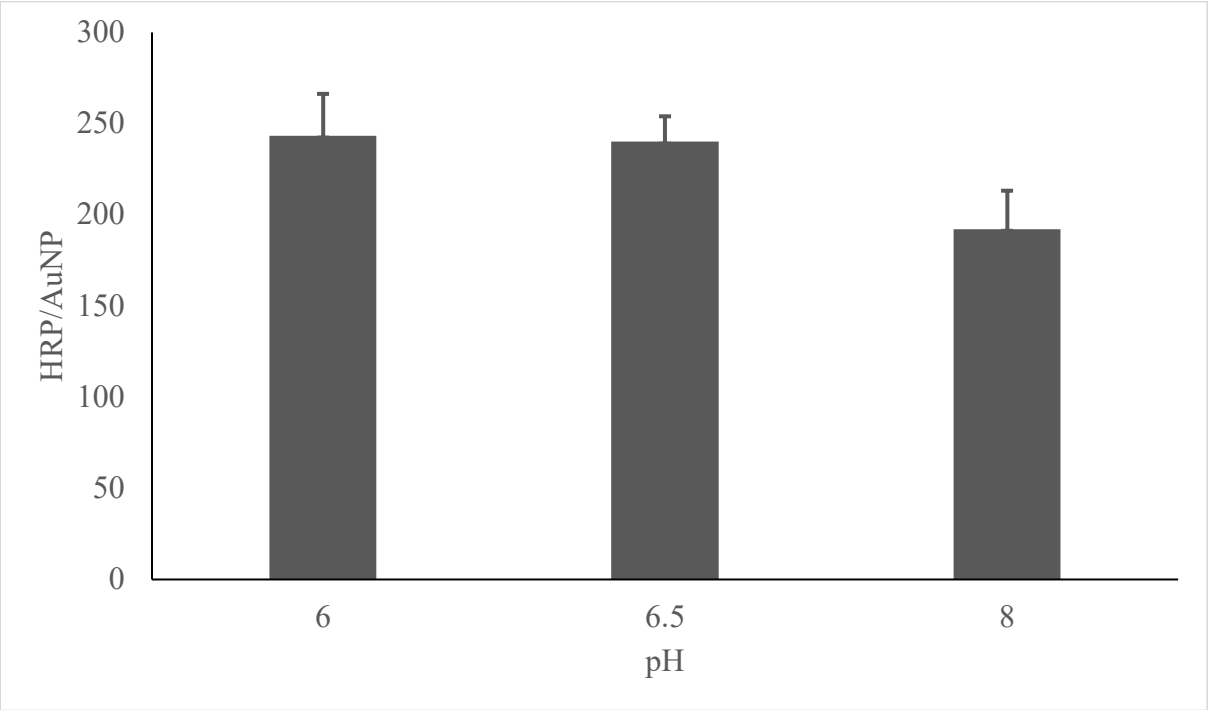

Figure 5. Quantitation of antigen binding activity of conjugates after resuspension into buffer of pH 6, 6.5 and 8. MAHRP-AuNP conjugate synthesized at pH 8 is resuspended in buffer of pH 6, 6.5 and 8.5 for 24 hours.

Buffer Exchange of Stable Antibody-AuNPs to Lower pH

In order to establish the mechanism by which antibody surface charge induces nanoparticle aggregation, a stable conjugate synthesized at pH 8.0 was titrated to lower pH by resuspension in buffer of pH 6 and 6.5 for four and twenty-four hours, after which the size (**Figure 6**), surface plasmon resonance (**Figure 7A and 7B**) and zeta potential (**Figure 7C)** of the conjugates were measured. Titration to lower pH was conducted to alter the adsorbed protein

surface charge, which, in effect, decreases the overall negative charge of the conjugates. We anticipated that if the mechanism of protein triggered aggregation proceeds by the reduction of the surface charge of nanoparticles, which may reduce the diffusion bilayer layer, then the nanoparticles are expected to aggregate upon titration to lower pH.

A

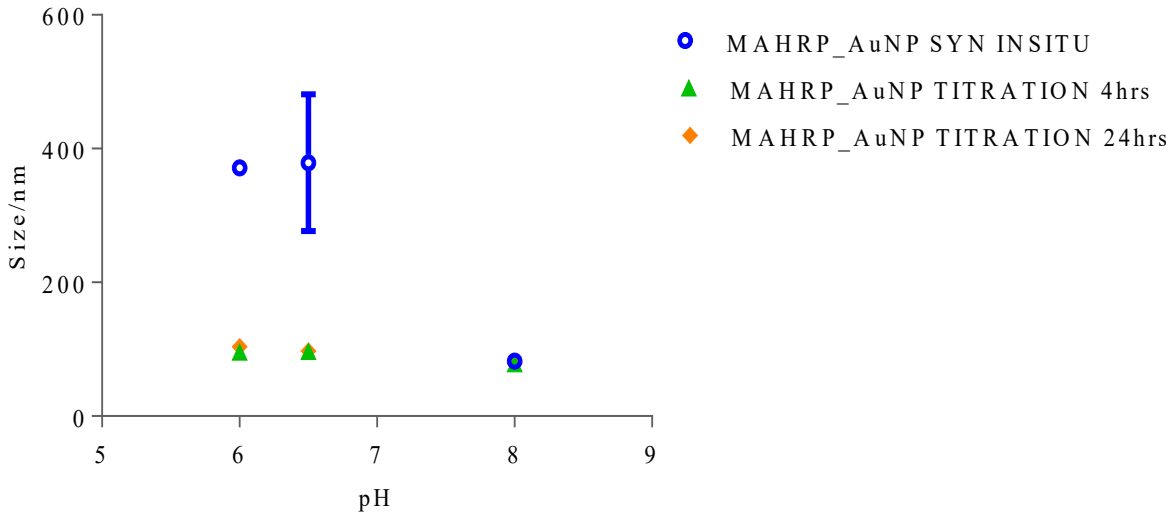

B

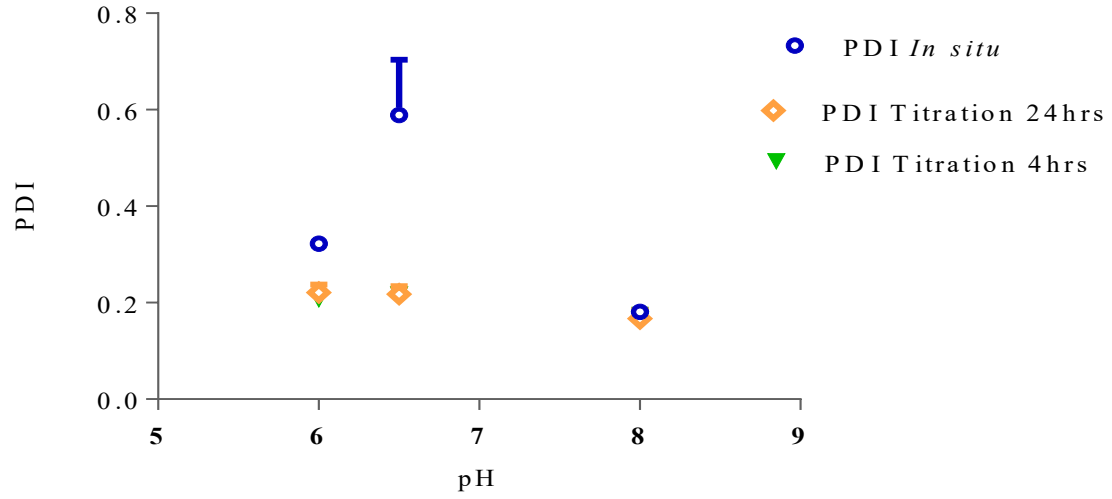

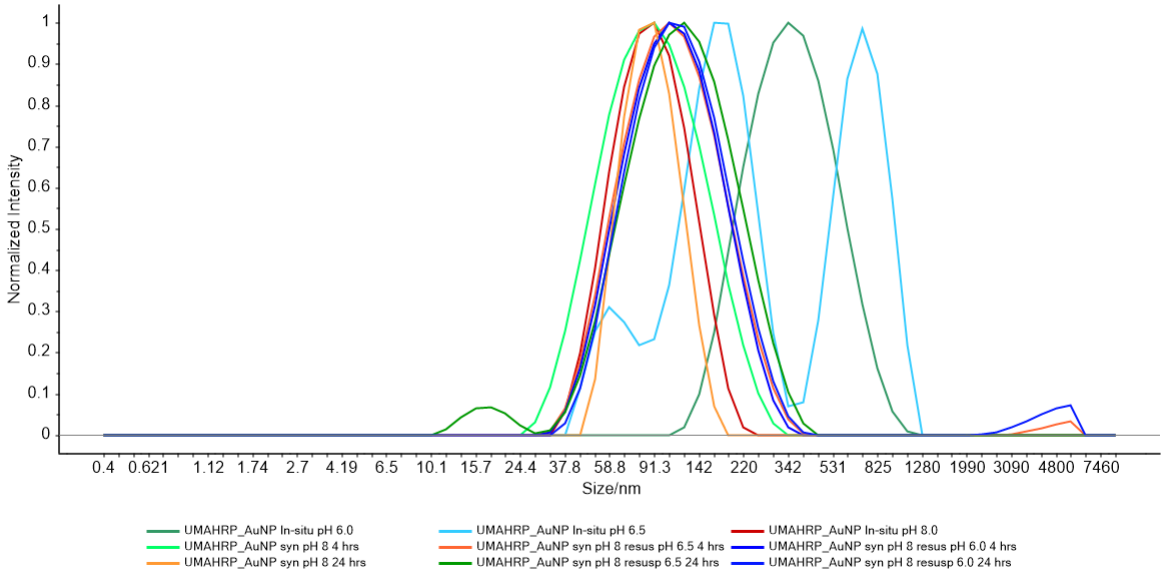

Figure 6. Size and particle distribution of MAHRP-AuNP conjugates synthesize at pH 6.0-8.5 *in situ* and stable conjuagtes titrated to pH 6.0-8.0. (A) Size of conjugates in nm for *in situ* synthesis and titrations. (B) Polydispersity Index (PDI) of *in situ* and titration conjugates. (C) DLS size.

However, there was no change in the size (Figures 6) and surface plasmon resonance (Figures 7A and 7B) even after the conjugates was resuspended in buffer of pH 6 and 6.5 for 24 hours. The results therefore, indicate no aggregates was formed after titration to lower pH.

Additionally, the results suggest reduction of the total nanoparticle surface charge by adsorbed antibodies or proteins is not the prevalent mechanism that causes nanoparticles to aggregate. Meanwhile, aggregates are also observed when excess antibodies are incubated with AuNPs at lower pH. Furthermore, when stable conjugates synthesized at pH 8.0 are resuspended in a lower pH buffer the overall negative potential on the conjugates is expected to decrease as more ionizable side chains are protonated. However, no significant change in zeta potential was

A

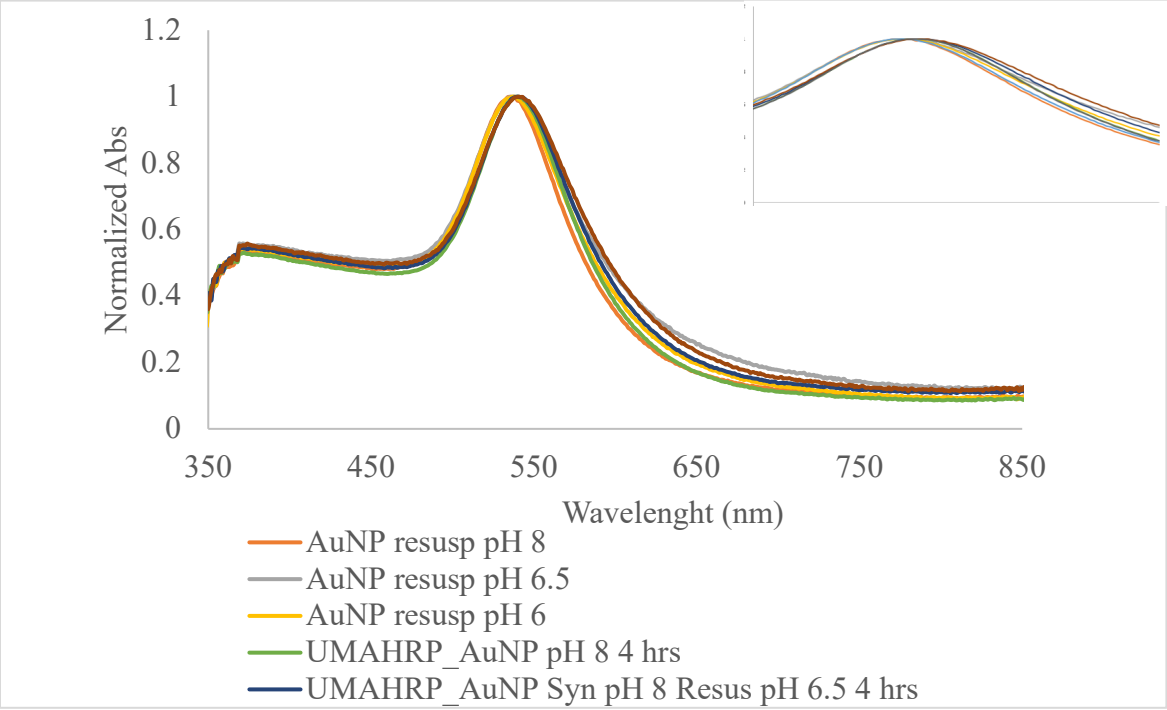
1.2
1
0.8
0.6
0.4
0.2
0
Normalized Abs
350
450
550
650
750
850
Wavelenght (nm)
AuNP resusp pH 8
AuNP resusp pH 6.5
AuNP resusp pH 6
UMAHRP_AuNP pH 8 4 hrs
UMAHRP_AuNP Syn pH 8 Resus pH 6.5 4 hrs

B

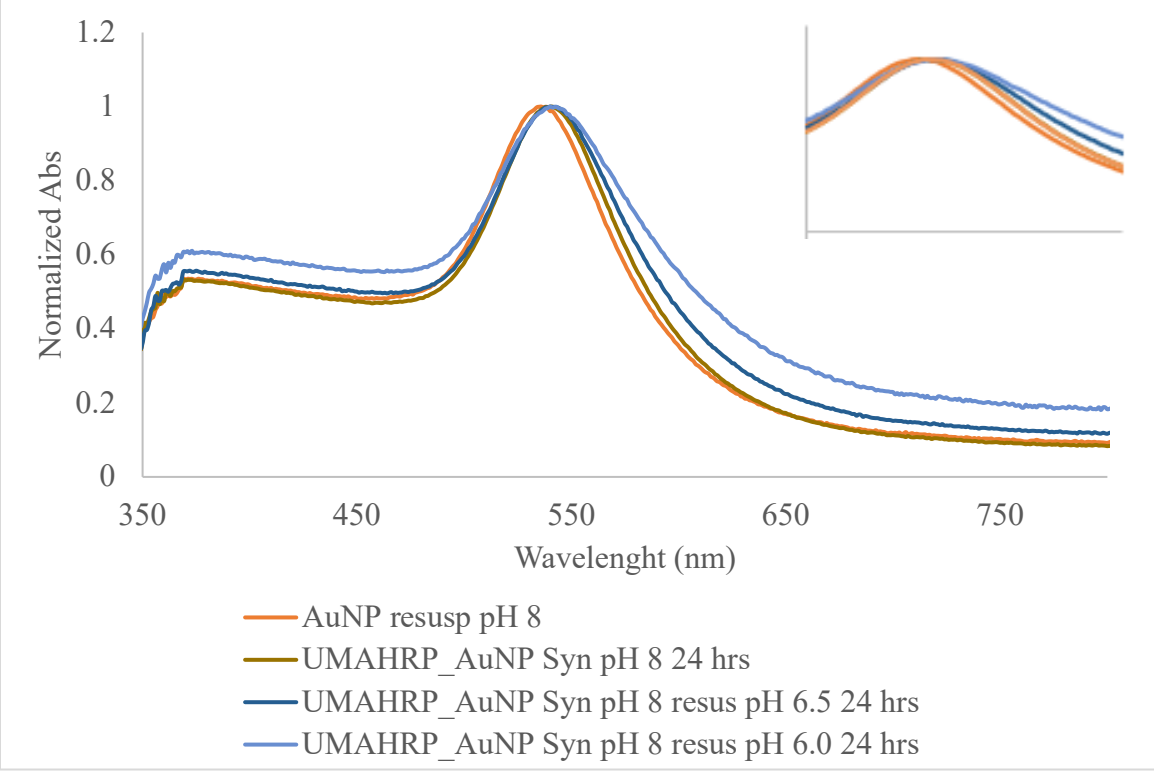
1.2
1
0.8
0.6
0.4
0.2
0
Normalized Abs
350
450
550
650
750
Wavelenght (nm)
AuNP resusp pH 8
UMAHRP_AuNP Syn pH 8 24 hrs
UMAHRP_AuNP Syn pH 8 resus pH 6.5 24 hrs
UMAHRP_AuNP Syn pH 8 resus pH 6.0 24 hrs

C

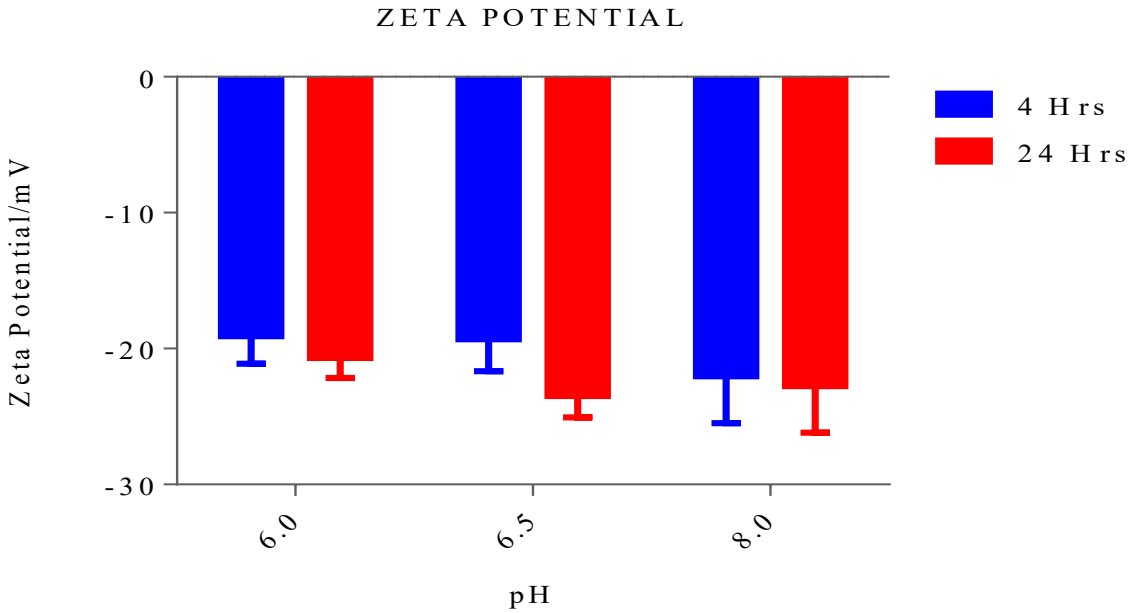

Figure 7. Surface plasmon resonance and Zeta potential of conjugates after titration into buffer of pH 6.0 and 6.5. (A) UV-visible spectra of MAHRP-AuNP conjuagtes synthesized at pH 8.0 and resuspended in buffer of pH 5.0-6.5 for 4 hours. (B) UV-visible spectra of MAHRP-AuNP conjuagtes synthesized at pH 8.0 and resuspended in buffer of pH 5.0-6.5 for 24 hours. (C) Zeta potential of conjugates after resupesnion in buffer pH 6.0 , 6.5 and 8.0 for 4 and 24 hours.

observed for our conjugates **(Figure 7C**). From these results, we inferred that, as the diffusion bilayer decreases upon resuspension of conjugates in a buffer of lower pH, steric interactions, including osmotic potential becomes significant at a distance less than twice the monolayer thickness.[44,47] These repulsive forces from adsorbed proteins contribute to the overall surface potential, which causes resistance to the collapse of diffusion bilayer and prevents the nanoparticle from aggregating. Additionally, the nanoparticle surface is fully saturated when incubated with excess antibody at pH 8.0, hence, there is no exposed surface for an antibody

with sufficient positive charge to act as an electrostatic bridge when resuspended at lower pH. These observations suggest AuNP aggregation at lower pH is a result of electrostatic bridging by antibodies.

Effects of Titration with NaOH on Reversibility of Aggregates

As discussed above, incubation of excess antibodies with citrate capped AuNPs at pH less than 7.5 triggers aggregation of the nanoparticles. To probe the reversibility of these aggregates over time, excess antibodies were added to 100 ml of AuNPs at pH 6.0 and 6.5 and the size of the aggregates was monitored after 5 min, 30 min, 5 h, and 24 h. As seen in **Figure 8**, large aggregates of nanoparticles were observed for all time points. The persistence of these aggregates over a period of 24 hours implies no propensity toward reversibility. However, upon addition of 0.1 M NaOH the color and size of the nanoparticles incubated with antibodies reversed to a normal stable conjugate size and color for samples incubated from 5 min to 5 h. A significant amount of aggregates was still present for the 24 hours incubation even after the addition of 0.1 M NaOH. From these observations we inferred that, aggregates are observed as a result of electrostatic bridging of positive patches on antibodies as pH decreases to negatively charged AuNPs for the first 5 hours since the change in antibody surface charge by the addition of NaOH leads to the reversibility of the aggregates. Nonetheless when these aggregates are allowed to stay for 24 hours van der Waals attraction between adjacent AuNPs held together by antibodies now overtake the electrostatic bridging hence the protein surface charge has no effect on the aggregate formation.

Reducing Antibody Positive Charge through Chemical Modification Allows Synthesis of Conjugates at Lower pH

The total surface charge of proteins is determined by the number and identity of ionizable side chains of its amino acids. Primary amines of lysine residues are mostly protonated at and below physiological pH, which increases the total positive charge on the protein surface. When these lysine residues are acroleinated, they lose the potential to possess a positive charge even at acidic pH. Mouse anti-HRP antibody was reacted with excess acrylic acid N-hydroxy succinimide (NHS) to acroleinate most solvent-accessible lysine residues. The extent of the antibody surface charge alteration upon chemical modification was monitored by measuring the antibody zeta potential before and after the chemical modification. The zeta potential of antibody decreased from -7.85 mV to -17.13 mV after chemical modification.

A

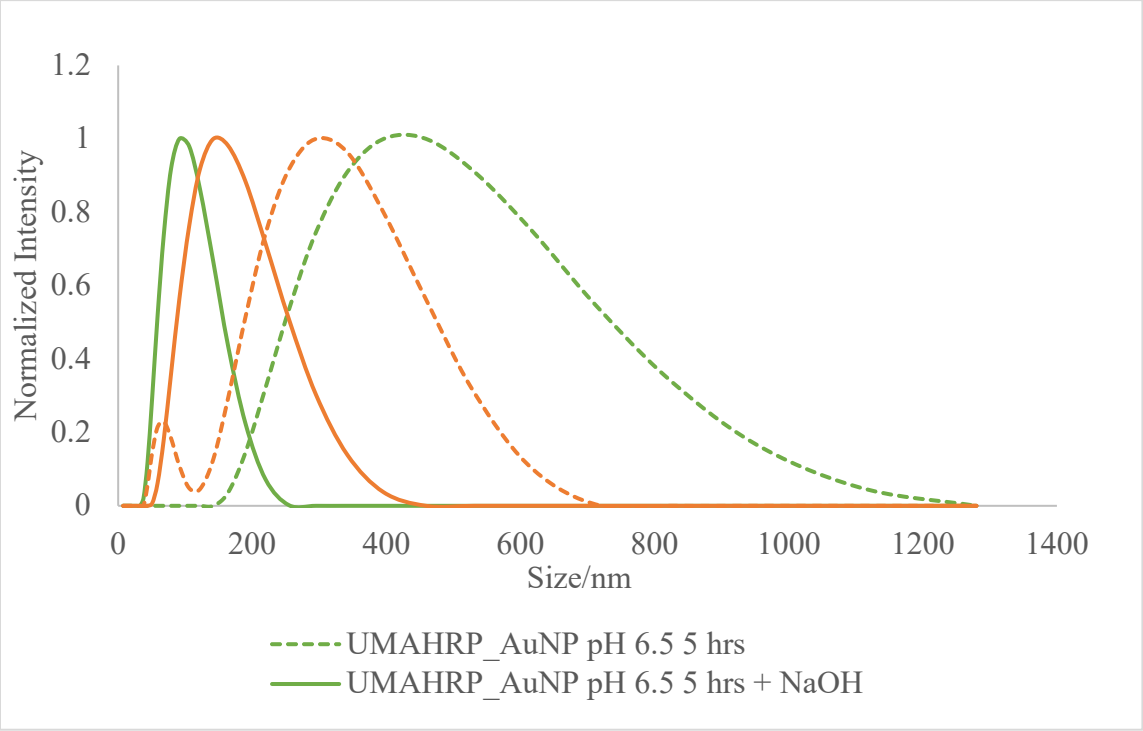

B

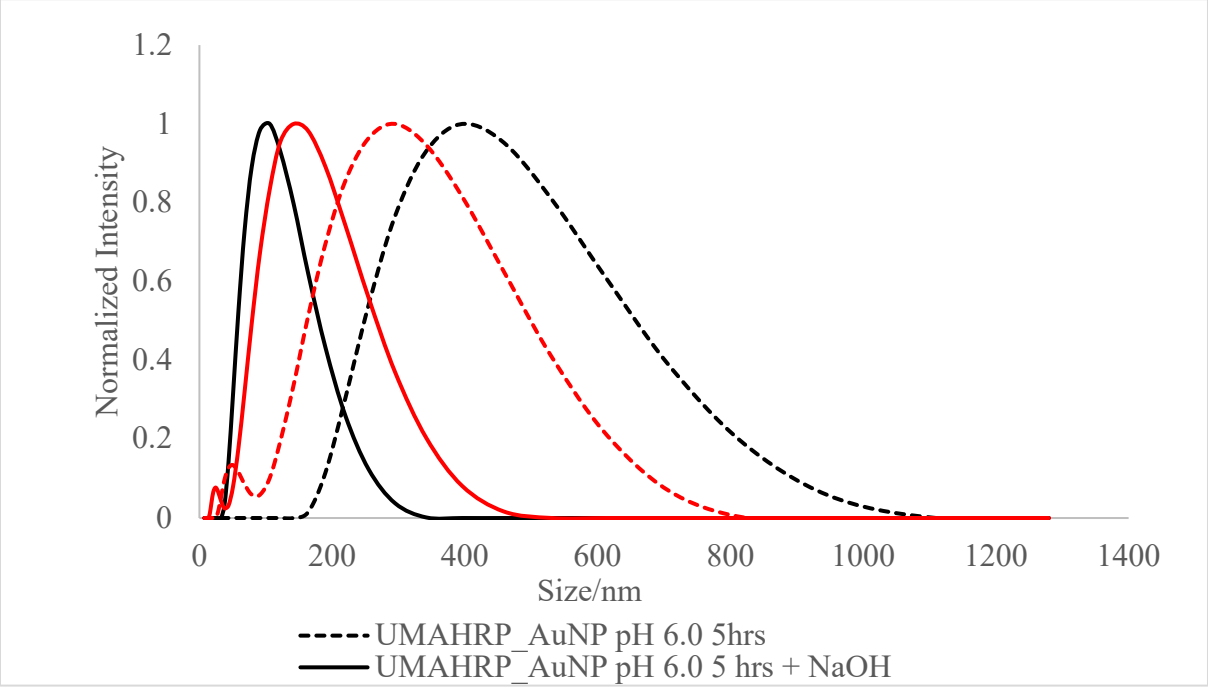

Figure 8. Reversibility of aggregation by addition of NaOH. (A) DLS Size distribution of conjugates synthesized at pH 6.0 (*in situ*) for 4 and 24 hours and titrated to higher pH by addition of 0.1 M NaOH. (B) DLS size distribution of conjugates incubated at pH 6.5 (*in situ*) for 4 and 24 hours. Dash lines represent size distribution of antibody-AuNP conjugates after addition of 0.1M NaOH.

UV-Vis analysis of AuNP antibody conjugates synthesized by incubating excess chemically modified antibodies with AuNPs revealed that the conjugates were stable at pH less than 7.5 (**Figure 9**). This result suggests that the protein surface charge controls the stability of AuNPs in solution. Moreover, the ability to synthesize stable AuNP antibody conjugates at lower pH after knocking out some of the positive charges on antibody suggests electrostatic bridging of

antibodies to citrate capped AuNPs to be the predominant interaction initiating the irreversible aggregation of AuNPs.

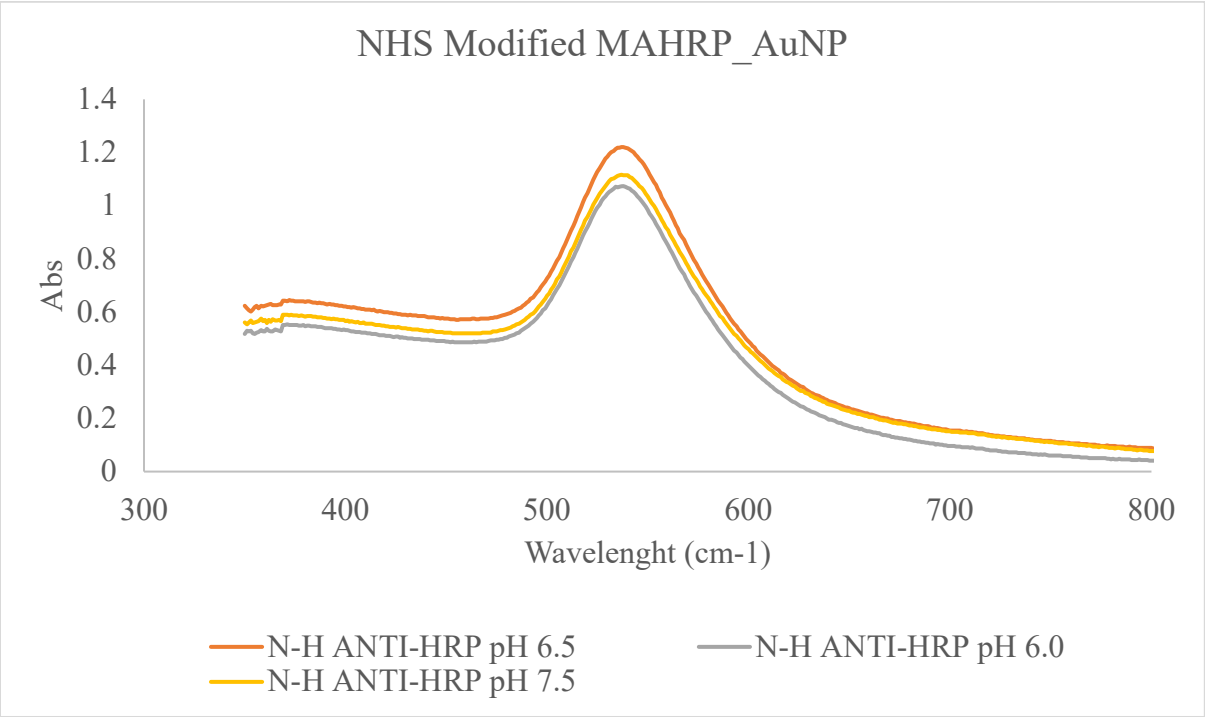

Figure 9. Surface plasmon resonance of acrylic acid NHS chemically modified MAHRP-AuNP conjugate synthesized in situ at pH 6.0, 6.5 and 7.5.

Conclusion

In summary, this study provides insight into the mechanism responsible for antibody induced AuNP aggregation. By using two different approaches to generate AuNP-antibody conjugates at different pH levels, we have proven the effect of protein (antibody) surface charge on AuNP stability. Several mechanisms have been proposed for protein triggered nanoparticle aggregation, here we confirm electrostatic bridging to be the prevalent mechanism by which antibodies induce AuNP aggregation at pH below 7.5. Also, we reaffirm steric interactions as one of the potentials contributing to the stability of protein functionalized AuNPs as proposed by

several theoretical models.[44–46] These findings support our hypothesis that pH plays a critical role in solution phase AuNP-antibody conjugate synthesis.

CHAPTER III: HIGH AFFINITY POINT OF INTERACTION ON ANTIBODY ALLOWS SYNTHESIS OF STABLE AND HIGHLY FUNCTIONAL ANTIBODY-AuNP CONJUGATES

Introduction

Enzyme-linked immunoassays (ELISAs), fluoroimmunoassays, and radioimmunoassays, have thoroughly been exploited for the detection of various disease biomarkers and infectious agents.[4,53,54] Although these assays are quite efficient, they require highly skilled personnel, specialized laboratories, long experiment times, and sometimes hazardous radiolabels. These limitations restrict the use of these assays for high throughput screening and point of care diagnosis. Recently various laboratories have employed AuNPs as sensing agents and heterogeneous labels for immunoassays[17,55] due to their unique optical and surface properties[56]. When incorporating AuNPs into immunoassays, the antibody or protein of interest must first be conjugated to the AuNPs. Various immobilization techniques, including covalent immobilization of antibody onto AuNP, direct antibody immobilization, and directionally oriented immobilization,[12,16,54,57,14,58] have been used to conjugate antibodies and other proteins onto AuNPs. Even though these conjugation techniques are promising, they present several challenges; including randomized orientation of bound targets, inefficient immobilization, aggregation, and sometimes protein unfolding.

Recently, our lab determined the effect of pH on the orientation of mouse monoclonal anti-horseradish peroxidase (MAHRP) antibody on citrate capped AuNPs. From our findings, the amount of available antigen-binding sites of antibodies on AuNPs increases with decreasing pH of the antibody-AuNP conjugation solution.[40] Thus, more antibodies were oriented correctly as the pH decreases. Our results suggest that lower pH improves the orientation of antibodies on

AuNPs; meanwhile, aggregation of AuNPs was observed below pH 7.5. In order to access lower pHs and improve antibody orientation, we have elucidated the mechanism by which this aggregation occurs at lower pH. Electrostatic bridging of antibodies to citrate capped AuNPs resulting from increased positive charged patches on antibody surface at acidic pH was determined to be the predominant pathway through which antibodies trigger AuNP aggregation. In summary, we have established that antibody surface charge is a critical parameter that controls both orientation and stability of antibody-AuNP conjugates.

Antibodies ubiquitously contains lysine residues, which contribute to its total surface charge depending on the pH of the solution. For example, almost all solvent accessible lysine residues are protonated and, therefore, positively charged at a pH below 7.0. Chemical modification of antibodies through reaction with lysine residues can, therefore, help mitigate charge effects that cause nanoparticle aggregation and enable the synthesis of highly oriented conjugates at lower pH. To this end, we have employed various chemical modifications to antibodies to help reduce the extent of positive charge, increase the points of interaction, and enhance conjugate stability.

Electrostatic interaction between proteins and nanoparticles is established as the initial driving force that facilitates the conjugation of proteins to AuNPs.[59,58,60] As these proteins and nanoparticle come into close proximity, cysteine residues interacts with AuNPs to form a Au-S bond.[18,35,61] Whereas free thiol is well established to form a stable covalent bond with AuNPs, amines have also been reported as a ligand for gold.[21,55] Here, we have employed several chemical modifications to lysine residues of antibodies to help identify and establish the chemical interactions that enable irreversible conjugation of antibodies to AuNPs. The kinetics of antibody corona formation (soft and hard) of both unmodified (native mouse anti-HRP)

antibody and chemically modified antibodies were also investigated using dynamic light scattering (DLS). We forecast that the identification of essential functionalities on proteins that interact with AuNPs will enable the synthesis of highly stable and orientated protein functionalized AuNPs.

Materials and Methods

Reagents

A 60 nm AuNP (Ted Pella Inc., Redding, CA) was employed in all studies. Mouse monoclonal anti-HRP IgG antibody (Clone 2H11) was obtained from My BioSource. ABTS (1-step ABTS), HRP, and dithiobissuccinimidyl propionate (DSP) were purchased from Thermo Scientific (Rockford, IL). ThermoFisher Scientific CBQCA protein quantification kits were used for antibody fluorescence assay validation. Phosphate buffers were prepared using anhydrous potassium phosphate dibasic and potassium phosphate monohydrate obtained from Mallinckrodt Chemicals, Inc. (Paris, KY) and Fischer Scientific (Fair Lawn, NJ), respectively. Acrylic acid N-hydroxysuccinimide ester (NHS-acrylic acid) and Amicon ultracentrifugal filter (MWCO 100 kDa) was acquired from Sigma-Aldrich (St Louis, MO).

Computational Simulation of Antibody Surface Charge

Adaptive Poison Boltzmann Solver (APBS) was used to calculate the surface charge of unmodified and lysine modified antibodies. Acetylated amines were parametrized using a cGenFF forcefield. The PDB file (PDB-ID 1IGT) obtained from RSCB Protein Data Bank (https://www.rcsb.org/) was converted to PQR using a PDB2PQR webserver (http://server.poissonboltzmann.org/). The conversion of PDB to PQR replaces the occupancy column and temperature factor in PDB with atomic charge (Q) and radius (R), respectively. Also, PDB2PQR adds all missing hydrogen and heavy atoms and assigns coordinate values to

them. All amino acid residues were parameterized using a CHARM forcefield. PROPKA was used to assign protonation states of ionizable groups at a particular pH.

Antibody Chemical Modification and Characterization

Activated ester acrylic acid N-hydroxy succinimide (NHS) and dithiobis(succimidyl propionate) (DSP) were used as antibody chemical modifiers. Two μL of 50 mM DSP reduced and acrylic acid NHS were added to 50 μg of mouse anti-HRP (MAHRP) antibody in separate reaction vials. The chemical modifier antibody solution reacted for 2 hours at room temperature with gentle shaking. Excess unreacted chemical modifiers were removed by the use of an Amicon Ultra Centrifuging filters (MWCO 100 kDa). Five hundred microliters of 2 mM phosphate buffer pH 7.5 was used to rinse out glycerol on the filter membrane by centrifuging at 10000 g for 5 minutes. The antibody chemical modifier reaction mixture was diluted to 500 µL and centrifuged at 14000 g for 12 minutes. The reverse spin capabilities of filter allowed it to be turned upside and centrifuged at 1000 g for 3 minutes to decant modified antibodies.
A NanoDrop 2000C spectrophotometer (Thermo Scientific, Rockford, IL) was used to measure the concentration of modified antibodies. The extent of chemical modification was monitored by measuring the zeta potential of the antibody before and after chemical modification using a Zetasizer Nano (Malvern Instruments).

Equilibrium dialysis and an HRP enzymatic assay were used to evaluate the antigen binding potential of chemically modified antibodies. Fifty microliters of 1.0 mg/mL (6.7 nM) of chemically modified, unmodified antibodies and mouse IgG isotype control was loaded into one chamber of the equilibrium dialysis tube (MWCO 100 kDa). The other chamber was filled with 0.45 µg/mL (9.9 nM) of HRP and allowed to equilibrate for three hours. After equilibration,

30μL of solution from the chamber originally filled with HRP was withdrawn and subjected to HRP/ABTS enzymatic assay.

Antibody-AuNP Synthesis

One hundred μL of 60 nm AuNPs were pelleted by centrifuging at 5000 g for 5 minutes. The pelleted AuNPs were resuspended in 100 μL of buffer of required pH after which 3 ug of desired antibody (chemically modified or unmodified) were added. For full protein saturation on AuNP, unmodified and DSP modified antibodies were incubated with AuNPs at room temperature for an hour while NHS modified antibodies were allowed to react with AuNPs for 24 hours.

Kinetic of Antibody Adsorption onto AuNPs

To study the time evolution of antibody corona on AuNPs, 3 mg of desired antibody (chemically modified or unmodified) were added to 100 μL of AuNPs in a low binding centrifuge tube and incubated for 1, 3, 6, 12, and 24 h. The size and zeta potential of the conjugates were measured *in situ*, thus without centrifugation. The conjugates were centrifuged at 5000 g for five minutes and the supernatant was discarded followed by resuspension in buffer of desired pH. The centrifugation/resuspension cycle was carried out three times to ensure the removal of any non-adsorbed antibody. The size and zeta potential of antibody-AuNPs synthesized at each time point were measured after purification.

Quantifying the Number of Antibodies bound Per AuNP

A native protein fluorescence assay was used to quantify the number of proteins adsorbed onto AuNP. Antibody-AuNP conjugates were purified to remove excess antibodies in solution by centrifuging at 5000 g for 5 minutes, the supernatant was removed by carefully pipetting the clear solution from the pellets. Pelleted antibody-AuNPs were resuspended in buffer of desired

pH and centrifuged at 5000 g for 5 minutes followed by decantation of supernatant. Three cycles of centrifugation/resuspension were carried out to certify the removal of any non-adsorbed antibody. To digest the gold and release antibodies into solution for easy protein quantification, 10 µL of 100 mM potassium cyanide was added to the pelleted antibody-AuNP conjugates. The reaction mixture was diluted to 110 μL with a 2 mM phosphate buffer (pH 7.5) after 2 hours of reaction at room temperature. Standard solutions of chemically modified and unmodified anti-HRP antibody (0-5 mg/mL) were prepared in a digested AuNP solution containing the same concentration of AuNP and KCN as in antibody-AuNP conjugates. Florescence spectra of standards and conjugates were obtained using an excitation wavelength of 280 nm and an emission range of 320-350 nm. Florescence intensity in the range of 335-342 nm was integrated and used for antibody quantification. To validate the native florescence assay we employed, a CBQCA (3-(4-carboxybenzoyl) quinoline-2-carboxaldehyde) highly sensitive florescence assay. For the CBQCA experiment, 10 μL of a 100 mM KCN was used to digest the pelleted antibody-AuNP conjugates for 2 hours. A 0.1 M phosphate buffer (pH 9.3) was used to dilute samples to 150 μL. Standard calibration solutions (0.5-5 μg/mL) of unmodified mouse anti-HRP antibody were prepared for the CBQCA florescence assay as well. To each standard concentration and sample was added 10 µL of 5 mM CBQCA reagent followed by incubation at room temperature for 2 hours. Aluminum foil was used to cover the samples and standards during incubation to prevent exposure to light. After incubation, protein florescence was measured at an excitation and emission wavelength of 465 and 550 nm, respectively.

The amount of AuNPs to which antibody is adsorbed was also determined using a Perkin Elmer optima 7300 V inductively coupled plasma-optical emission spectroscopy (ICP-OES). Fifty µL of digested antibody-AuNP conjugates used for the antibody florescence assay were

diluted to 5 ml with 2% HNO_3. Standard solutions of gold (0.1 – 1 mg/L) were prepared in 2% HNO_3. The number of AuNPs was calculated by dividing the mass of total gold extrapolated from ICP-OES standard calibration by the mass of a 60 nm AuNP ($2.18 \times 10^{-15}\ g$).

Quantitation of Conjugates Antigen Binding Site

The antigen binding activity of antibodies adsorbed onto AuNPs was determined by an HRP enzymatic assay. One hundred mL of purified antibody-AuNP conjugate were incubated with 3 mg of HRP for 1 hour. Excess unbound HRP was removed by three centrifuge/wash cycles at 5000g for 5 mins. Standard concentrations (0.1-0.7 μg/mL) of HRP were prepared and used to quantify the amount of HRP captured by conjugates. A 10 µL aliquot of standards and conjugates was mixed with 1-step ABTS solution. The enzymatic rate was determined by measuring the absorbance of the oxidized product at 415 nm for 20 mins at 10 s intervals using Bio-Rad microplate plate reader. To correlate the number of HRP captured to the number of antibodies per AuNP, the exact number of AuNPs present in the 100 μL antibody-AuNP conjugate suspension used for the HRP assay was determined using an ICP-OES.

Dissecting Antibody Orientation on AuNP

To determine the impact of overcrowding of antibodies on AuNPs on antigen capture, the enzymatic activity of conjugates formed by incubating different concentrations of unmodified anti-HRP antibodies was evaluated. For this experiment, 1.5, 2, 3 and 4 mg of unmodified anti-HRP antibody was added to 100 μL of AuNP in a 2 mM phosphate buffer (pH 7.5). The antibody-AuNP suspension was left to incubate for an hour. After incubation, the number of antibodies per AuNP and antigen binding site was determined using the procedures discussed above. Three μL of a 1 mg/mL solution was incubated with purified conjugates before HRP incubation to block all available AuNP surface.

Instrumentation

Dynamic Light Scattering (DLS). Hydrodynamic diameter and zeta potential of chemical modified, unmodified antibodies, and conjugates were measured using a Zetasizer Nano ZSP (Malvern Instruments) equipped with non-invasive back scatter optics. Antibodies were filtered with a 0.02 μm filter prior to DLS analysis. A capillary cuvette was filled with filtered buffer and a 20 μL aliquot of antibodies or conjugates was carefully introduced to the bottom of the cuvette. Hydrodynamic diameter and zeta potential were measured in triplicate. Fifteen runs were averaged for each measurement. A built-in Smoluchowksi method for aqueous media was adopted for all DLS measurement.

UV-visible Measurement. A Cary 1 Bio UV-visible dual-beam spectrophotometer was used to obtain extinction spectra of protein-AuNP conjugates. The spectra were collected over a range of 350-900 nm at 0.5 nm increment with a spectral bandwidth of 0.2 nm. HRP enzymatic assay absorbance was collected using an iMark Bio-Rad high throughput microplate reader. Enzyme kinetics was monitored at 415 nm for 20 mins at 10 s intervals.

Results and Discussion

Antibody Chemical Modification

Primary amines of lysine can act as efficient nucleophiles at a basic pH, which can react with electrophiles with good leaving groups. The product of this addition-elimination reaction prevents protonation of lysine residues at lower acidic pH as well as the interaction of primary amines with other ligands. Chemical modification of antibodies through the reaction of primary amines eliminates its positive charge, thereby decreasing the overall positive charge on the surface of antibodies. In order to substantiate that chemical modification of lysine alters antibody surface charge, lysine residues of a fully characterized IgG (PDB-ID 1IGT) were acetylated in-

silico using UC-Chimera, and its surface charge computed using a Poisson Boltzmann solver on CHARM-GUI.[62,63] The results indicate a decrease in positive surface charge for modified antibody compared to the unmodified antibody, as shown in **Figure 10** with blue and red patches denoting regions of positive and negative charges, respectively.

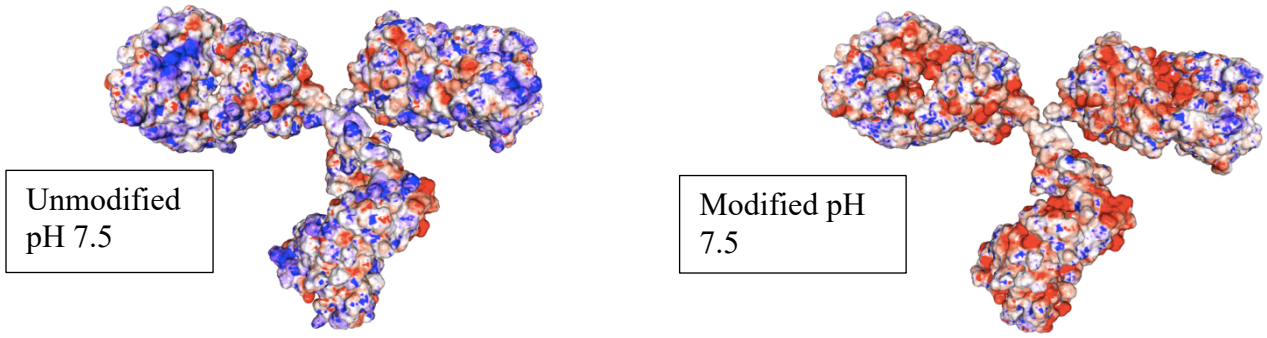

Figure 10. Calculation of antibody (PDB-ID 1IGT) surface charge. Adaptive Poison Boltzmann equation solver on a CHARM-GUI was used for protein surface charge simulation. Blue and red regions represent positive and negative potential, respectively, in a range of −5 kbT/e to + 5 kbT/e.

Antibody chemical modification was carried out experimentally using acrylic acid N-hydroxy succinimide (acrylic acid NHS) and reduced dithiobissuccinimidyl propionate (DSP). We envisaged that acrolein and a thio propionate group will be covalently bonded to primary amines of lysine residues upon reacting with acrylic acid NHS and reduced DSP, respectively (**Figure 11**). A Malvern Zetasizer Nano ZSP was employed to monitor the extent and effect of chemical modification on antibody surface charge by measuring the protein zeta potential. As anticipated, the surface charge on the unmodified antibody increases (becomes less negative) as the pH decreases, as a result of protonating basic amino acids (**Figure 12**). Importantly, both of

the modified antibodies present a substantially more negative surface charge at pH 7.5 than the unmodified antibody at a similar pH. These data confirm chemical modification of lysine residues through the primary amine and establish that antibody surface charge can be manipulated via chemical modification.

Although both chemical modifiers used can alter antibody surface charge, DSP increases the number of free thiols, thereby promoting strong conjugation to AuNPs. Thus, the DSP-modified antibody was further characterized to determine the extent of chemical modification by measuring the number of additional free thiols on the protein. Molecular modeling of an IgG protein (PDB-ID 1IGT) establishes that the thiols of the cysteine residues are all involved in disulfide bonds and not present as free thiols (**Figure 13**).

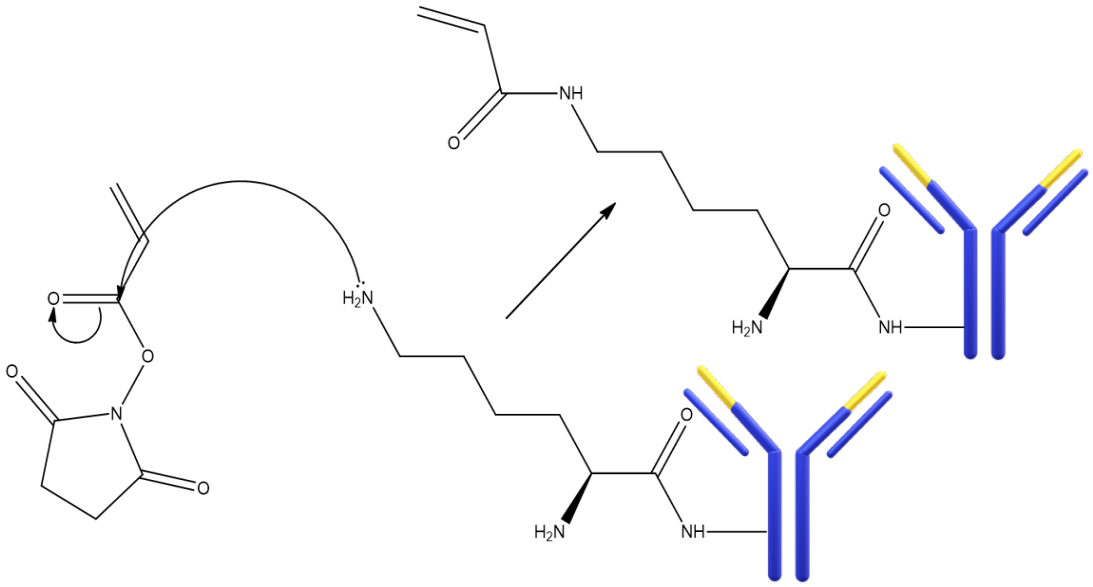

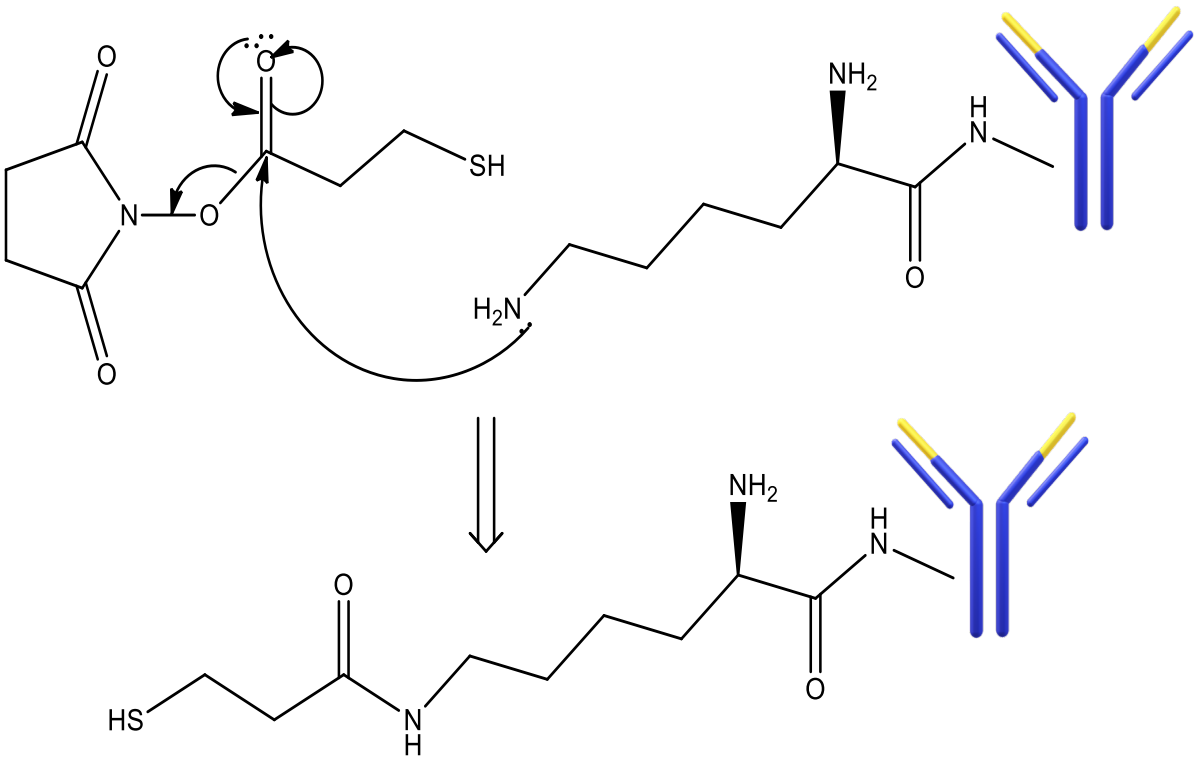

Figure 11. Chemical modification of the lysine residue with acrylic acid NHS (top) and reduced DSP (bottom).

The number of free thiols on the unmodified protein were quantified using Ellman's reagent and a previously established protocol (**Figure 14**).[64] No free thiols were detected on the unmodified antibody, consistent with molecular models showing that each cysteine residue is involved in a disulfide bond and therefore not detectable by Ellman's reagent. However, ten free thiols were detected for each DSP-modified antibody. These results further confirm chemical modification of the antibody and show that free thiols can be added to proteins which may impact their adsorption to AuNPs.

Equilibrium dialysis was performed to examine the antigen-binding activity of the anti-HRP antibodies before and after chemical modification.

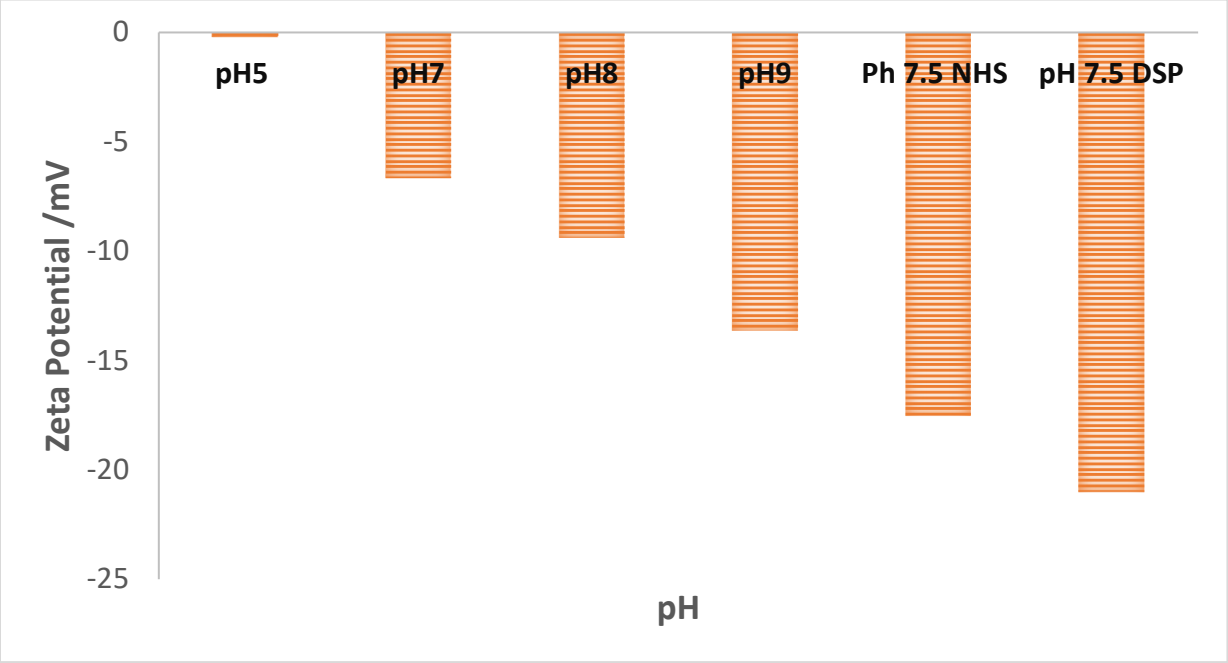

Figure 12. Characterization of chemically modified and unmodified antibodies. Zeta potential of unmodified chemically modified antibodies at different pHs.

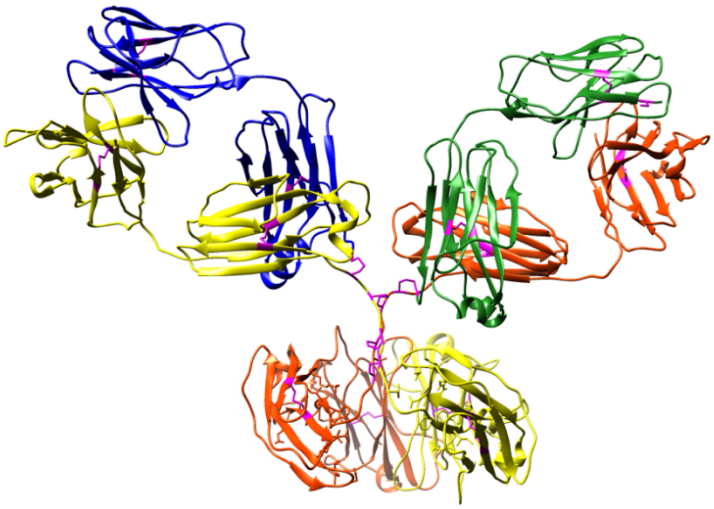

Figure 13. Structure of antibody showing all cysteine residue (pink) are engaged in disulfide bond.

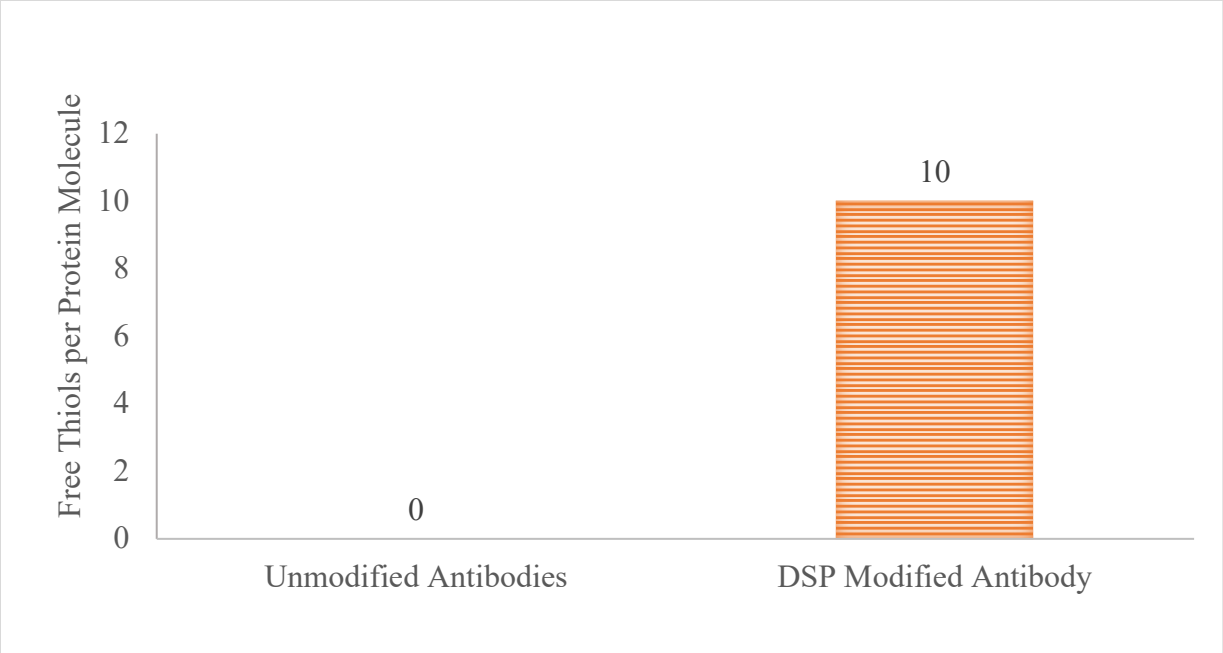

Figure 14. Characterization of chemically modified and unmodified antibodies. The number of free thiols on unmodified and DSP-modified antibodies determined using Ellman's reagent.

To this end, an HRP solution was added to one chamber of the dialysis device and an equimolar concentration of sample was added to the adjacent chamber. The sample solutions included unmodified anti-HRP antibody, DSP-modified anti-HRP, NHS-modified anti-HRP, an IgG isotype control, and buffer. The chambers were separated by a 100 kDa membrane and equilibrated for 3 h to allow HRP (MW 44 kDa) to equilibrate between the chambers while the IgG was confined to its original chamber (MW 150 kDa). After equilibration, the solution was removed from the chamber originally filled with HRP and the remaining HRP was measured based on enzymatic activity for the substrate ABTS. **Figure 15** shows that no enzymatic activity was observed for the unmodified or either modified antibody. This result confirms the antibody binds the HRP antigen and extracts it from its original chamber. For the IgG isotype control and

buffer, the HRP solution equilibrates in both chambers to equal concentrations since no binding occurs to concentrate the HRP in the sample chamber; thus, significant enzymatic activity is observed for the equilibrated solution removed from the HRP chamber, as is evident in **Figure 15**. The results suggest no decrease in antigen binding affinity of antibodies after chemical modification as unmodified and chemically modified antibodies had similar enzyme kinetic rates after equilibrating with HRP. Likewise, there was no significant change of protein size (16 ± 2) nm observed by DLS before and after chemical modification indicating a low possibility of protein unfolding upon chemical modification.

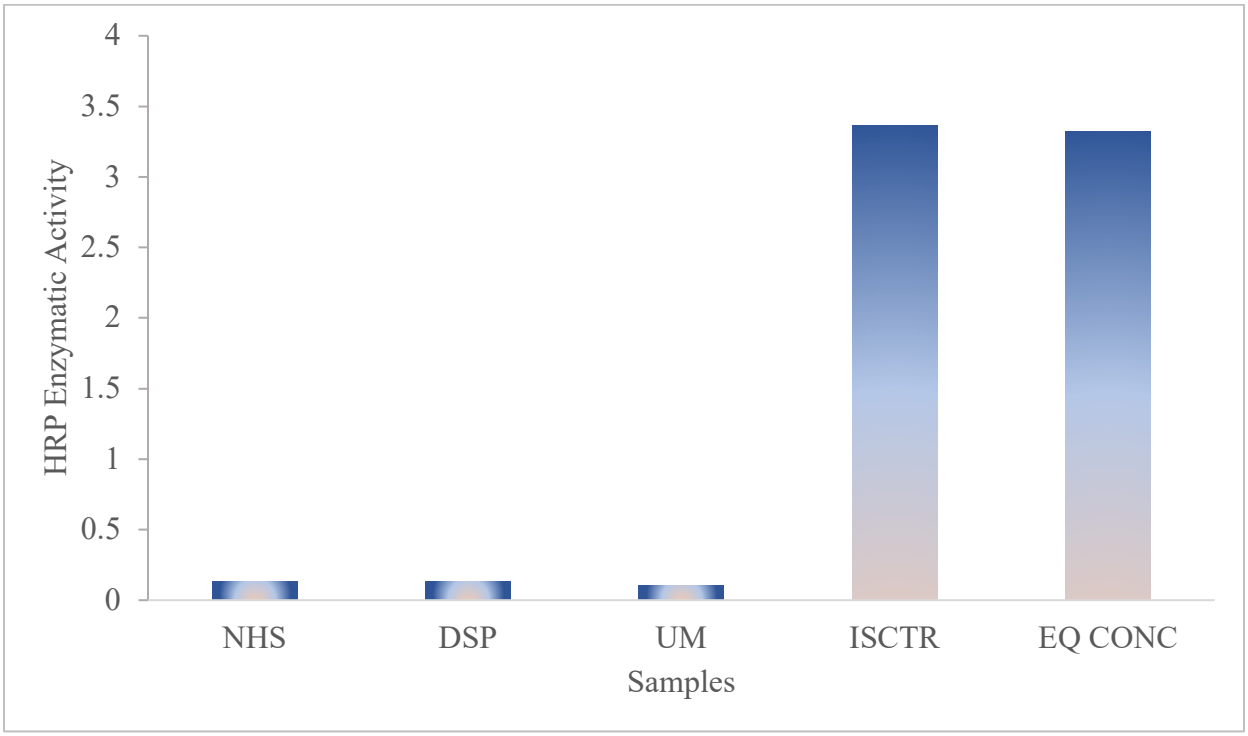

Figure 15. Characterization of chemically modified and unmodified antibodies. Result of equilibrium dialysis to determine the antigen-binding activity of the unmodified (UM) and modified antibodies (NHS and DSP). Negative control samples include an IgG isotype (ISCTR) control and buffer (EQ CONC).

Kinetics of Hard and Soft Antibody Corona Formation on AuNPs

Previously, we have determined that a monolayer coverage of anti-HRP antibodies is formed on AuNPs within an hour. To this end, excess chemically modified and unmodified antibody were incubated with AuNPs for 1h at pH 7.5. UV-vis spectrophotometry, dynamic light scattering (DLS), and nanoparticle tracking analysis (NTA) were used to measure the presence and thickness of the antibody monolayer.

Upon the adsorption of proteins, the refractive index of AuNPs changes. This change in refractive index results in a shift in extinction maximum of the nanoparticle surface plasmon resonance, which can be monitored using a UV-Vis spectrophotometer. Unconjugated 60 nm AuNPs exhibited an extinction maximum at 536 nm (**Figure 16**). An extinction maximum was observed at 540-541 nm for the 60 nm AuNPs incubated with unmodified and DSP-modified antibody for 1 h (Figure 6). This 4-5 nm red shift is characteristic of an adsorbed protein monolayer. Surprisingly, however, no shift in the extinction spectrum was observed for the 60 nm AuNPs incubated with the NHS-modified antibodies, and this result suggests that the NHS-modified antibody did not adsorb onto the AuNP within the 1 h incubation period.

DLS size and zeta potential measurements corroborate the UV-visible spectrophotometry results. An increase in size and a decrease in the zeta potential of AuNPs is observed when proteins are adsorbed on nanoparticles. DLS analysis confirms a monolayer thickness of 20 nm ± 5 nm and 14 nm ± 3 nm for the DSP-modified and unmodified antibody AuNP conjugates after purification. Meanwhile, no significant change in AuNP size was detected for NHS-modified antibody AuNP conjugates for the one-hour incubation time.

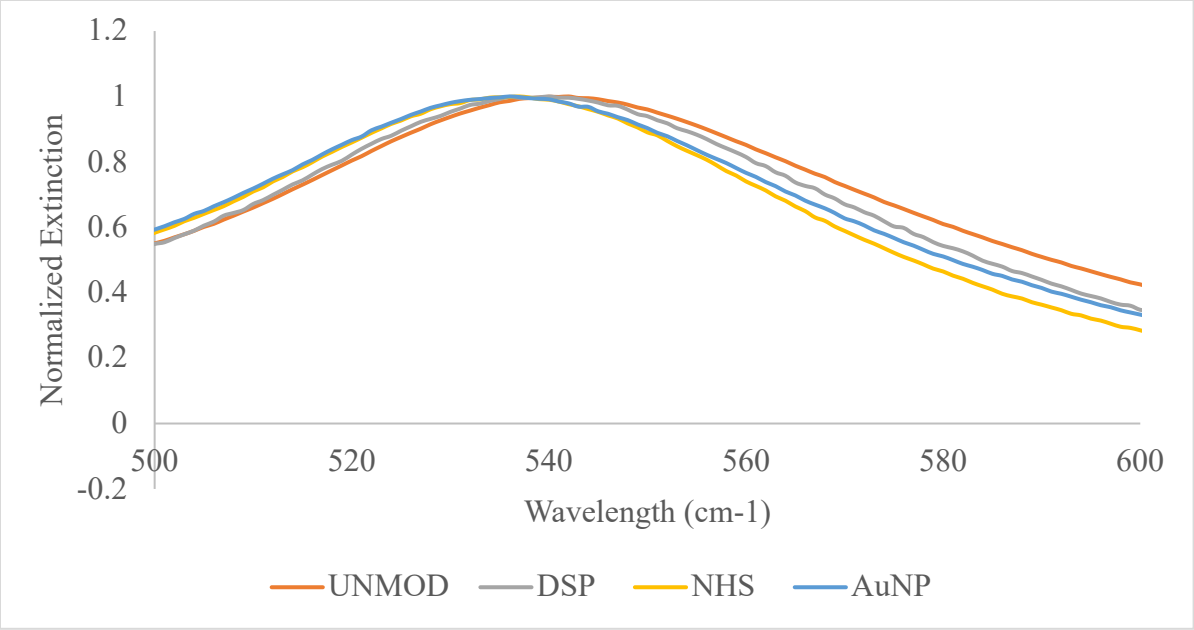

Figure 16. Extinction spectra of Antibody-AuNP conjugates incubated for an hour.

To understand why there was no adsorption of NHS-modified antibodies onto AuNPs at an hour of incubation, we investigated the time evolution of the soft and hard antibody corona on AuNPs. Both hard and soft protein coronas have been established to be present in AuNP protein conjugates. A thiol gold bond is well-established to be responsible for the hard corona formation. In contrast, electrostatic interaction between gold and charged surfaces of proteins facilitate the formation of the soft corona. It has been shown that centrifugation can remove the soft protein corona while the hard corona remains adsorbed.[20,31,65] Herein, we employed centrifugation (**Figure 17**) and DLS size measurements to probe the time evolution of the soft and hard antibody corona on a AuNP. Antibody AuNPs size and zeta potential were monitored for 24 hours using a Zetasizer Nano ZSP (Malvern Instrument). AuNP-antibody conjugates size was measured before and after centrifuging. Conjugate size measured before centrifuging represents both hard and soft corona of antibody. In contrast, only hard corona remains after centrifuging.

The change in antibody-AuNP conjugates size for chemically modified and unmodified antibodies after centrifuging represents the soft corona thickness at each time point (**Figure 18**).

A soft corona of antibodies was observed within an hour of incubation for both chemically modified and unmodified antibody-AuNP conjugates. There was no considerable difference in the thickness of the antibody soft corona for all time points. Nonetheless, after centrifuging to remove the soft corona, the unmodified and DSP modified antibody-AuNP conjugates recorded the presence of antibody hard corona on AuNP at all time point (**Figures 18A and 18C**). The size of acrylic acid NHS modified antibody-AuNP conjugates returned to 62 nm for the 1, 3 and 6 h (**Figure 18B**) time points after centrifuging, signifying the absence of antibody hard corona for these incubation time.

Similarly, Zeta potential of purified conjugates suggests the rapid formation of hard antibody corona for unmodified and DSP modified antibodies, where NHS modified antibodies only showed a substantial change in AuNP Zeta potential at 12 hours and beyond (**Figure 19**).

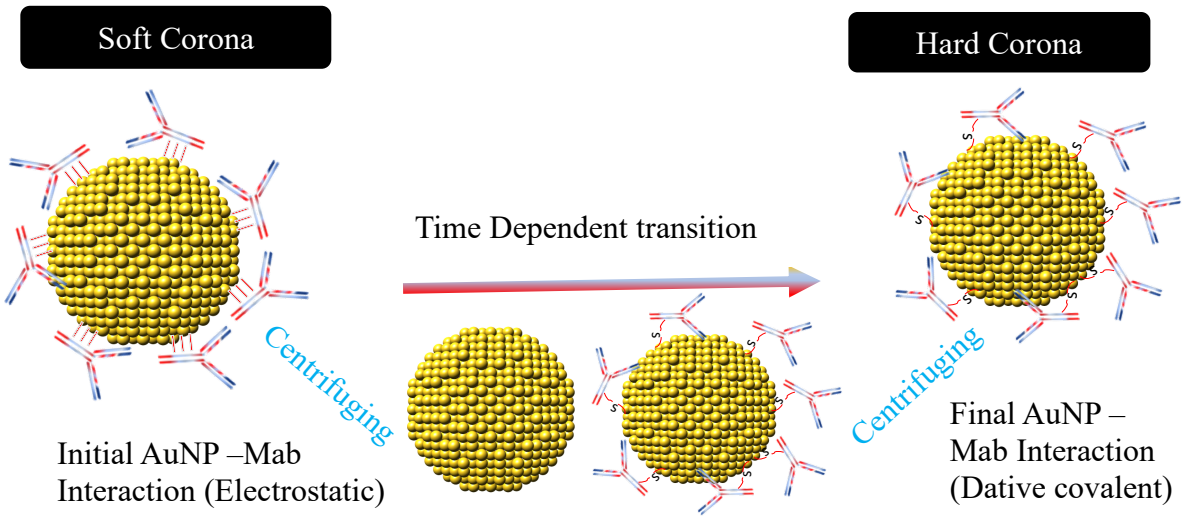

Figure 17. Time evolution of antibody corona on AuNP. Demonstration of effect of centrifuging on antibody soft and hard corona.

These results suggest that electrostatic attraction between antibodies and AuNP which facilitate soft corona formation as well as the initial coordination of proteins to nanoparticles is rapid.

Although the free thiol of the cysteine residue forms a stronger bond with gold and is the most preferred ligand, amines have been shown to display moderate affinity toward gold.[66–68,21] Computational analysis of a fully characterized IgG2A (PDB ID 1IGT) similar to our antibody revealed all cysteine residues to be engaged in disulfide bonds (**Figure 13**). In contrast, numerous solvent-accessible lysine residues were identified. We inferred from the computational studies that AuNPs would initially interact with readily available primary amines of antibody lysine residues.

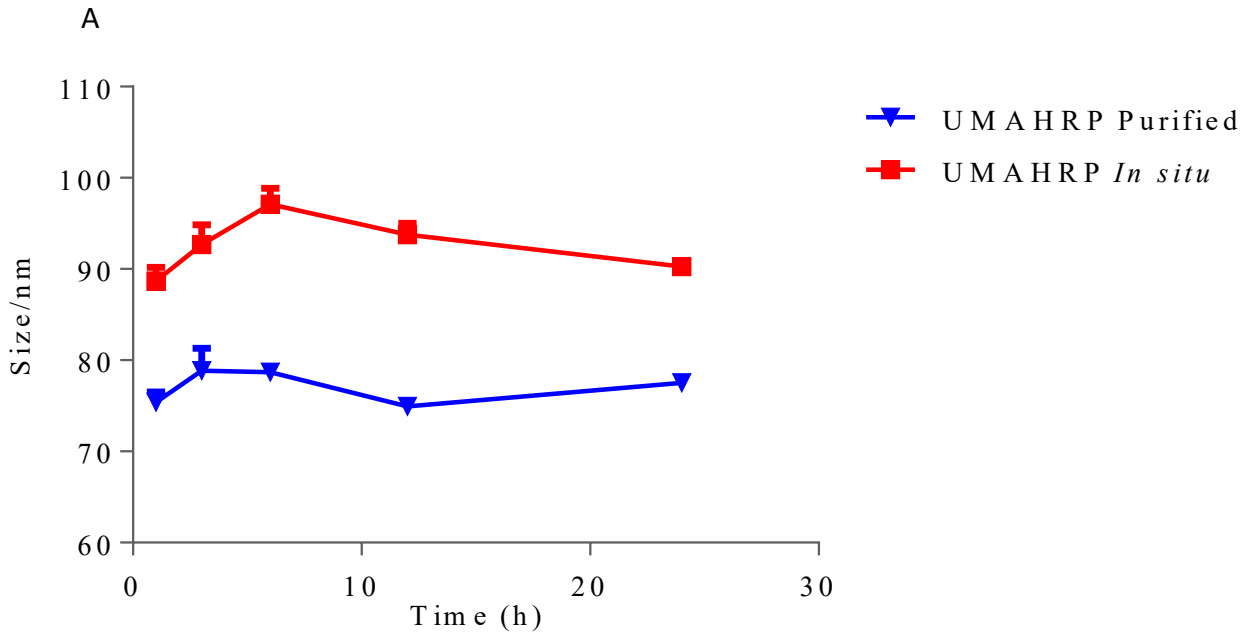

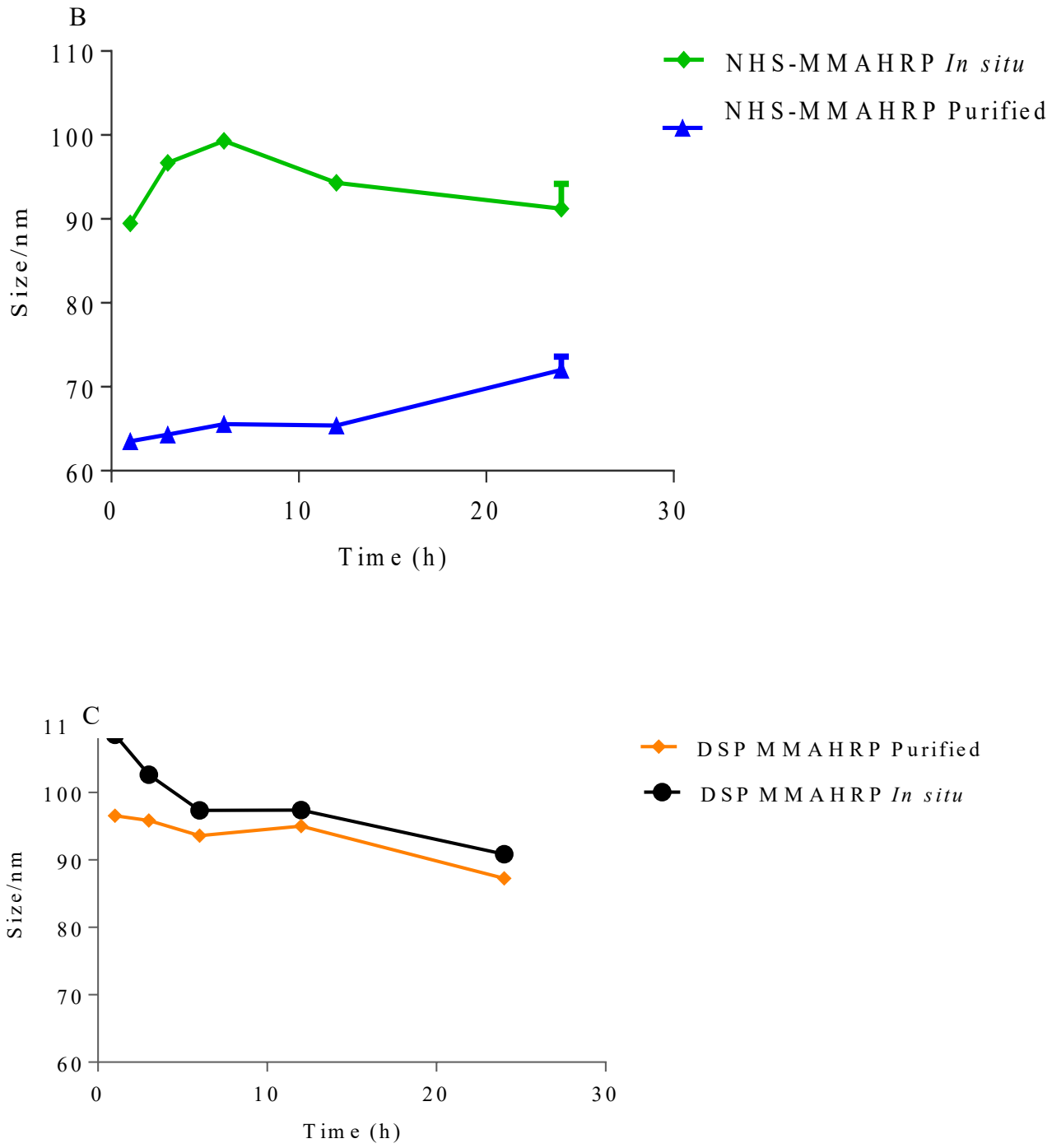

Figure 18. Kinetic of hard and soft antibody corona formation. (A) DLS size meaured of unmodified antibody-AuNP conjugates before removal of excess antibodies through centrifugation (*in situ)* and after removal of excess antibodies (purified). (B) Size of acrylic acid

NHS-modified antibody-AuNP conjugates *in situ* and after purification. (C) DSP- modified antibody-AuNP conjugates size before (in-situ) and after (purified) purification.

The formation of the hard antibody corona on AuNPs was not observed until 12h for the acrylic acid NHS modified antibody; meanwhile, a soft corona of acrylic acid NHS modified antibody was formed under 1 hour. From this observation, we suggest primary amines to be an essential functional group to promote adsorption of proteins onto AuNPs in the absence of free thiol. The DSP-modified antibodies readily formed a stable hard corona within an hour (**Figure 18C**) with a small change in conjugate size after centrifuging, demonstrating a rapid formation of gold sulfur bond by the free thiol.

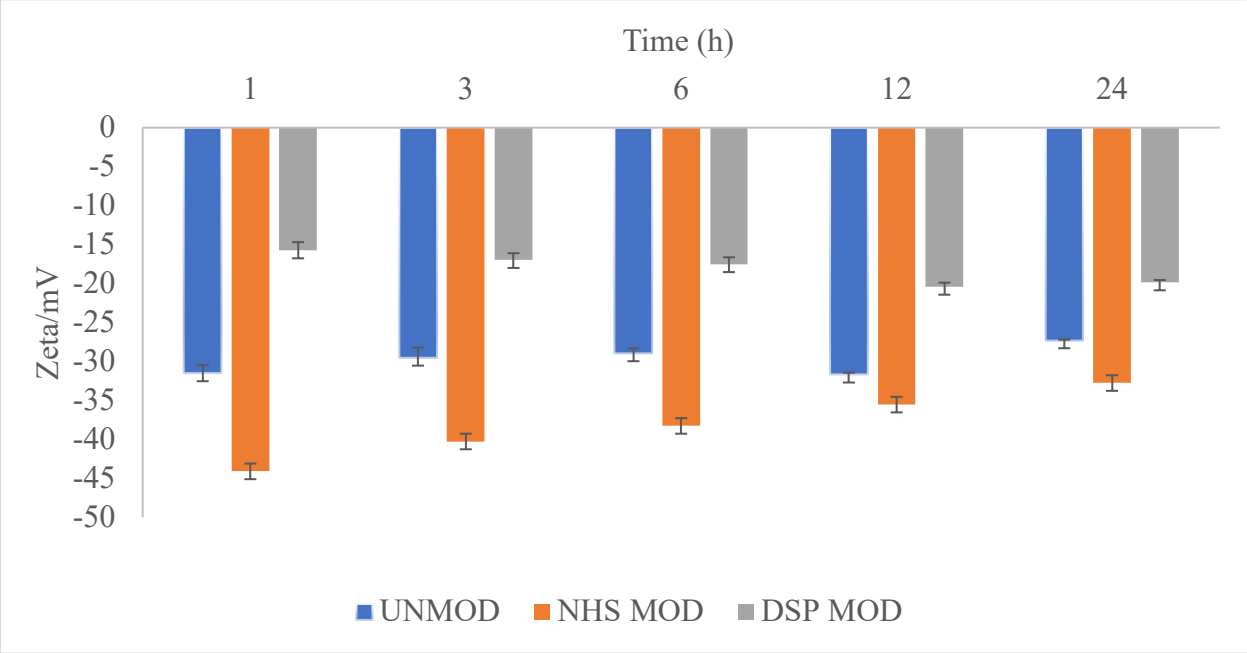

Figure 19. Zeta potential of unmodified and modified antibody-AuNP conjugates incubated for different time.

Catalytic reduction of para-nitrophenol to aminophenol by sodium borohydride on a AuNP surface[69] was employed to validate the time-dependent formation of a hard protein corona and formation of the antibody-AuNP conjugate. This reduction occurs on the exposed surface of

AuNPs; hence we hypothesized that when the AuNP surface is fully saturated with antibodies, the reduction reaction will be inhibited. To test our hypothesis, purified acrylic acid NHS modified and unmodified antibodies synthesized at different time points were used to undertake this reduction reaction. Acrylic acid NHS modified antibody-AuNP conjugates synthesized at 1h, 3h and 6h catalyzed the reduction reaction, whereas the unmodified antibody-nanoparticle conjugates did not (**Figure 20**). The requirement of long incubation time for acrylic acid-NHS modified antibodies to adsorb onto gold demonstrates the importance of free amines in adsorption of proteins onto AuNPs.

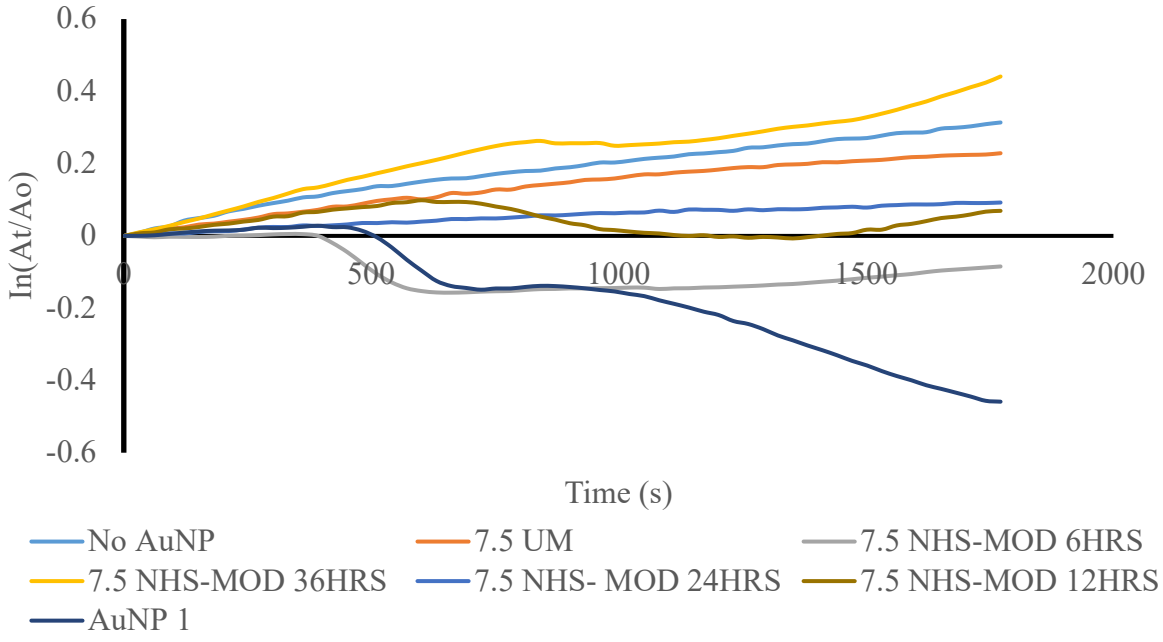

Figure 20. Kinetics of catalytic activity of acrylic acid NHS-modified and unmodified antibody-AuNP conjugates. Reduction of para-nitrophenol to aminophenol by AuNP was evaluated to determine the time required for full saturation of AuNP surface by acrylic acid NHS-modified antibodies.

In summary, we have demonstrated that the presence of free thiols or amines on proteins is essential for robust and fast adsorption of proteins onto a AuNP.

Effect of pH on the Synthesis of AuNP-Antibody Conjugates

Antibody-AuNP conjugates were formed by allowing 24h for protein adsorption, and three factors were considered in evaluating the formation and stability of antibody-AuNP conjugates at different pH: (1) the surface plasmon resonance of AuNPs, (2) the monolayer thickness of antibodies on AuNP, and (3) the zeta potential of antibody-AuNP conjugate. UV-Visible spectrophotometry, dynamic light scattering (DLS), and nanoparticle tracking analysis were used to monitor and measure antibody-AuNP stability and protein monolayer thickness in solution.

UV-visible spectrophotometry has been extensively utilized to monitor nanoparticle size, stability, and adsorption to other molecules such as proteins due to its ability to measure the surface plasmon resonance of nanoparticles. A significant red shift and the broadening of the UV-visible spectra (**Figure 21**) at pH less than 7.5 for the unmodified antibody-AuNP conjugates show the presence of aggregates. Electrostatic bridging of antibodies to AuNPs at lower pH has been determined to be the mechanism by which these aggregates are formed (**see Chapter II**). From this observation, we hypothesized that chemical modification of lysine residues of antibodies to remove some of the positive charges should allow the synthesis of antibody-AuNP conjugates at lower pH.

NHS and DSP chemically modified antibodies formed a highly stable conjugate with AuNP. A 3-5 nm red shift in extinction maximum of the AuNPs (**Figure 10**) and a monolayer thickness of 8-18 nm (**Figure 22**) confirms the formation of a stable antibody AuNP conjugate at pH 6, 6.5, and 7.5 for the modified antibodies. A decrease in the zeta potential of AuNP from -45

± 3 to -18 ± 4 and -28 ± 5 mV for DSP and NHS chemically modified antibody-AuNP conjugates respectively, also denotes the formation of an antibody corona on AuNP.

A

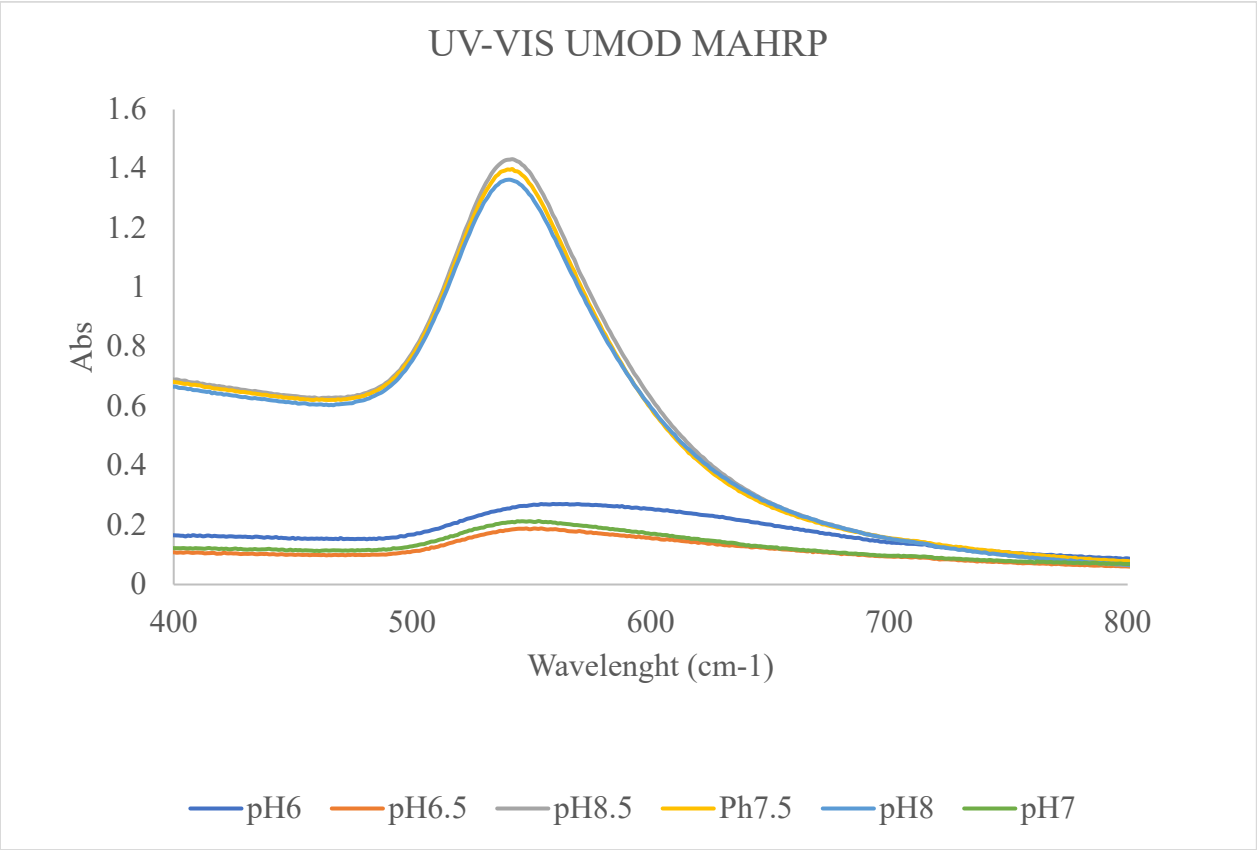

B

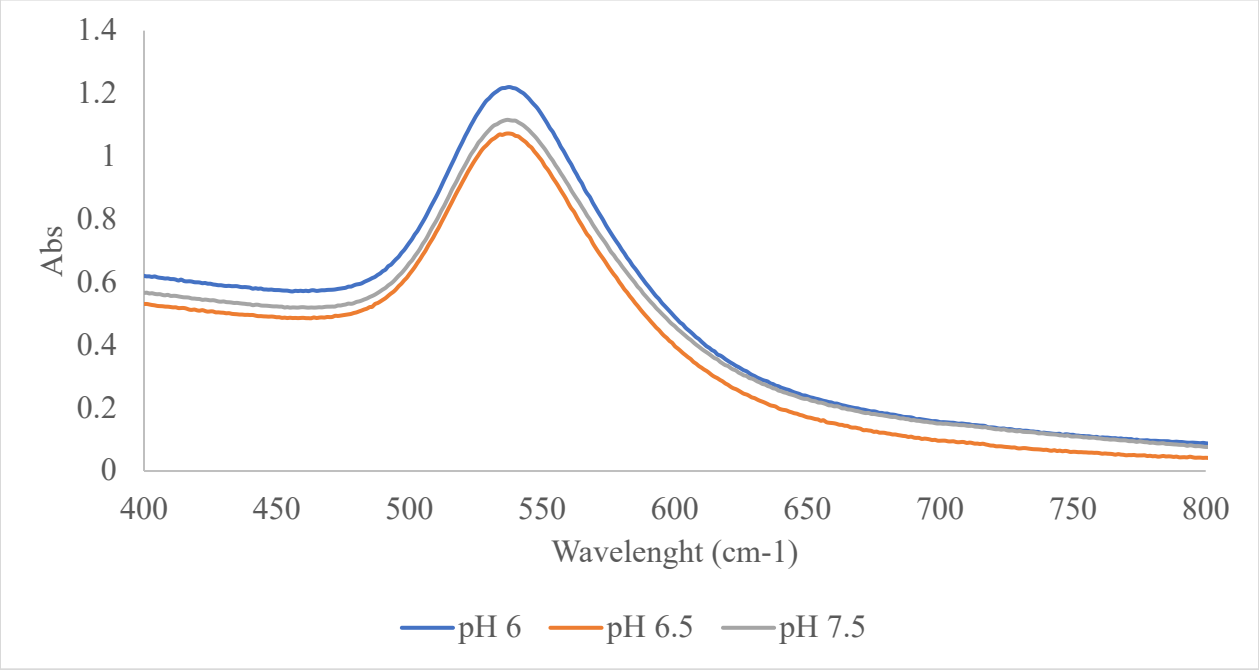

C

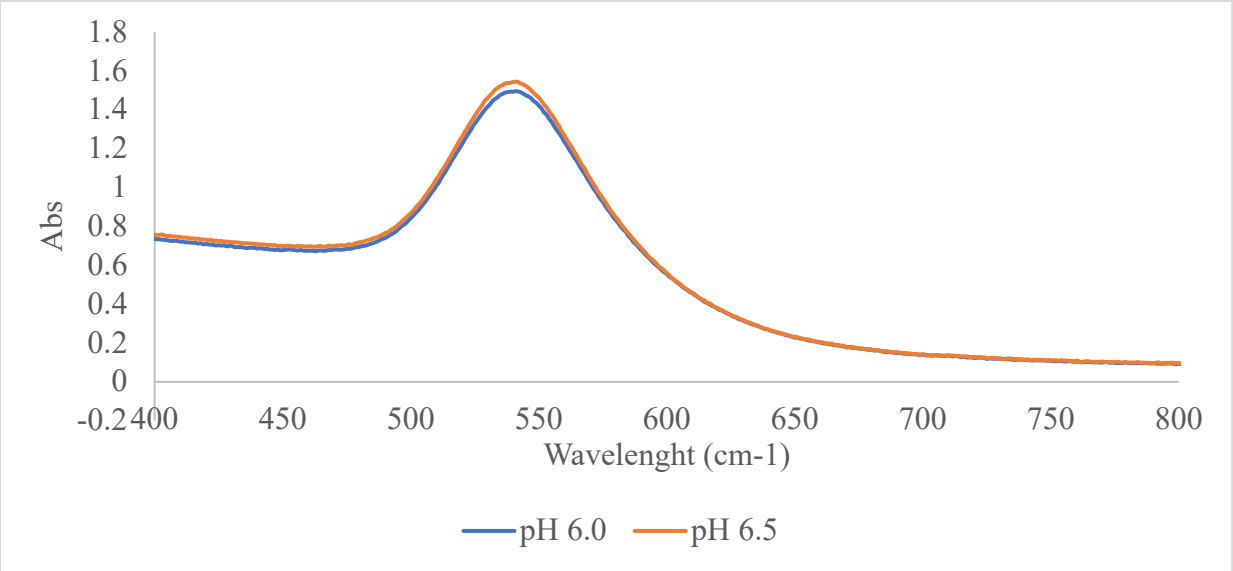

Figure 21. Evaluating antibody-AuNP conjugate stability *at different pH.* Extinction spectra of (A) unmodified antibody-AuNP, (B) acrylic acid NHS-modified antibody-AuNP, and (C) DSP-modified antibody-AuNP conjugates at different pH.

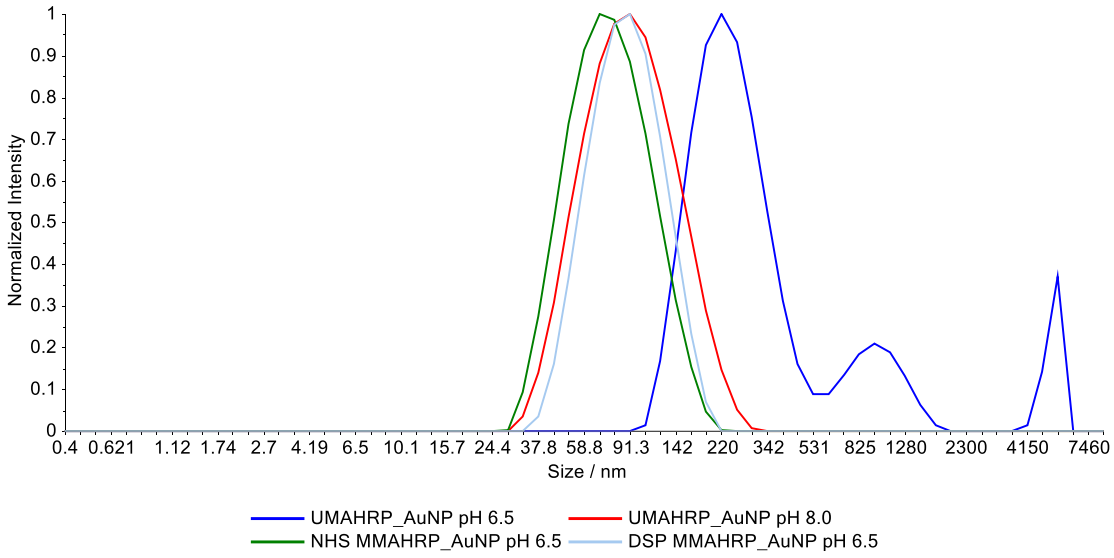

Figure 22. Hydrodynamic diameter of unmodified and modified antibody-AuNP conjugates at pH 6.5 measured with DLS.

Quantifying Antibody bound Per AuNP

Antibody density is an important parameter to determine in order to evaluate the orientation and number of functional antibodies adsorbed onto the AuNP. Most existing analytical techniques employed to quantify antibody on AuNPs measures supernatant concentration after centrifuging where the antibody bound is determined by the difference in the amount added and the amount in the supernatant. Antibodies quantified by these procedures deviate slightly from the actual amount adsorbed onto AuNP; hence, it is essential to search for new alternatives for quantifying the number of antibodies on AuNP. Here, a fluorescence and inductively coupled plasma optical emission spectroscopic technique was developed (**Figure 23**) to quantify antibodies and nanoparticles in solution simultaneously. A highly sensitive, but cost prohibitive, CBQCA fluorescence assay was used to validate our developed native protein fluorescence assay.

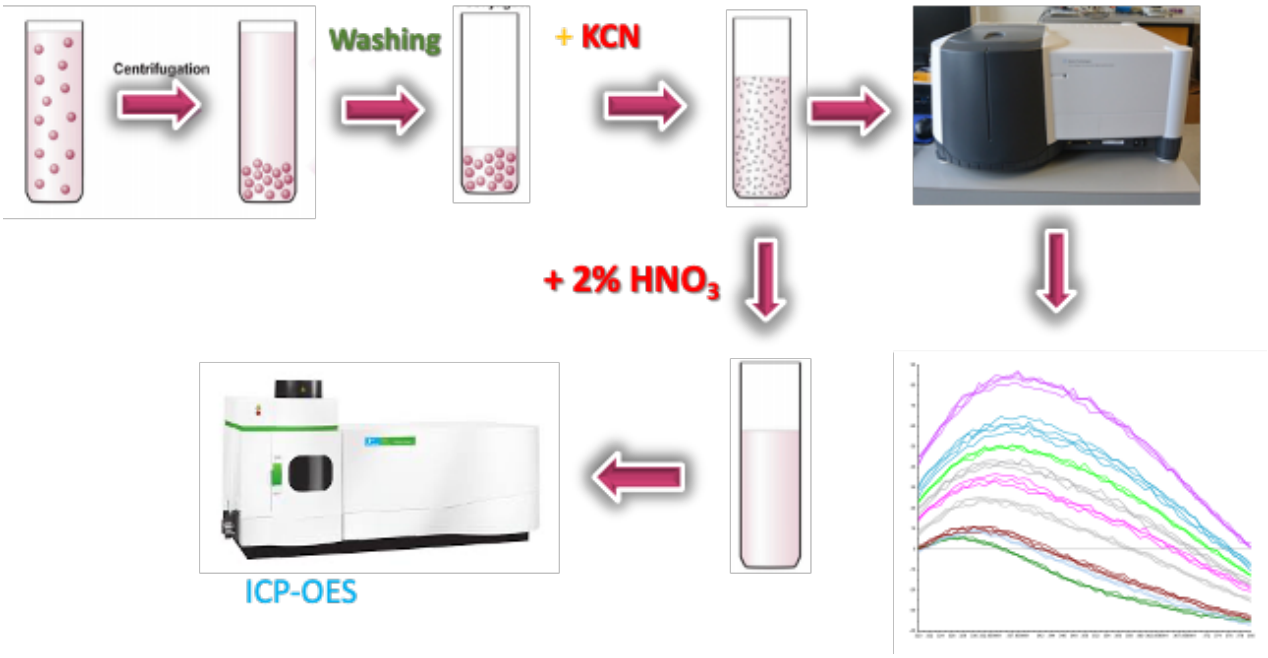

Figure 23. Schematic illustration of workflow for quantitation of the number of antibodies per AuNP using florescence and ICP-OES.

In applying this developed method to quantify adsorbed antibodies, the purified antibody AuNP conjugates were digested with KCN to dissolve the gold and release adsorbed antibodies into the solution for fluorescence quantification. The number of antibodies bound to each AuNP was estimated from a standard antibody fluorescence calibration, whereas the number of AuNP was extrapolated from a gold standard calibration. Digested AuNPs of equivalent concentration as the one used in preparing conjugates was used as a diluent in all standard fluorescence solutions, in an effort to matrix match and to ensure accurate protein quantification. The number of AuNPs was calculated by dividing the mass of gold obtained from the ICP-OES experiment by the mass of a 60 nm AuNP. The antibody loading per AuNP as a function of the amount of antibody added to the AuNP suspension was determined using this newly developed method (**Figure 24**). The measured quantity of adsorbed antibody was similar when using the native

fluorescence of the antibody or the costly CBQCA fluorescence assay. Both methods show that a monolayer coverage is formed with the addition of ≥ 2 mg of antibody per 100 mL of AuNP. After validating the analytical methodology, antibody loading on the AuNP was quantified for both modified and unmodified antibodies at different pHs where stable conjugates could be synthesized (**Figure 24**). For the unmodified antibodies, only pH 7.5 was considered since aggregation occurs below pH 7.5. Unmodified antibodies reached a saturated loading of 274 ± 44 antibodies per AuNP at pH 7.5. At pH 7.5 and 6.5, 137 ± 4 and 131 ± 11 antibodies were found bound per AuNP, respectively, for the NHS modified antibody conjugates.

DSP modified antibody conjugates recorded 320 ± 14, 410 ± 5, and 621 ± 24 at pH 7.5, 6.5, and 6.0, respectively. From the above data, DSP modified antibody conjugates recorded the highest number of antibodies per AuNP, followed by the unmodified antibody conjugates with the NHS modified having the least number of antibodies per AuNP.

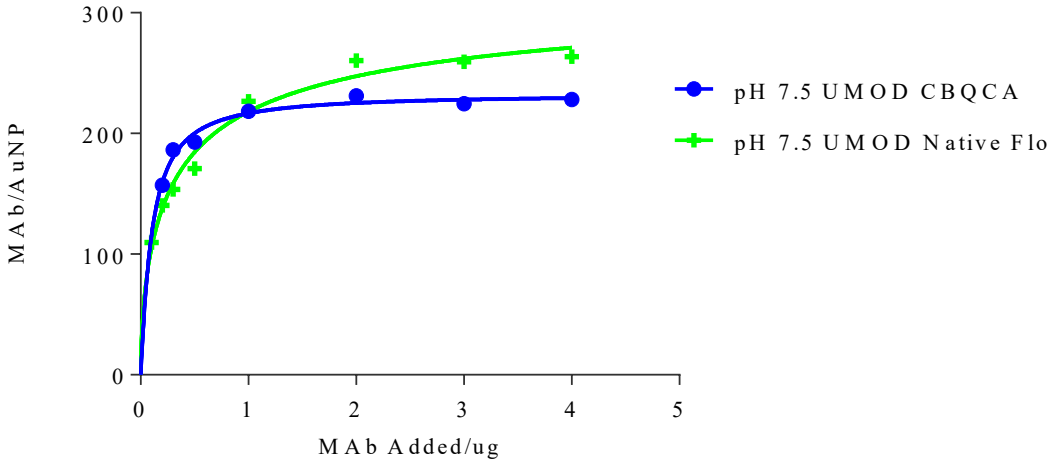

Figure 24. Quantitation of number of antibody/AuNP. (A) Florescence adsorption isotherm of unmodified antibody on AuNP obtained using native protein florescence and a highly sensitive CBQCA florescence assay.

These observations align with the DLS size measurement as the size of the antibody monolayer thickness follows the same trend (**Figure 18 & 22**). From our results, we observed an increase in the number of antibodies per AuNPs as the point of interaction on proteins to AuNP increased. Thus, acrylic acid NHS-modified antibodies with fewer points of interaction with gold recorded the least number of antibodies per AuNP. Chemical modification of antibody with DSP adds free thiols to the antibody, which increases the points of interaction with AuNPs. Increasing the number of free thiols, therefore, enhances the antibody's binding affinity which promote the loading of more antibodies onto AuNP. These accounts explain why more DSP modified antibodies are adsorbed per AuNP.

Based on a geometrical argument, the total number of antibodies theoretically needed to saturate a 60 nm AuNP was calculated to determine if the number of antibodies bound per AuNP is within a monolayer coverage. Using standard antibody dimension (14 × 8.5 × 4) a theoretical minimum and maximum of 95 and 333 antibodies per AuNP were estimated for a 60 nm AuNP with a total surface area of 11311 nm^2. Both unmodified and NHS modified conjugates recorded antibodies per AuNP within the theoretical monolayer layer saturation range. However, the number of antibodies per AuNP for DSP modified antibody conjugates was above the theoretical maximum for a monolayer saturation signifying overcrowding of antibodies on the AuNP surface. As discussed above, DSP modified antibodies have approximately 10 free thiols, which is expected to interact with gold most strongly. Also, there is a possibility of a disulfide bond forming between two antibodies which can affect antibody loading and antigen binding, however the consistency in the size of antibody before and after the chemical modification which was determined as 16 ± 2 nm indicates no disulfide formation.

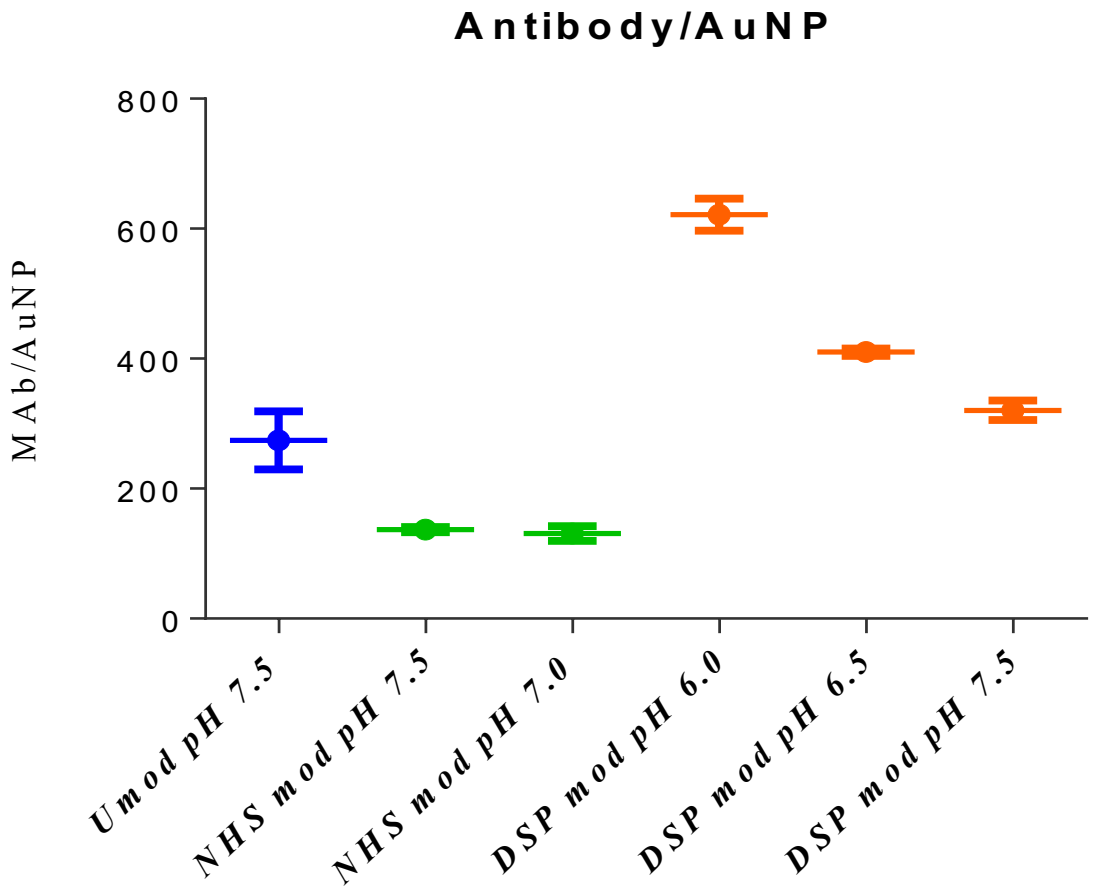

Figure 25. Quantitation of number of antibody/AuNP at selected pHs for chemically modified and unmodified antibodies.

Hydrodynamic diameters measured by DLS may include the hydration shell which tends to increase the size by a few nanometers. Also, the occurrence of very few large particles may have a major influence on the average conjugate size measured since DLS is biased towards measuring larger particles. To confirm, if multilayers of antibodies are present on AuNP, nanoparticle tracking analysis (NTA) was used to validate conjugate size. From **Figure 26** an antibody layer thickness of 15 ± 3 nm was observed signifying a monolayer coverage. The NTA

results indicate that, the likelihood of disulfide bonds between antibodies leading to the formation of multilayers of antibody on AuNP is minimal.

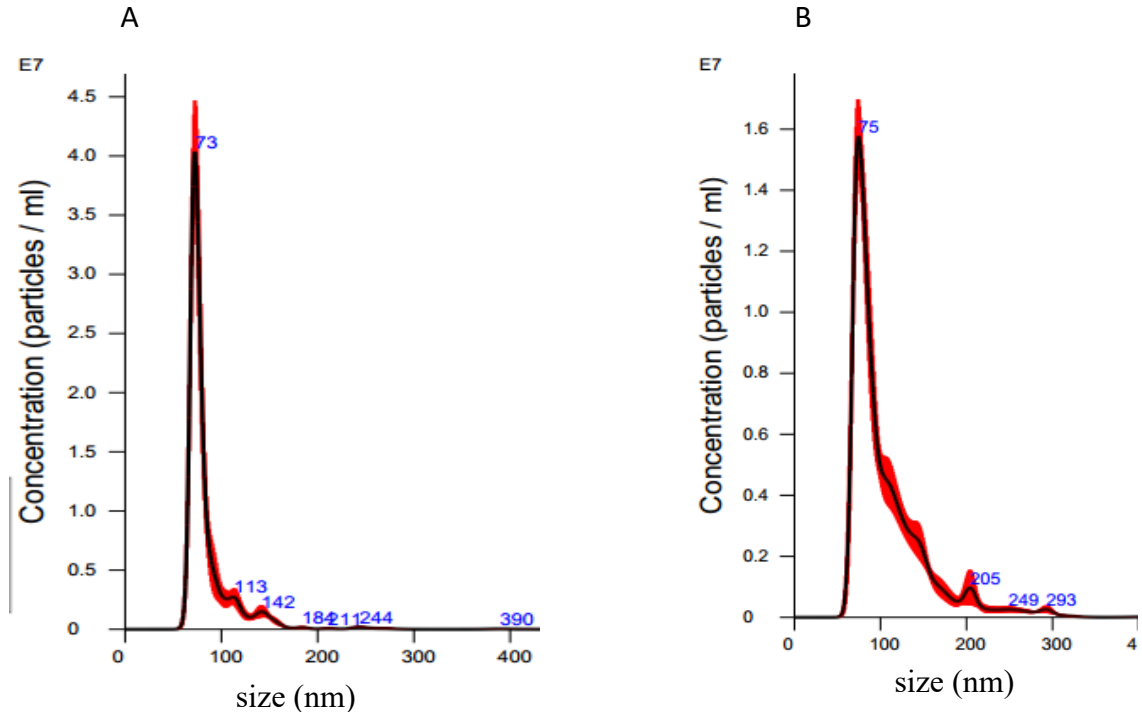

Figure 26. NTA size distribution of DSP-modified antibody-AuNP conjugate at (A) pH 6.5 and (B) pH 6.0.

Steric adjustment of antibodies at the expense of their conformation to allow more antibody packing have been previously reported.[70] The high number of DSP modified antibodies can be attributed to the over packing of antibodies on AuNP due to the high affinity of these antibodies for AuNPs. Herein we propose over packing of antibodies through steric adjustment as the pathway leading to a higher density of DSP modified antibodies on AuNP.

We have previously reported the impact of a solution pH on the number of antibodies on AuNP. Thus, the number of antibodies per AuNP increases as pH decreases from 8.5 to 7.5 for mouse anti-HRP. This observation was attributed to the different orientation of antibodies at

these pHs. Likewise, the number of antibodies per AuNP increased significantly from pH 7.5 to 6.0 for the DSP modified antibodies (**Figure 25**). The solution pH alters the surface charge of antibodies which influences its orientation as well as loading on AuNP. At lower pHs, more positive patches are created on the antibody, which directs its orientation on AuNP since electrostatic interaction between antibodies and AuNP is the primary force that initiates antibody adsorption onto AuNP. The increase in the number of antibodies with decreasing pH can therefore be attributed to antibody orientation facilitating more antibody loading.

Quantitation of Antigen-binding Activity of Conjugates

Antibody-AuNP conjugates can only bind antigen if an intact Fab region of the antibody is exposed. Determining the antigen-binding activity, therefore, gives insight into the orientation of antibodies on AuNP. Horseradish peroxidase (HRP) is a metalloenzyme that catalyzes the oxidation of various organic substrates using hydrogen peroxide. HRP can catalyze the oxidation of 2,2′-Azinobis-(3-Ethylbenzothiazoline-6-Sulfonic Acid) (ABTS). The reaction product is a metastable cation with an absorption maximum of 419 nm, while the substrate has a maximum of 342 nm; hence, the reaction product of this enzymatic oxidation can be measured with no interference from the substrate.[71] To this end, mouse anti-HRP antibody, which binds specifically to HRP, was used in all our studies.

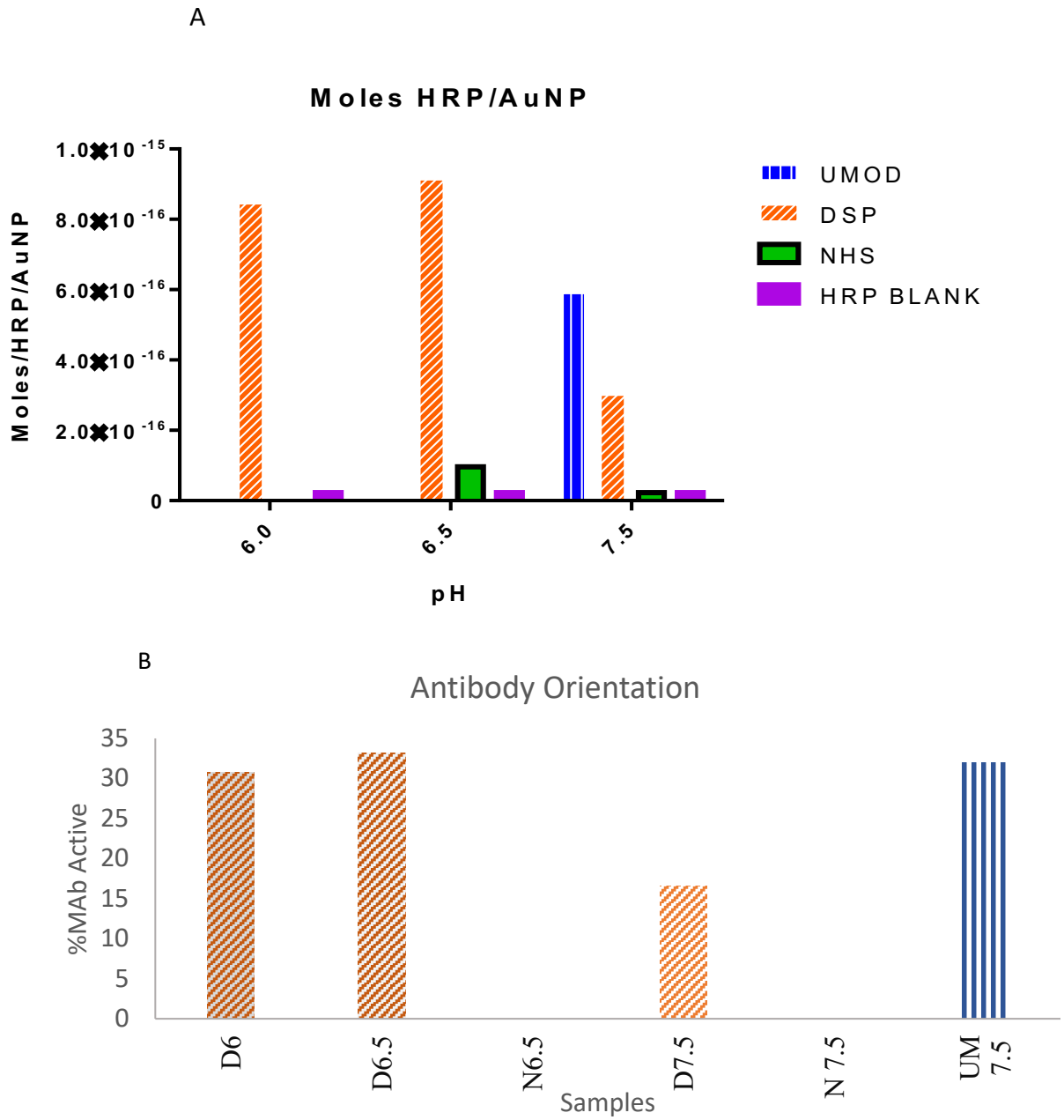

Figure 27. Determination of antigen binding activity of chemically modified and unmodified antibody-AuNP conjugates. (A) Moles of HRP captured by each conjugate at selected pH. ICP-OES Au intensity at 242 nm was used to normalize HRP data.(B) Percentage of adsorbed antibody available for antigen binding.

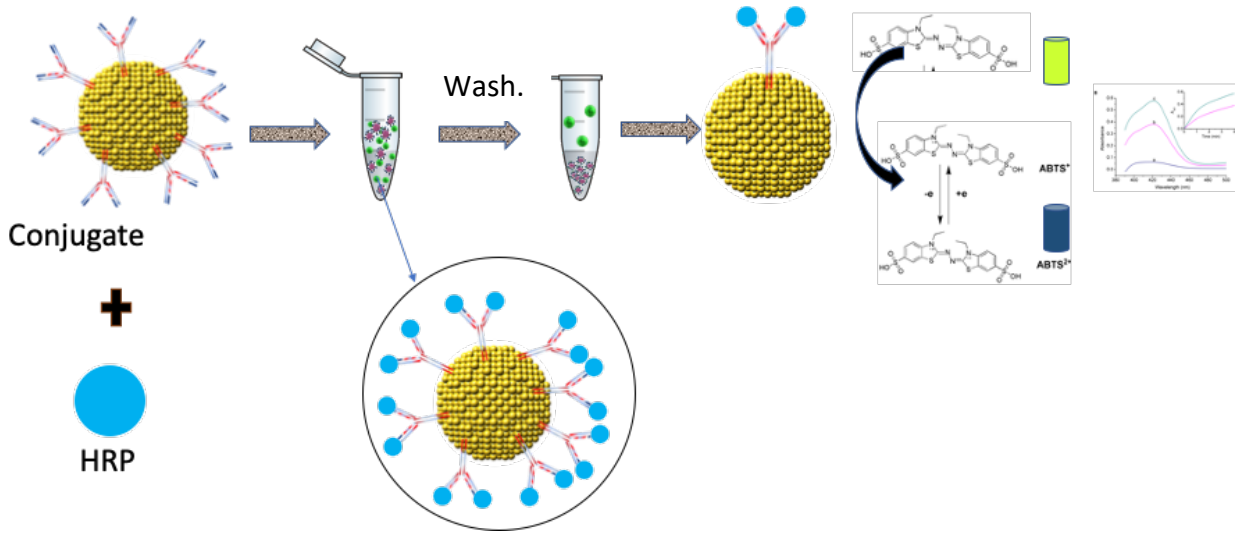

Figure 28. Workflow of HRP enzymatic assay for evaluating the antigen binding affinity of antibody-AuNP conjugates.

Briefly, MAHRP-AuNP conjugates were saturated with excess HRP for 3 h to allow efficient binding to antibodies. After purification to remove free HRP in solution, an HRP enzymatic assay was conducted, and the amount of HRP captured by the conjugates was estimated from an HRP calibration standard. Previously we have demonstrated that there is no significant difference between the catalytic activity of HRP bound by antibody and free HRP in solution.[72] Hence, we could determine the number of HRP molecules captured by each antibody-AuNP conjugate from an HRP calibration curve. Also, a measured gold intensity via ICP-OES for each antibody-AuNP was used for normalization to conjugate concentration for easy comparison between sample preparations. **Figure 27A** shows the number of moles of HRP captured by each antibody-AuNP conjugate. The DSP modified antibody-AuNP conjugate recorded the highest number of HRP followed by the unmodified antibody-AuNP conjugates. No HRP was captured by conjugates synthesized using the NHS modified antibodies, although there was a substantial number of antibodies per nanoparticle from our fluorescence assay. In

accounting for these observations, the number of HRP captured by each conjugate was correlated to the number of antibodies per AuNP (**Figure 27B**). As previously discussed, DSP modified antibody-AuNP conjugate had the highest antibody loading as well.

Consequently, the high number of antigens bound by DSP modified antibody-AuNP conjugates compared to the unmodified counterpart can be attributed to the density of antibody per AuNP. The fraction of antibody on AuNP accessible for antigen-binding was also computed by multiplying the total number of antibodies per AuNP by two and dividing by the total number of HRP it captures. This calculation was adopted due to the bivalency of antibodies. The fraction of accessible antigen-binding sites was 33-39% for conjugates made with DSP modified antibodies at pH 6.0 and 6.5. Similarly, 34% of the unmodified antibodies adsorbed per AuNP were available for antigen binding at pH 7.5.

Antibodies on AuNP can have a different orientation, which can impact its loading density. This result suggests the increase in antigen binding of DSP modified antibody-AuNP conjugates is a result of high antibody loading per AuNP, which is influenced by the orientation of these antibodies on AuNP. Moreover, the percentage of antibodies accessible for antigen binding increased from pH 7.5 to 6.0 for the DSP modified antibodies.

Although free thiol has a high affinity for gold compared to amines, all cysteine residue in the antibody we used for this experiment are engaged in disulfide bonds and are relatively inaccessible to solvent. Meanwhile, multiple solvent-accessible lysine residues are present in immunoglobulin G 2a (IgG2A). Therefore, primary amines of lysine residues are a primary target for the initial coordination of the antibodies to AuNP. Acroleinating primary amines of lysine through chemical modification of antibodies with acrylic NHS, inhibit interaction of primary amines of lysine with AuNP. In other to firmly anchor acrylic acid NHS modified

antibodies onto AuNP, the antibody would, therefore, have to unfold to expose functional groups that can actively interact with the nanoparticles. Antibody unfolding may stimulate the loss of tertiary structure and may lead to loss of antigen-binding. Herein, we propose antibody unfolding to be the primary reason why acrylic acid NHS-modified antibody-AuNP conjugate captured no antigen.

Dissecting the Effect of Antibody on AuNP

It has been previously reported that antibody crowding on the AuNP surface can lead to a decrease in the percentage of active antibodies. Moreover, the number of proteins loaded onto nanoparticles have been reported to be dependent on the concentration of added protein. To investigate the possibility of overcrowding in limiting antigen binding by antibodies, different amount (1.5, 2, 3, 4 ug) of unmodified mouse anti-HRP antibody was added to a fixed concentration of AuNP at pH 7.5. The fraction of antibodies available for antigen binding was deduced at each concentration using an HRP enzymatic assay.

A

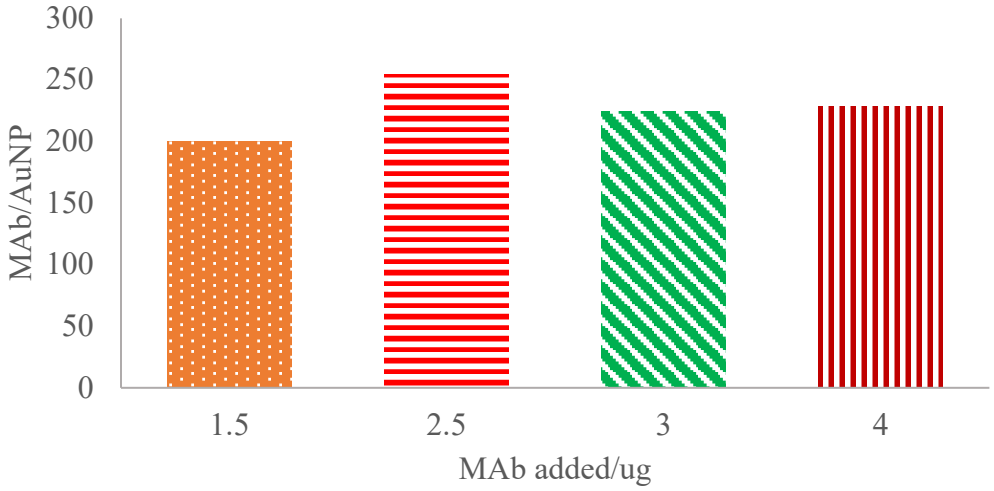

B

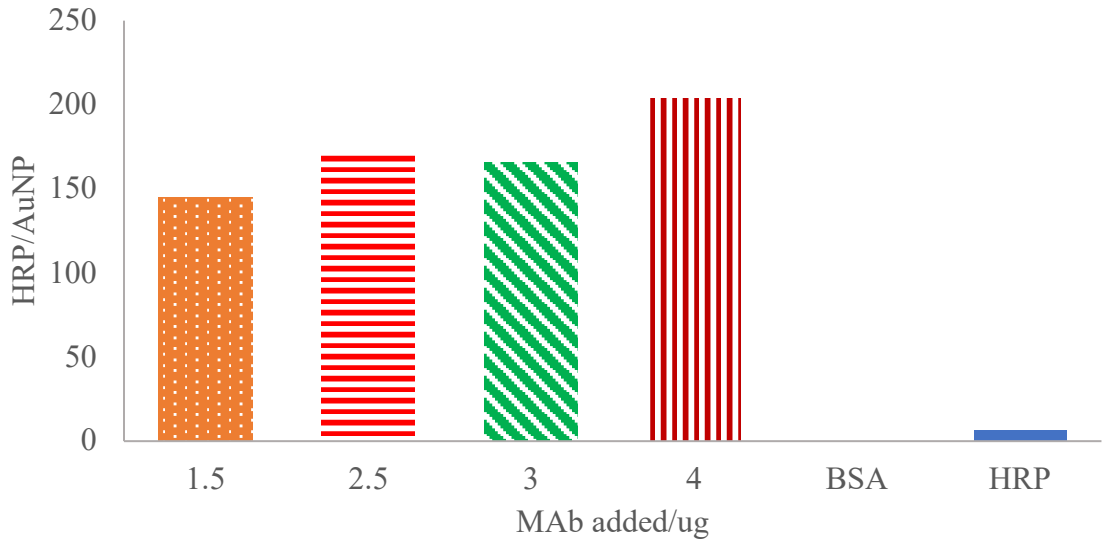

C

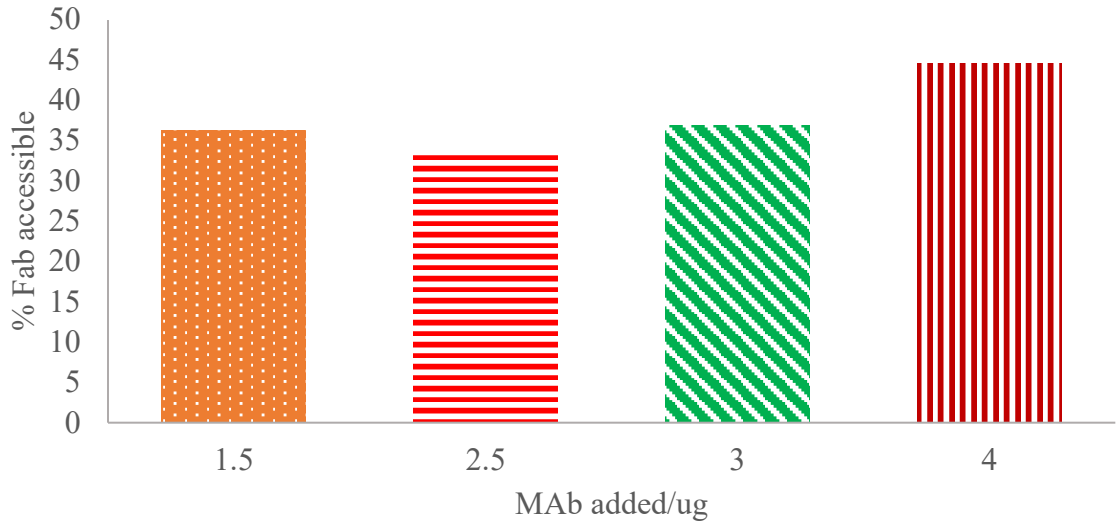

Figure 29. Evaluating the effect of antibody overcrowding on antigen capture efficiency. (A) Number of antibodies per AuNP at different antibody incubation concentration. (B) Number of HRP captured by antibody-AuNP conjugates synthesized at each added antibody concentration. (C) Fraction of antibody accessible to antigens at each antibody concentration.

Theoretically, the maximum number of antibodies needed to saturate a 60 nm AuNP entirely is 333 for a side on close packing. Employing the use of our developed fluorescence-ICP-OES assay to determine the number of antibodies adsorb at each added concentration, we recorded 151 ± 7, 184, 230, 231, and 239 antibodies per AuNP at 0.5, 1.5, 2.5, 3 and 4 □g respectfully (Figure 29A). The data suggest a monolayer saturation at 2.5 □g. The HRP enzymatic assay revealed that 33-44% of antibodies were active, and the activity was independent of the amount of anti-HRP antibody added (**Figure 29C**). The independency of the fraction of active antibodies on the amount of added antibody indicates that the percentage of antibodies on AuNP available for antigen binding is solely dictated by antibody orientation, which has been found to be impacted by the pH of the solution for unmodified mouse anti-HRP antibody.

Conclusion

It is well established that protein adsorption onto AuNP is governed by both electrostatic and covalent interactions. Initially, we had observed aggregation of AuNPs when incubated with antibodies at pH less than 7.5. By controlling the surface charge of antibodies through chemical modification with acrylic acid NHS and reduced DSP, stable conjugates were synthesized at pH 6.0 and 6.5. Also, we have established that the presence of free thiols and primary amines on protein promote quick adsorption of proteins onto AuNP. These studies demonstrate that primary amine and free thiol are important functionalities that facilitate the adsorption of proteins on AuNP. Introduction of free sulfhydryl on antibody enhanced the formation of stable and functional antibody-AuNP conjugates. Although stable conjugates where formed even at acidic pH when interaction of amines with AuNP was eliminated, through chemical modification of antibodies with acrylic acid NHS, the conjugates could capture no antigen. Moreover, we have

confirmed that solution pH is a significant parameter which controls orientation of antibodies on AuNP. From our studies we can also conclude that the fraction of accessible Fab of antibodies on AuNP is solely dependent on antibody orientation and not affected by overcrowding of antibodies on AuNP, at least within our working concentration.

CHAPTER IV: CONCLUSIONS AND OUTLOOKS

Research Summary

There is growing concern on the fate of nanoparticles for in-vitro and in-vivo biomedical application due to the potential of biomolecules altering the physicochemical properties of these nanoparticles.[24,37,39,41,42] In this work, the impact of antibody surface charge on the stability of AuNPs and the mechanism by which antibodies induces aggregation of AuNPs have been fully evaluated. A systematic workflow was used to synthesize and titrate AuNPs-antibody conjugates at different pHs. AuNP aggregates were observed when excess antibodies were incubated with nanoparticles at pH less than 7.5. However, when a stable conjugate was titrated to a pH less than 7.5 no aggregates were observed. Also, no aggregation of nanoparticles was detected at pH<7.5 when the surface charge of antibodies was modulated through chemical modification using acrylic acid NHS which reacts and form an amide with primary amines of lysine residues. Protein induced AuNP aggregation was intrinsically irreversible when aggregates were allowed to stand in buffer for 24 hours, however, upon titrating to higher pH by the addition of NaOH, the aggregates reversed to a normal conjugate size for the first five hours of incubation. Meanwhile there was no, or little reversibility of aggregates incubated for 24 hours.

From our findings, we conclude that protein surface charge which is dictated by a solution pH is an important factor to consider when functionalizing AuNPs surface with proteins. Electrostatic bridging of antibodies between AuNPs was also determined to be the mechanism by which antibodies triggers AuNP aggregation, since a fully saturated nanoparticle with no exposed surface is stable after resuspension in buffer (pH 6-6.5) for 24 hours. Moreover, the ability to synthesize antibody-nanoparticle conjugates after altering the surface charge of

antibodies through chemical modification also reaffirms the assertion that electrostatic bridging of antibodies is the predominant interaction which initiates the aggregation of AuNPs.

The impact of a solutions pH on the orientation of antibodies on AuNPs have been fully studied in our lab.[32] The fraction of accessible antigen binding site of antibodies on AuNP have been determined to increase as pH of the incubating solution decreases, however aggregation of AuNPs is observed at pH<7.5. As discussed above, the surface charge of antibodies at these pHs is solely responsible for triggering aggregation of nanoparticles. Chemical modification of antibodies through reaction primary amines of lysine residues alters antibody surface charge and allows synthesis of conjugates at pH<7.5. Here, the adsorption dynamics, kinetics and antigen binding activity of chemically modified antibody-AuNP conjugates have been investigated. UV-visible spectrophotometry, nanoparticle tracking analysis and dynamic light scattering was employed to undertake all these studies. Chemical modification of antibodies with acrylic acid NHS and reduced DSP results in the formation of an amide between primary amines of lysine residues and carboxylate carbonyl chemical modifiers. Reaction of reduced DSP with antibodies introduces free thiol onto the antibody which enhances antibody adsorption onto AuNP. The possibility of interaction between primary amines and AuNP is eliminated when reacted with acrylic acid NHS.

From our observations we conclude that free thiol and amines are important functionalities for rapid and efficient adsorption of proteins onto AuNPs.

Outlooks and Future Direction

Gold-nanoparticle enabled immunoassays are rapid and cost effective, however applicability is limited due to low sensitivity resulting from ineffective immobilization of antibodies on AuNP. This works provides insight on the possible mechanism by which antibodies can trigger AuNP aggregation and how this aggregation can be avoided through chemical modification of antibodies.

Although the presence of highly active points of interaction on the protein, such as free thiols, increased the number of antigens captured by antibody-AuNP conjugates which may enhance the sensitivity of AuNP-enabled immunoassay, the orientation of antibodies on AuNP was random and pH dependent. A site directed immobilization of the Fc portion of antibody on AuNP after chemical modification of antibodies will improve orientation and prevent aggregation thereby improving the sensitivity and utility of antibody functionalized AuNPs for disease diagnosis.

The possibility of antibody unfolding which may reduce antigen binding activity can also be investigated by employing the use of circular dichroism and FTIR. This study will help substantiate the effect of the number of points of interaction on protein unfolding when adsorbed onto nanoparticles.

REFERENCES

(1) Kozlowski, R.; Ragupathi, A.; Dyer, R. B. Characterizing the Surface Coverage of Protein-AuNP Bioconjugates. *Bioconjug. Chem.* **2018**, *29* (8), 2691–2700. https://doi.org/10.1021/acs.bioconjchem.8b00366.

(2) Tsai, C.-W.; Jheng, S.-L.; Chen, W.-Y.; Ruaan, R.-C. Strategy of Fc-Recognizable Peptide Ligand Design for Oriented Immobilization of Antibody. *Anal. Chem.* **2014**, *86* (6), 2931–2938. https://doi.org/10.1021/ac4029467.

(3) Filbrun, S. L.; Filbrun, A. B.; Lovato, F. L.; Oh, S. H.; Driskell, E. A.; Driskell, J. D. Chemical Modification of Antibodies Enables the Formation of Stable Antibody-AuNP Conjugates for Biosensing. *Analyst* **2017**, *142* (23), 4456–4467. https://doi.org/10.1039/c7an01496a.

(4) Darwish, I. A. Immunoassay Methods and Their Applications in Pharmaceutical Analysis: Basic Methodology and Recent Advances. *Int. J. Biomed. Sci.* **2006**, *2* (3), 217–235.

(5) Eyimegwu, P. N.; Lartey, J. A.; Kim, J. H. Gold-Nanoparticle-Embedded Poly(N-Isopropylacrylamide) Microparticles for Selective Quasi-Homogeneous Catalytic Homocoupling Reactions. *ACS Appl. Nano Mater.* **2019**, *2* (9), 6057–6066. https://doi.org/10.1021/acsanm.9b01594.

(6) Das, M.; Shim, K. H.; An, S. S. A.; Yi, D. K. Review on AuNPs and Their Applications. *Toxicology and Environmental Health Sciences*. 2011, pp 193–205. https://doi.org/10.1007/s13530-011-0109-y.

(7) Zhang, W.; Meckes, B.; Mirkin, C. A. Spherical Nucleic Acids with Tailored and Active Protein Coronae. *ACS Cent. Sci.* **2019**, *5*, 1983–1990. https://doi.org/10.1021/acscentsci.9b01105.

(8) Mahmoudi, M.; Lynch, I.; Ejtehadi, M. R.; Monopoli, M. P.; Bombelli, F. B.; Laurent, S. Protein−Nanoparticle Interactions: Opportunities and Challenges. *Chem. Rev.* **2011**, *111* (9), 5610–5637. https://doi.org/10.1021/cr100440g.

(9) Casals, E.; Pfaller, T.; Duschl, A.; Oostingh, G. J.; Puntes, V. Time Evolution of the Nanoparticle Protein Corona. *ACS Nano* **2010**, *4* (7), 3623–3632. https://doi.org/10.1021/nn901372t.

(10) Hermanson, G. T. *Bioconjugate Techniques: Third Edition*; Elsevier Inc., 2013. https://doi.org/10.1016/C2009-0-64240-9.

(11) Mandl, A.; Filbrun, S. L.; Driskell, J. D. Asymmetrically Functionalized Antibody-AuNP Conjugates to Form Stable Antigen-Assembled Dimers. *Bioconjug. Chem.* **2017**, *28* (1), 38–42. https://doi.org/10.1021/acs.bioconjchem.6b00459.

(12) Karyakin, A. A.; Presnova, G. V.; Rubtsova, M. Y.; Egorov, A. M. Oriented Immobilization of Antibodies onto the Gold Surfaces via Their Native Thiol Groups. *Anal. Chem.* **2000**, *72* (16), 3805–3811. https://doi.org/10.1021/ac9907890.

(13) Shang, L.; Yang, L.; Seiter, J.; Heinle, M.; Brenner-Weiss, G.; Gerthsen, D.; Nienhaus, G. U. Nanoparticles Interacting with Proteins and Cells: A Systematic Study of Protein Surface Charge Effects. *Adv. Mater. Interfaces* **2014**, *1* (2). https://doi.org/10.1002/admi.201300079.

(14) Pollok, N. E.; Rabin, C.; Smith, L.; Crooks, R. M. Orientation-Controlled Bioconjugation of Antibodies to Silver Nanoparticles. *Bioconjug. Chem.* **2019**, *30*, acs.bioconjchem.9b00737. https://doi.org/10.1021/acs.bioconjchem.9b00737.

(15) Tollefson, E. J.; Allen, C. R.; Chong, G.; Zhang, X.; Rozanov, N. D.; Bautista, A.; Cerda, J. J.; Pedersen, J. A.; Murphy, C. J.; Carlson, E. E.; et al. Preferential Binding of Cytochrome c to Anionic Ligand-Coated AuNPs: A Complementary Computational and Experimental Approach. *ACS Nano* **2019**, *13* (6), 6856–6866. https://doi.org/10.1021/acsnano.9b01622.

(16) De Juan-Franco, E.; Caruz, A.; Pedrajas, J. R.; Lechuga, L. M. Site-Directed Antibody Immobilization Using a Protein A-Gold Binding Domain Fusion Protein for Enhanced SPR Immunosensing. *Analyst* **2013**, *138* (7), 2023–2031. https://doi.org/10.1039/c3an36498d.

(17) Jans, H.; Huo, Q. AuNP-Enabled Biological and Chemical Detection and Analysis. *Chem. Soc. Rev.* **2012**, *41* (7), 2849–2866. https://doi.org/10.1039/c1cs15280g.

(18) De Paoli Lacerda, S. H.; Park, J. J.; Meuse, C.; Pristinski, D.; Becker, M. L.; Karim, A.; Douglas, J. F. Interaction of AuNPs with Common Human Blood Proteins. *ACS Nano* **2010**, *4* (1), 365–379. https://doi.org/10.1021/nn9011187.

(19) Ruiz, G.; Ryan, N.; Rutschke, K.; Awotunde, O.; Driskell, J. D. Antibodies Irreversibly Adsorb to AuNPs and Resist Displacement by Common Blood Proteins. **2019**. https://doi.org/10.1021/acs.langmuir.9b01900.

(20) Vilanova, O.; Mittag, J. J.; Kelly, P. M.; Milani, S.; Dawson, K. A.; Rädler, J. O.; Franzese, G. Understanding the Kinetics of Protein-Nanoparticle Corona Formation. *ACS Nano* **2016**, *10* (12). https://doi.org/10.1021/acsnano.6b04858.

(21) Pong, B.-K.; Lee, J. Y.; Trout, B. L. A Computational Study to Understand the Surface Reactivity of AuNPs with Amines and DNA. *Http://Hdl.Handle.Net/1721.1/30380* **2006**, 1–6.

(22) De Roe, C.; Courtoy, P. J.; Baudhuin, P. A Model of Protein-Colloidal Gold Interactions. *J. Histochem. Cytochem.* **1987**, *35* (11), 1191–1198. https://doi.org/10.1177/35.11.3655323.

(23) Zhang, D.; Neumann, O.; Wang, H.; Yuwono, V. M.; Barhoumi, A.; Perham, M.; Hartgerink, J. D.; Wittung-Stafshede, P.; Halas, N. J. AuNPs Can Induce the Formation of Protein-Based Aggregates at Physiological PH. *Nano Lett.* **2009**, *9* (2), 666–671. https://doi.org/10.1021/nl803054h.

(24) Dominguez-Medina, S.; Kisley, L.; Tauzin, L. J.; Hoggard, A.; Shuang, B.; D. S. Indrasekara, A. S.; Chen, S.; Wang, L. Y.; Derry, P. J.; Liopo, A.; et al. Adsorption and Unfolding of a Single Protein Triggers Nanoparticle Aggregation. *ACS Nano* **2016**, *10* (2), 2103–2112. https://doi.org/10.1021/acsnano.5b06439.

(25) Neupane, S.; Pan, Y.; Takalkar, S.; Bentz, K.; Farmakes, J.; Xu, Y.; Chen, B.; Liu, G.; Qian, S. Y.; Yang, Z. Probing the Aggregation Mechanism of AuNPs Triggered by a Globular Protein. *J. Phys. Chem. C* **2017**, *121* (2), 1377–1386. https://doi.org/10.1021/acs.jpcc.6b11963.

(26) Bharti, B.; Meissner, J.; Klapp, S. H. L.; Findenegg, G. H. Bridging Interactions of Proteins with Silica Nanoparticles: The Influence of PH, Ionic Strength and Protein Concentration. *Soft Matter* **2014**, *10* (5), 718–728. https://doi.org/10.1039/c3sm52401a.

(27) Shang, L.; Nienhaus, K.; Jiang, X.; Yang, L.; Landfester, K.; Mailänder, V.; Simmet, T.; Nienhaus, G. U. Nanoparticle Interactions with Live Cells: Quantitative Fluorescence Microscopy of Nanoparticle Size Effects. *Beilstein J. Nanotechnol.* **2014**, *5* (1), 2388–2397. https://doi.org/10.3762/bjnano.5.248.

(28) Safari, J.; Zarnegar, Z. Advanced Drug Delivery Systems: Nanotechnology of Health Design A Review. *Journal of Saudi Chemical Society*. April 2014, pp 85–99. https://doi.org/10.1016/j.jscs.2012.12.009.

(29) Smith, A. M.; Marbella, L. E.; Johnston, K. A.; Hartmann, M. J.; Crawford, S. E.; Kozycz, L. M.; Seferos, D. S.; Millstone, J. E. Quantitative Analysis of Thiolated Ligand Exchange on AuNPs Monitored by 1 H NMR Spectroscopy. **2015**. https://doi.org/10.1021/ac504081k.

(30) Zhao, L.; Zhao, L.; Li, H.; Sun, P.; Wu, J.; Li, K.; Hu, S.; Wang, X.; Pu, Q. Facile Evaluation of Nanoparticle-Protein Interaction Based on Charge Neutralization with Pulsed Streaming Potential Measurement. *Anal. Chem.* **2019**. https://doi.org/10.1021/acs.analchem.9b03778.

(31) Giri, K.; Shameer, K.; Zimmermann, M. T.; Saha, S.; Chakraborty, P. K.; Sharma, A.; Arvizo, R. R.; Madden, B. J.; Mccormick, D. J.; Kocher, J. A.; et al. Understanding Protein−Nanoparticle Interaction: A New Gateway to Disease Therapeutics Karuna. *Bioconjug. Chem.* **2014**, *25*, 1078–1090.

(32) Ruiz, G.; Tripathi, K.; Okyem, S.; Driskell, J. D. PH Impacts the Orientation of Antibody Adsorbed onto AuNPs. *Bioconjug. Chem.* **2019**, *30* (4), 1182–1191. https://doi.org/10.1021/acs.bioconjchem.9b00123.

(33) Vines, J. B.; Yoon, J. H.; Ryu, N. E.; Lim, D. J.; Park, H. AuNPs for Photothermal Cancer Therapy. *Frontiers in Chemistry*. Frontiers Media S.A. April 5, 2019, p 167. https://doi.org/10.3389/fchem.2019.00167.

(34) Her, S.; Jaffray, D. A.; Allen, C. AuNPs for Applications in Cancer Radiotherapy: Mechanisms and Recent Advancements. *Advanced Drug Delivery Reviews*. Elsevier B.V. January 15, 2017, pp 84–101. https://doi.org/10.1016/j.addr.2015.12.012.

(35) Matei, I.; Buta, C. M.; Turcu, I. M.; Culita, D.; Ionita, G. Molecules Formation and Stabilization of AuNPs in Bovine Serum Albumin Solution. **2019**. https://doi.org/10.3390/molecules24183395.

(36) Neupane, S.; Pan, Y.; Takalkar, S.; Bentz, K.; Farmakes, J.; Xu, Y.; Chen, B.; Liu, G.; Qian, S. Y.; Yang, Z. Probing the Aggregation Mechanism of AuNPs Triggered by a Globular Protein. *J. Phys. Chem. C* **2017**, *121* (2), 1377–1386. https://doi.org/10.1021/acs.jpcc.6b11963.

(37) Fei, L.; Perrett, S. Effect of Nanoparticles on Protein Folding and Fibrillogenesis. *International Journal of Molecular Sciences*. Multidisciplinary Digital Publishing Institute (MDPI) February 2009, pp 646–655. https://doi.org/10.3390/ijms10020646.

(38) Bharti, B.; Meissner, J.; Klapp, S. H. L.; Findenegg, G. H. Bridging Interactions of Proteins with Silica Nanoparticles: The Influence of PH, Ionic Strength and Protein Concentration. *Soft Matter* **2014**, *10* (5), 718–728. https://doi.org/10.1039/c3sm52401a.

(39) Chegel, V.; Rachkov, O.; Lopatynskyi, A.; Ishihara, S.; Yanchuk, I.; Nemoto, Y.; Hill, J. P.; Ariga, K.; Lashkaryov, V. E. AuNPs Aggregation: Drastic Effect of Cooperative Functionalities in a Single Molecular Conjugate. *J. Phys. Chem. C* **2012**, *116*, 2683–2690. https://doi.org/10.1021/jp209251y.

(40) Ruiz, G.; Tripathi, K.; Okyem, S.; Driskell, J. D. PH Impacts the Orientation of Antibody Adsorbed onto AuNPs. *Bioconjug. Chem.* **2019**, *30* (4), 1182–1191. https://doi.org/10.1021/acs.bioconjchem.9b00123.

(41) Cukalevski, R.; Ferreira, S. A.; Dunning, C. J.; Berggård, T.; Cedervall, T. IgG and Fibrinogen Driven Nanoparticle Aggregation. *Nano Res.* **2015**, *8* (8), 2733–2743. https://doi.org/10.1007/s12274-015-0780-4.

(42) Hotze, E. M.; Phenrat, T.; Lowry, G. V. Nanoparticle Aggregation: Challenges to Understanding Transport and Reactivity in the Environment. *J. Environ. Qual.* **2010**, *39* (6), 1909–1924. https://doi.org/10.2134/jeq2009.0462.

(43) Phan, H. T.; Haes, A. J. What Does Nanoparticle Stability Mean? HHS Public Access. *J Phys Chem C Nanomater Interfaces* **2019**, *123* (27), 16495–16507. https://doi.org/10.1021/acs.jpcc.

(44) Wijenayaka, L. A.; Ivanov, M. R.; Cheatum, C. M.; Haes, A. J. Improved Parametrization for Extended Derjaguin, Landau, Verwey, and Overbeek Predictions of Functionalized Gold Nanosphere Stability. *J. Phys. Chem. C* **2015**, *119* (18), 10064–10075. https://doi.org/10.1021/acs.jpcc.5b00483.

(45) Saunders, S. R.; Eden, M. R.; Roberts, C. B. Modeling the Precipitation of Polydisperse Nanoparticles Using a Total Interaction Energy Model. *J. Phys. Chem. C* **2011**, *115*, 4603–4610. https://doi.org/10.1021/jp200116a.

(46) Vincent, B.; Edwards, J.; Emmett, S.; Jones, A. Depletion Flocculation in Dispersions of Sterically-Stabilised Particles ("soft Spheres"). *Colloids and Surfaces* **1986**, *18* (2–4), 261–281. https://doi.org/10.1016/0166-6622(86)80317-1.

(47) Xi, W.; Phan, H. T.; Haes, A. J. How to Accurately Predict Solution-Phase Gold Nanostar Stability Graphical Abstract HHS Public Access. *Anal Bioanal Chem* **2018**, *410* (24), 6113–6123. https://doi.org/10.1007/s00216-018-1115-6.

(48) Woods, K. E.; Perera, Y. R.; Davidson, M. B.; Wilks, C. A.; Yadav, D. K.; Fitzkee, N. C. Understanding Protein Structure Deformation on the Surface of AuNPs of Varying Size. *J. Phys. Chem. C* **2016**, *120* (49). https://doi.org/10.1021/acs.jpcc.6b08089.

(49) Dolinsky, T. J.; Nielsen, J. E.; McCammon, J. A.; Baker, N. A. PDB2PQR: An Automated Pipeline for the Setup of Poisson-Boltzmann Electrostatics Calculations. *Nucleic Acids Res.* **2004**, *32* (WEB SERVER ISS.), W665–W667. https://doi.org/10.1093/nar/gkh381.

(50) Dong, F.; Olsen, B.; Baker, N. A. Computational Methods for Biomolecular Electrostatics. *Methods Cell Biol.* **2008**, *84*, 843–870. https://doi.org/10.1016/S0091-679X(07)84026-X.

(51) Baker, N. A.; Sept, D.; Joseph, S.; Holst, M. J.; Andrew McCammon, J. *Electrostatics of Nanosystems: Application to Microtubules and the Ribosome*; 2001; Vol. 98.

(52) Reynolds, H. Y. *Immunoglobulin G and Its Function in the Human Respiratory Tract**Based on a Medical Grand Rounds Presentation at the Mayo Clinic, April 22, 1987.*; 1988; Vol. 63. https://doi.org/10.1016/S0025-6196(12)64949-0.

(53) Overbaugh, J.; Morris, L. The Antibody Response against HIV-1. *Cold Spring Harb. Perspect. Med.* **2012**, *2* (1), a007039. https://doi.org/10.1101/cshperspect.a007039.

(54) Jung, Y.; Jin, H.; Min, J.; Ok, S.; Soo, W. Controlled Antibody Immobilization onto Immunoanalytical Platforms by Synthetic Peptide. **2008**, *374*, 99–105. https://doi.org/10.1016/j.ab.2007.10.022.

(55) Welch, N. G.; Scoble, J. A.; Muir, B. W.; Pigram, P. J. Orientation and Characterization of Immobilized Antibodies for Improved Immunoassays (Review). *Biointerphases* **2017**, *12* (2), 02D301. https://doi.org/10.1116/1.4978435.

(56) Daraee, H.; Eatemadi, A.; Abbasi, E.; Aval, S. F.; Kouhi, M.; Akbarzadeh, A. Application of AuNPs in Biomedical and Drug Delivery. *Artificial Cells, Nanomedicine and Biotechnology*. 2016, pp 410–422. https://doi.org/10.3109/21691401.2014.955107.

(57) Sotnikov, D. V.; Berlina, A. N.; Ivanov, V. S.; Zherdev, A. V.; Dzantiev, B. B. Adsorption of Proteins on AuNPs: One or More Layers? *Colloids Surfaces B Biointerfaces* **2019**, *173*, 557–563. https://doi.org/10.1016/j.colsurfb.2018.10.025.

(58) Oliveira, J. P.; Prado, A. R.; Keijok, W. J.; Antunes, P. W. P.; Yapuchura, E. R.; Guimarães, M. C. C. Impact of Conjugation Strategies for Targeting of Antibodies in AuNPs for Ultrasensitive Detection of 17β-Estradiol. *Sci. Rep.* **2019**, *9* (1). https://doi.org/10.1038/s41598-019-50424-5.

(59) Wang, A.; Perera, Y. R.; Davidson, M. B.; Fitzkee, N. C. Electrostatic Interactions and Protein Competition Reveal a Dynamic Surface in AuNP−Protein Adsorption. **2016**. https://doi.org/10.1021/acs.jpcc.6b08469.

(60) Assfalg, M.; Ragona, L.; Pagano, K.; D'Onofrio, M.; Zanzoni, S.; Tomaselli, S.; Molinari, H. The Study of Transient Protein-Nanoparticle Interactions by Solution NMR Spectroscopy. *Biochimica et Biophysica Acta - Proteins and Proteomics*. 2016. https://doi.org/10.1016/j.bbapap.2015.04.024.

(61) Pensa, E.; Cortés, E.; Corthey, G.; Carro, P.; Vericat, C.; Fonticelli, M. H.; Benítez, G.; Rubert, A. A.; Salvarezza, R. C. The Chemistry of the Sulfur-Gold Interface: In Search of a Unified Model. *Acc. Chem. Res.* **2012**, *45* (8), 1183–1192. https://doi.org/10.1021/ar200260p.

(62) Jo, S.; Kim, T.; Iyer, V. G.; Im, W. CHARMM-GUI: A Web-Based Graphical User Interface for CHARMM. *J. Comput. Chem.* **2008**, *29* (11), 1859–1865. https://doi.org/10.1002/jcc.20945.

(63) Jo, S.; Vargyas, M.; Vasko-Szedlar, J.; Roux, B. B.; Im, W. PBEQ-Solver for Online Visualization of Electrostatic Potential of Biomolecules. *Web Serv. issue Publ. online* **2008**, *36*. https://doi.org/10.1093/nar/gkn314.

(64) Badyal, J. P.; Cameron, A. M.; Cameron, N. R.; Coe, D. M.; Cox, R.; Davis, B. G.; Oates, L. J.; Oye, G.; Steel, P. G. A Simple Method for the Quantitative Analysis of Resin Bound Thiol Groups. *Tetrahedron Lett.* **2001**, *42* (48), 8531–8533. https://doi.org/10.1016/S0040-4039(01)01820-2.

(65) Yadav, I.; Kumar, S.; Aswal, V. K.; Kohlbrecher, J. Structure and Interaction in the PH-Dependent Phase Behavior of Nanoparticle-Protein Systems. *Langmuir* **2017**, *33* (5). https://doi.org/10.1021/acs.langmuir.6b04127.

(66) Siddiqui, M. R. H. Protected AuNPs with Thioethers and Amines as Surrogate Ligands. *J. Chem.* **2013**, *2013*, 1–4. https://doi.org/10.1155/2013/780939.

(67) Sainsbury, T.; Ikuno, T.; Okawa, D.; Pacilé, D.; Fréchet, J. M. J.; Zettl, A. Self-Assembly of AuNPs at the Surface of Amine- and Thiol-Functionalized Boron Nitride Nanotubes. *J. Phys. Chem. C* **2007**, *111* (35), 12992–12999. https://doi.org/10.1021/jp072958n.

(68) Kumar, A.; Mandal, S.; Selvakannan, P. R.; Pasricha, R.; Mandale, A. B.; Sastry, M. Investigation into the Interaction between Surface-Bound Alkylamines and AuNPs. *Langmuir* **2003**, *19* (15), 6277–6282. https://doi.org/10.1021/la034209c.

(69) Kuroda, K.; Ishida, T.; Haruta, M. Reduction of 4-Nitrophenol to 4-Aminophenol over Au Nanoparticles Deposited on PMMA. *J. Mol. Catal. A Chem.* **2009**, *298* (1–2), 7–11. https://doi.org/10.1016/j.molcata.2008.09.009.

(70) Saha, B.; Evers, T. H.; Prins, M. W. J. How Antibody Surface Coverage on Nanoparticles Determines the Activity and Kinetics of Antigen Capturing for Biosensing. *Anal. Chem.* **2014**, *86* (16), 8158–8166. https://doi.org/10.1021/ac501536z.

(71) Cheng, X.; Challier, L.; Etcheberry, A.; Noël, V.; Perez, H. The ABTS-HRP System as an Alternative Method to RRDE for the Determination of the Selectivity of the Oxygen Reduction Reaction. *Int. J. Electrochem. Sci.* **2012**, *7* (7), 6247–6264.

(72) Tripathi, K.; Driskell, J. D. Quantifying Bound and Active Antibodies Conjugated to AuNPs: A Comprehensive and Robust Approach to Evaluate Immobilization Chemistry. *ACS Omega* **2018**, *3* (7), 8253–8259. https://doi.org/10.1021/acsomega.8b00591.